

Doctoral Dissertation

博士論文

Nutrient absorption in the developing embryo of oviparous
cloudy catshark, *Scyliorhinus torazame*

(卵生軟骨魚類トラザメの胚発生期における消化吸収機構に関する研究)

A Dissertation Submitted for the Degree of Doctor of Philosophy
December 2020

令和 2 年 12 月博士（理学）申請

Department of Biological Sciences, Graduate School of Science,
The University of Tokyo

東京大学大学院理学系研究科 生物科学専攻

Yuki Honda

本田 祐基

Abstract

All animals are heterotroph, so that they must consume food to obtain nutrients for survival. Digestion and absorption of nutrients take place in a coordinated process of digestive organs. Among them, intestine is the major site for nutrient absorption. Since embryos generally do not have functional intestine, they need different systems to obtain nutrients. The aim of my PhD research is to clarify digestion and absorption mechanisms in the developing embryos. For this purpose, I focused on cartilaginous fish (sharks, skates, rays and chimaeras). They are copulating animals, and produce a small number of offsprings. Their reproductive modes vary from oviparous to aplacental or placental viviparous. Embryos of oviparous species rely on yolk as a sole source of nutrients while viviparous embryos obtain additional nutrients, such as uterine milk and trophic eggs, in the uterus. Even in oviparous species, yolk is known to be directed into the embryonic intestine from the external yolk sac from the mid-embryonic stage, suggesting that embryos of cartilaginous fish undergo a shift of nutrient absorption surface during the development. In the present study, I chose the oviparous cloudy catshark (*Scyliorhinus torazame*) as a model animal. Cloudy catshark lays egg throughout the year, and have several advantages including the availability of genome and transcriptome data.

It is well known that tetrapods and teleosts have long intestinal tract to increasing surface area of intestinal lumens for efficient nutrient absorption. On the other hand, cartilaginous fish have relatively short intestine with helical intestinal mucosa, known as spiral intestine. In **Chapter 1**, I investigated the morphological and functional development of the spiral intestine. By detailed histological observation, I found that spiral formation starts at stage 24 and finished at stage 31. At the middle of stage 31, about two months after oviposition, the egg case opens to allow seawater flow into the egg case, a phenomenon known as “pre-hatching”. The spiral formation was completed

prior to the pre-hatching event. The yolk in the external yolk sac began to flow into the embryonic intestine within 48 hours after the pre-hatching via the yolk stalk. The mRNA levels of the peptide transporter *pept1* and neutral amino acid transporter *slc6a19* were increased in the embryonic intestine after pre-hatching, showing that absorption capacity. These results suggested that the pre-hatching is the turning point for nutrient absorption in catshark embryo.

The results in Chapter 1 implied that, before the pre-hatching event, the yolk sac membrane (YSM) is considered to be sole organ to absorb nutrients. I hypothesized that functional shift of nutrient absorption from the YSM to the intestine occurs during the catshark development. In **Chapter 2**, I investigated expression of genes involved in digestion and absorption of nutrients to verify the hypothesis. I conducted RNA-seq analysis of the YSM and the intestine, and identified amino acid transporters, lipid absorption molecules, and digestive enzymes. Quantification of the mRNA levels throughout the embryonic period revealed that most genes increased their expression in the intestine after the pre-hatching period, in accord with the above hypothesis. However, contrary to the expectation, many of genes related to digestion and absorption in the YSM increased after the formation of functional intestine. These results imply that nutrient digestion and absorption in cloudy catshark embryo is more active in later developmental stage with both the intestine and YSM as nutrient absorption surfaces to achieve rapid growth. Embryonic body weight was markedly increased from stage 32, supporting this notion. In addition, the gene expression profiles suggest that the nutrient absorption mechanisms are different between the YSM and the intestine. While the embryonic intestine uptakes peptides/amino acids via specific transporters, the endodermal epithelial cells of YSM likely incorporate nutrient by endocytosis together with amino acid

transporters.

In the last part of this thesis, I will discuss my findings on nutrition absorption mechanisms in developing embryos of oviparous cloudy catshark from the viewpoints of the functions of the spiral intestine, reproductive strategies, and evolutionary history of cartilaginous fish. I propose a hypothesis that the pre-hatching of oviparous cartilaginous fish is equivalent to the hatching in teleosts. The hatched larvae of cloudy catshark stay inside the egg case until the completion of yolk absorption to increase survival by reducing predation risk. This would be important for the strategy of “low birth and premature death rates” in oviparous cartilaginous fish.

Contents

1. General Introduction	1
2. Chapter 1	13
Morphological and functional development of the spiral intestine in cloudy catshark (<i>Scyliorhinus torazame</i>)	
3. Chapter 2	46
Molecular investigation of nutrient absorption in the yolk sac membrane and the intestine of the developing embryo of cloudy catshark (<i>Scyliorhinus torazame</i>)	
4. General Discussion	91
5. Acknowledgements	103
6. References	106

General Introduction

All animals must consume food to obtain nutrients for growth, maintenance of the body metabolism, and reproduction. Vertebrates possess a digestive system composed of a gastrointestinal tract and accessory organs, such as liver, pancreas and gall bladder, to digest and absorb nutrient efficiently. Among these organs, intestine is major for nutrient absorption. Ingested food is broken down by physical and chemical digestion in the gastrointestinal tract. Digested peptides, amino acids, sugars and lipids are then absorbed by specific mechanisms according to the types of molecules (Kiela and Ghishan, 2016). Di- or Tri-peptides, amino acids and sugars are absorbed through specific peptide transporters (Daniel, 2004), amino acid transporters (Bröer, 2008; Bröer and Fairweather, 2018), and sugar transporters (Drozdowski and Thomson, 2006), respectively. On the other hand, mono-, di- and triacylglycerol, cholesterol and phospholipid are aggregated into micelles and then incorporated by simple diffusion or via specific transporters (Wang et al., 2013; Hussain, 2014). These nutrients are then released into the systemic circulation and supplied to the whole body.

Unique intestine of cartilaginous fish: spiral intestine

For efficient absorption of nutrient in the intestine, extensive luminal surface area is necessary. Three structural hierarchies contribute to the enlargement of the intestinal surface area: 1) the presence of intense microvilli on the apical surface of enterocytes at ultrastructural level, 2) extensive villi or mucosal folding at microscopic level, and 3) elongated gut tube at macroscopic level (Romer and Parsons, 2007; Walton et al., 2016). Relative intestinal length to body cavity is approximately 2-fold in carnivorous teleosts and 8-fold in herbivorous teleosts (Bucking, 2015). Besides, relative intestinal length to body length is approximately 4- to 6-fold in carnivorous mammals and 10- to 27-fold in

herbivores mammals (Kararli, 1995). On the other hand, the length of cartilaginous fish intestine is shorter than body cavity. Instead of the increase in intestinal length, they have spirally-shaped mucosa, which increases luminal surface at macroscopic level at relatively short length. The spiral intestine is a plesiomorphic feature of vertebrates and is common not only in cartilaginous fish, but also in lungfish, coelacanth, polypterus, sturgeon, and gar (Khanna, 2004). The external appearance of the spiral intestine is relatively short, straight tubule (Bucking, 2015). However, inside the intestinal lumen, a spiral staircase-like structure known as spiral valve is formed by mucosa and submucosa folds to compartmentalize the intestine for larger surface area. In cartilaginous fish, the anatomy of the spiral intestine has been well described in several species of shark and ray (Perrault, 1671; Parker, 1880; Hadley, 1929; Khanna, 2004; Chatchavalvanich et al., 2006). The spiral intestine can be classified as a spiral, a ring or a scroll type depending on the spiral shape (White, 1937; Compagno et al., 2005). The number of spirals is different among species. For example, 14-1/2 coils are present in spiny dogfish (*Squalus acanthias*), twelve coils are found in lesser spotted dogfish (*Scyliorhinus canicula*), while eight coils are reported in Port Jackson shark (*Heterodontus portusjacksoni*) (Khanna, 2004). The number of spiral turns is thought to be related to the diet (Holmgren and Nilson, 1999). The extensive villi and microvilli on the spiral valve further increase the absorption surface area in the intestine (Chatchavalvanich et al., 2006).

The spiral intestine is major absorptive section in shark digestive tract (Jhaveri et al., 2015) and several studies on digestion and absorption of the spiral intestine of elasmobranchs have been conducted (Leigh et al., 2017). Clearance of digesta from the gastrointestinal tract takes 68-82 hours in lemon shark (*Negaprion acutidens*) (Wetherbee et al., 1987). In the case of carnivorous teleosts such as bluegill (*Lepomis macrochirus*),

green sunfish (*Lepomis cyanellus*) and white catfish (*Ameiurus catus*), food passage time is less than 50 hours at 20-25°C (Lane and Jackson, 1969; Fange and Grove, 1979), indicating that food passage time in sharks is comparatively longer than those of teleosts (Wetherbee et al., 1990). Furthermore, high levels of proteolytic and lipolytic activities were evident in the spiral intestine of bonnethead shark (*Sphyrna tiburo*) (Jhaveri et al., 2015) and in the pancreas tissue of shortfin mako shark (*Isurus oxyrinchus*) (Newton et al., 2015), suggesting efficient digestion activity in shark intestines. High proteolytic and lipolytic activities are reasonable because main energy sources are protein and lipid in elasmobranchs (Ballantyne, 1997). For nutrient absorption, functional peptide transporter 1 (PepT1) was detected in the spiral intestine of bonnethead shark (*Sphyrna tiburo*). To our best knowledge, however, the bonnethead shark study is the only report of transporters contributing to nutrient absorption in the spiral intestine of cartilaginous fish. In mammals and teleosts, the intestine can be divided into functionally distinct segments, such as small intestine and large intestine in mammals, and anterior, middle and posterior portions in teleost intestine (Canan et al., 2012). Meanwhile, no comparative distinction has been reported in spiral intestine of cartilaginous fish (Romer and Parsons, 2007), probably due to a lack in morphological characterization. A single report showed that distal portion of the spiral intestine was different in histological structure and water absorption capacity from other parts in little skate (*Leucoraja erinacea*) (Theodosiou et al., 2007; Theodosiou and Simeone, 2012), suggesting functional segmentation is also true in the spiral intestine.

Reproductive modes and development of cartilaginous fish

While developing embryos still do not have functional digestive organs, they need

to use other systems to obtain nutrient. The ways to get nutrient depend on reproductive modes. Vertebrates have two reproductive modes, oviparity and viviparity (Blackburn, 1999). Oviparity refers to females laying eggs. In oviparous vertebrates, the embryo relies on yolk as the sole nutrient source. In contrast, viviparity refers to females keeping their embryos inside uterus and giving birth to live individuals. In viviparous vertebrates, the embryos obtain nutrient inside the uterus.

Cartilaginous fish are unique in their reproductive strategies among fishes. All cartilaginous fish are copulating animals. They breed a small number of offsprings, and the developmental period of offspring is generally long, ranging from months to years (Conrath and Musick, 2012). Furthermore, reproductive modes of cartilaginous fish were diversely evolved (Musick and Ellis, 2005). Reproductive modes of cartilaginous fish can be generally divided into oviparity and viviparity, and viviparity is further divided into several subtypes by the means of nutrition supply to the embryos. In oviparity, two subtypes were known. One subtype is single oviparity, in which female keeps one egg case in each oviduct for a short period and then lays egg case on breeding ground (Compagno, 1988). Another subtype is multiple oviparity where female keeps multiple eggs in an oviduct for a longer period and then lays egg case containing well developed embryo (Compagno, 1990; Compagno, 2001; Goto, 2001). Recently, Nakaya et al. (2020) found new subtype of oviparity known as sustained single oviparity. Yolk sac viviparity is the lecithotrophic mode in viviparity (Compagno, 1990). In this mode, an embryo relies on yolk for sole nutrient source, although the embryo remains inside the maternal body. On the other hand, an embryo of matrotrophic species obtains additional nutrient in the uterus. In a histotrophic species southern stingray (*Dasyatis americana*), embryos obtain nutrients by ingesting lipid-rich histotroph called uterine milk (Hamlett et al., 1996).

Embryos of the tiger shark (*Galeocerdo cuvier*) drink clear liquid in egg case and authors proposed this new type of nourishing process as “embryotrophy” (Castro et al., 2016). In crocodile shark (*Pseudocarcharias kamoharai*), embryos ingest trophic eggs, a phenomenon known as oophagy (Fujita, 1981). In the sand tiger shark (*Carcharias taurus*), embryos consume not only encapsulated yolk supply, but also their siblings inside uterus (Gilmore et al., 1983). This type is thus called adelphophagy. Placental viviparity is limited in carcharhiniform sharks (the order Carcharhiniformes). The placenta, also known as yolk sac placenta, is composed of embryonic yolk sac membrane (YSM) and uterine wall, and nutrient materials transfer to embryo via blood (Hamlett, 1986; Jones and Hamlett, 2004).

Nutrient absorption is vitally necessary for the proper development of embryos. Given the diverse reproductive modes in cartilaginous fish mentioned above, it is reasonable that the digestion and absorption mechanisms of embryos are also diverse. The histotrophic, oophagous and adelphophagous embryos ingest milk or food, so that their digestive tracts must develop corresponding digestive and absorptive mechanisms during the embryonic development. On the other hand, although the gastrointestinal tract is anatomically formed, a placental viviparous embryo receives required nutrients through the placenta. However, up to now, little is known about digestion and absorption mechanisms in cartilaginous fish embryos, possibly due to the difficulty in obtaining necessary sample because of long developmental period. This is especially true in viviparous species because estimating the developmental stages of embryos from outside is difficult. Therefore, most developmental studies have been conducted using oviparous species in cartilaginous fish (Balfour, 1878; Smith, 1942; Harahush et al., 2007; Rodda and Seymore, 2008; Musa et al., 2018).

Detailed developmental stages have been described in lesser spotted dogfish (*Scyliorhinus canicula*) (Ballard et al., 1993), and brownbanded bamboo shark (*Chiloscyllium punctatum*) (Onimaru et al., 2018). In oviparous cartilaginous fish, a fertilized egg is enclosed in a protective egg case composed of collagen fibrils, and is laid on the sea floor (Knight and Hunt, 1976; Rusaouën et al., 1976; Knupp and Squire, 1998). One side of egg case has a slit but it is sealed by mucous plug to isolate the embryo physically from the surrounding seawater (Thomason et al., 1994). In the middle of development, the slit opens to allow seawater flow into the egg case, a phenomenon known as “pre-hatching” (Lechenault et al., 1993). This phenomenon is considered to be advantageous to facilitate embryonic respiration in circulating seawater (Diez and Davenport, 1987), and to provide space for embryonic growth (Mellinger et al., 1986, 1989). Even though some oviparous species are established models for investigating developmental events among cartilaginous fish, little is known about nutrient absorption during the embryonic period.

Embryonic nutrition in oviparous vertebrates

As mentioned above, developing embryos, in general, do not have a functional digestive system. Mammalian embryo obtains macronutrients, such as glucose, amino acids, and fatty acids, via molecule exchanges in placenta (Lager and Powell, 2012; Brett et al., 2014). On the other hand, oviparous vertebrate embryos consume deposited yolk during embryogenesis. The major component of yolk protein is from vitellogenin, which is synthesized in the female liver and is transported into oocyte (Wallace, 1985). Vitellogenin is then cleaved into lipoproteins, lipovitellin and phosvitin (Yamamura et al., 1995). Unlike placental mammals, embryos of oviparous vertebrates need to digest yolk

protein to absorb nutrients.

In amphibian embryos, yolk platelets are allocated into embryonic cells during cleavage and then processed by intracellular digestion (Jorgensen et al., 2009). The intracellular digestion is conducted by late endosomes containing primary lysosomes (Komazaki and Hiruma, 1999; Komazaki et al., 2002). On the other hand, the egg yolk of teleosts, reptiles and birds is abundant, so that cleavage proceeds only in the limited area at the animal pole lacking yolk, and thereby yolk is stored in the yolk sac. In teleost embryo, yolk mass is adjacent to yolk syncytial layer (YSL), which is a multi-functional extra-embryonic tissue (Carvalho and Heisenberg, 2010). Yolk platelets were degraded in the YSL, which were evident from ultrastructure studies with transmission electron microscopy (TEM) in trout (*Salmo trutta fario* L.) (Walzer and Schönenberger, 1979), rockfish (*Sebastes schlegeli*) (Shimizu and Yamada, 1980), perch (*Perca fluviatilis* L.) (Krieger and Fleig, 1999), and plaice (*Pleuronectes platessa*) (Skjærven et al., 2003). Cathepsin is a group of lysosomal proteolytic enzymes and is involved in yolk digestion in the YSL (Imamura et al., 2008). Indeed, activity of cathepsins D and L (Sire et al., 1994) and mRNA expression of cathepsins B and L (Tingaud-Sequeira and Cerdà, 2007; Tingaud-Sequeira et al., 2011) were observed in the YSL. In avian embryos, yolk is incorporated into endodermal epithelial cells lining the innermost layer of the yolk sac membrane (Lambson, 1970; Mobbs and McMillan, 1981). Cathepsin is involved in yolk degradation in avian embryo, similar to that of teleosts. Enzymatic activity of cathepsin D was detected in the YSM of chicken (Wouters et al., 1985), and activities of cathepsins B and D were detected in the YSM of Japanese quail (*Coturnix japonica*) (Gerhartz et al., 1997). Immunohistochemical study showed that cathepsins B and D were found in the endodermal epithelial cells of YSM of quail (Gerhartz et al., 1999). Furthermore, mRNAs

encoding cathepsins A and B were detected in the transcriptome data of the chicken embryo yolk sac (Yadgary et al., 2014). Recent studies further found that intestinal nutrient transporters such as peptide transporter (PepT1), amino acid transporters (excitatory amino acid transporter 3 [Slc1a1], sodium-dependent neutral amino acid transporter [Slc6a19], cationic amino acid transporter [Slc7a1]), monosaccharide transporters (fructose transporter [Slc2a5] and sodium glucose transporter [Slc5a1]), and brush border enzymes (aminopeptidase N and sucrase-isomaltase), were also expressed in the chicken yolk sac membrane (Yadgary et al., 2011; Speier et al., 2012; Yadgary et al., 2014; Zhang and Wong, 2017). It was thus assumed that the transporter-mediated nutrient absorption occurs in the avian yolk sac membrane, in addition to endocytotic uptake pathway (Wong and Uni, 2020).

In oviparous or viviparous cartilaginous fish at early developmental stages, the vascularized yolk sac membrane is most likely a place for nutrient absorption (Hamlett, 1986). Both endodermal epithelium and YSL were observed in the yolk sac membrane of cartilaginous fish embryos (Jollie and Jollie, 1967; Hamlett and Worums, 1984). Yolk platelets are degraded in the YSL and the processed yolk droplets are endocytosed into the endodermal cells (Hamlett et al., 1987). Lysosomal digestion of yolk protein is prominent according to ultrastructural observation (Hamlett et al., 1987). Furthermore, maximum proteolytic activity of dogfish (*Scyliorhinus canicula*) yolk protein was found in low pH (3.5), which is the optimal pH for lysosomal enzymes. The observation suggested that lysosomal enzyme is involved in yolk protein digestion in cartilaginous fish (Diez and Davenport, 1990). On the other hand, in the mid-embryonic stage, the yolk from the external yolk sac is directed into the embryonic intestine (Tewinkel, 1943; Iwai, 1957). From that stage onwards, the digestion of yolk most likely occurs inside the

intestine, because emulsified yolk platelet and zymogen granules were observed in the intestinal lumen and the pancreatic cells, respectively (Beard, 1896). Glycogen and fat droplet were detected in the epithelial cells of embryonic intestine in *Squalus acanthias* (Tewinkel, 1943). Accumulation of yolk-derived substances were also found in the epithelial cells of intestine in freshwater stingray embryo (Teshima and Tomonaga, 2016), supporting the notion that yolk digestion and absorption occur in the intestine of cartilaginous fish embryo. However, most literature provided only the histochemical and morphological evidence, physiological and mechanistic data were not available. From a developmental perspective, when and how do spiral intestine form? From a physiological perspective, when the embryonic intestine become functional?

Aim of this study

The final goal of my study is to reveal digestion and absorption mechanisms during the development of oviparous cartilaginous fish embryos. To this end, I selected cloudy catshark (*Scyliorhinus torazame*) as the research model for the present study. There are three advantages of cloudy catshark for this purpose: (1) cloudy catshark is closely related to lesser spotted dogfish in which detailed developmental stages was established (Ballard et al., 1993), where comparable stages can be identified according to morphological features. (2) Since cloudy catshark spawn throughout a year, I can collect many fertilized eggs provided by collaborators in the Ibaraki Prefectural Oarai Aquarium. (3) The genome and transcriptome database are available for cloudy catshark (Hara et al., 2018), which allow me to perform discovery search for candidate genes in relation to the physiological processes of interests.

In **Chapter 1**, I focus on morphological and functional development of the spiral

intestine. Formation of spiral valves, secondary folds and microvilli, and opening of esophagus and rectum were examined morphologically and histologically. Spiral formation is completed prior to pre-hatching event at the end of the first third of development. I found that yolk-to-intestine transfer occurred coincided the pre-hatching event. After pre-hatching, I found that peptide transporter 1 (PepT1) and neutral amino acid transporter (Slc6a19) mRNAs were expressed in the embryonic intestine, implying an increase in nutrient absorption capacity of embryonic intestine. Expression of PepT1 and Slc6a19 were regional- and temporal-specific in the intestine of developing embryo. These patterns may infer the shift in nutrient absorption strategies in embryos.

In **Chapter 2**, I focus on genes involved in digestion and absorption in the YSM and intestine of developing embryos. From Chapter 1, I have established that embryonic intestine is functional after the pre-hatching event. Therefore, the pathways for nutrition absorption must be different before and after pre-hatching period. To examine nutrition absorption mechanisms comprehensively, RNA-seq analysis was conducted on the embryonic intestine and YSM of cloudy catshark. Genes encoding amino acid transporters, lipid absorption molecules, and cathepsins were harvested from the transcriptome data. Subsequently, I further examined the detailed expression profiles of these candidate genes in the YSM and intestine throughout the developmental period. Since the embryonic intestine becomes functional after pre-hatching period, nutrient absorption in the YSM was expected to decrease in later stages of development. However, contrary to my expectation, many of genes related to digestion and absorption in the YSM increased even after the formation of functional intestine. Taken together, it is suggested that cloudy catshark embryo absorb nutrient via both intestine and YSM after pre-hatching to fulfill the demand of rapid growth in the late embryonic stages.

In general discussion, I will discuss my findings on nutrition absorption mechanisms in developing embryos of oviparous cloudy catshark from the viewpoints of the functions of the spiral intestine, reproductive strategies, and evolutionary history of cartilaginous fish. In particular, the physiological meanings and implication of the pre-hatching event will be discussed.

Chapter 1

**Morphological and functional development of the
spiral intestine in cloudy catshark (*Scyliorhinus torazame*)**

ABSTRACT

Cartilaginous fish have a comparatively short intestine known as the spiral intestine that consists of a helical spiral of intestinal mucosa. However, morphological and functional development of the spiral intestine has not been fully described. Unlike teleosts, cartilaginous fish are characterized by an extremely long developmental period *in ovo* or *in utero*; for example, in the oviparous cloudy catshark (*Scyliorhinus torazame*), the developing fish remains inside the egg capsule for up to 6 months, suggesting that the embryonic intestine may become functional prior to hatching. In this chapter, I describe the morphological and functional development of the spiral intestine in the developing catshark embryo. Spiral formation of embryonic intestine was completed at the middle of stage 31, prior to ‘pre-hatching’, which is a developmental event characterized by the opening of the egg case at the end of the first third of development. Within 48 h of the pre-hatching event, egg yolk began to flow from the external yolk sac into the embryonic intestine via the yolk stalk. At the same time, there was a rapid increase in mRNA expression of the peptide transporter *pept1* and neutral amino acid transporter *slc6a19*. Secondary folds in the intestinal mucosa and microvilli on the apical membrane appeared after pre-hatching, further supporting the onset of nutrient absorption in the developing intestine at this time. I demonstrate the acquisition of intestinal nutrient absorption at the pre-hatching stage of an oviparous elasmobranch.

INTRODUCTION

Cartilaginous fish (sharks, rays and chimaeras) have evolved many unusual physiological features, including aspects of osmoregulation (Smith, 1936; Hyodo et al., 2014), reproduction (Musick and Ellis, 2005) and gastrointestinal morphology (Wilson and Castro, 2010). The spiral intestine is considered to be a plesiomorphic feature of vertebrate and is found in the non-teleostean actinopterygii, non-tetrapod sarcopterygii, elasmobranchii and holocephalii (Argyriou et al., 2016). The comparatively short intestine in these fishes is offset by the spiral arrangement of the mucosa (Khanna, 2004), significantly increasing the surface area of the intestine up to 3- and 6-fold depending on morphology and species (Bertin, 1958). One explanation for the physiological advantage of the spiral intestine in elasmobranchs is to maximize intestinal surface area in a limited body space that is dominated by a large lipid-dense liver (White, 1937). Digesta rotate along the longitudinal axis of the intestine, resulting in a slower evacuation time and further increasing absorptive capacity (Wetherbee et al., 1987). In cartilaginous fishes, the anatomy of the intestine has been well described in several species of shark and ray (Perrault, 1671; Parker, 1880; Khanna, 2004; Chatchavalvanich et al., 2006), and the spiral structures have been classified as spiral, ring or scroll type (White, 1937; Compagno et al., 2005; Leigh et al., 2017). However, we know little regarding the morphological and functional development of the intestine in elasmobranchs.

Unlike teleosts, cartilaginous fish are characterized by an extremely long developmental period *in ovo* or *in utero*. During early development, the richly vascularized yolk sac membrane contributes to absorption of nutrients by the developing embryos (Jollie and Jollie, 1967; Hamlett et al., 2011; Conrath and Musick, 2012). In viviparous species, embryos begin to use the gastrointestinal tract around the middle of

gestation. In southern stingray (*Dasyatis americana*), lipid-rich histotroph known as uterine milk is secreted by the uterine villi and embryos drink the milk *in utero* (Hamlett et al., 1996), and in the crocodile shark (*Pseudocarcharias kamoharai*), embryos ingest trophic eggs *in utero* (Fujita, 1981). Conversely, oviparous embryos depend entirely on yolk; however, yolk has been shown to be present within the lumen of the embryonic intestine during development (Lechenault et al., 1993; Haines et al., 2005). In the oviparous lesser spotted dogfish (*Scyliorhinus canicula*), yolk internalization occurred approximately after the first third of embryonic life (Ballard et al., 1993) and in the ovoviviparous spiny dogfish (*Squalus acanthias*) yolk was firstly observed in the intestinal lumen of 70 mm length embryo, and then fat droplets were observed in intestinal epithelial cells when the embryos were approximately 150 mm in length (Tewinkel, 1943). These findings raise the hypothesis that, even in oviparous elasmobranchs, the spiral intestine is formed and probably functional for nutrient absorption well before hatching (Tewinkel, 1943; Rodda and Seymour, 2008). In the present study, I focused on the timing of the ‘pre-hatching’ event in the onset of nutrient absorption by the embryonic intestine. Pre-hatching occurs in oviparous elasmobranchs at the end of the first third of development and is a period when the egg casing is known to open to the environment to facilitate embryonic respiration and growth (Mellinger et al., 1986; Diez and Davenport, 1987; Mellinger et al., 1989). This hypothesized developmental trajectory is distinctly different from oviparous ray-finned fishes that typically hatch before complete development of the gastrointestinal tract (Ng et al., 2005). Unravelling the functional development of the spiral intestine is thus important for our understanding of embryonic growth in cartilaginous fish.

In this chapter, I describe the functional development of the spiral intestine in the

oviparous cloudy catshark [*Scyliorhinus torazame* (Tanaka 1908)]. To this end, I investigated (1) formation of the spiral structure, esophageal opening and rectum opening, (2) formation of the secondary folds and microvilli that are related to nutrient absorption and (3) the timing of when yolk first appears in the embryonic intestine. In addition, as protein is a major diet component in fishes (Clements and Raubenheimer, 2006), and peptide transporter 1 (PepT1) and the neutral amino acid transporter Slc6a19 are known to contribute to nutrient absorption across the teleost intestine (Verri et al., 2003; Rønnestad et al., 2007; Terova et al., 2009; Rimoldi et al., 2015; Xu et al., 2016; Orozco et al., 2017, 2018), spatiotemporal expression was also examined on mRNAs encoding PepT1 and Slc6a19 in the intestine as functional gene expression markers. I provide evidence of a functional intestine in the oviparous cloudy catshark shortly after the pre-hatching event, suggesting that pre-hatching represents a physiological turning point in the embryonic development of oviparous cartilaginous fish.

MATERIALS AND METHODS

Animals

Spawned cloudy catshark (*S. torazame*) eggs collected from captive individuals were transported from Ibaraki Prefectural Oarai Aquarium to the Atmosphere and Ocean Research Institute at the University of Tokyo. They were kept in a 1000-liter tank with recirculating natural seawater under a constant photoperiod (12 h:12 h light:dark) at 16°C.

Embryos were staged according to the developmental stages established in lesser spotted dogfish, *S. canicula* (Ballard et al., 1993). Approximately 2 months post-fertilization at the end of the first third of development classified as the middle of developmental stage 31, the anterior part of the egg capsule opens and is known as the

‘pre-hatching’ or ‘eclosion’ (Ballard et al., 1993; Takagi et al., 2017). For the present experiment, I further subdivided this stage into two phases: the first half prior to pre-hatch (stage 31 early or 31E) and the second half following pre-hatch (stage 31 late or 31L). Occurrence of pre-hatching was confirmed by gentle pressure on the egg capsule; if intracapsular fluid was released, pre-hatching had occurred. Once hatched, juveniles were maintained under similar environmental conditions and fed a diet of chopped squid twice a week *ad libitum*. Embryos and juveniles were sampled throughout the year from 2015 to 2020. For sampling, both embryos and juveniles were anesthetized in 0.02% ethyl 3-aminobenzoate methanesulfonate (Sigma-Aldrich, St Louis, MO, USA). All animal experiments were conducted according to the Guidelines for Care and Use of Animals approved by the ethics committee of the University of Tokyo (A16-13).

Histological observation

The embryos from developmental stage 23 to 34 and juveniles were used for histological observation. For juveniles and embryos at developmental stages 32, 33 and 34, spiral intestines were dissected out, and were fixed in formalin with picric acid (saturated picric acid:formalin 3:1) at 4°C overnight. Spiral intestines of embryos earlier than stage 32 were fixed *in toto*. Fixed tissues were washed twice in 70% ethanol, dehydrated in graded concentrations of ethanol, cleared with benzene, and embedded in Paraplast (McCormick Scientific, Richmond, IL, USA). Serial sections were cut at 6 µm thickness and mounted onto glass slides (Matsunami Glass, Osaka, Japan). The sections were stained with hematoxylin and eosin. First, rehydrated tissue sections were treated with hematoxylin solution (Wako Pure Chemical Industries, Osaka, Japan) for 5 min and then washed in running tap water for 30 min. The sections were then stained with eosin

(Chroma Gesellschaft Schmid, Koengen, Germany) for 10 min, dehydrated through graded concentrations of ethanol, cleared with xylene, and mounted with Permount (Thermo Fisher Scientific, Waltham, MA, USA). Micrographs were obtained using a digital camera (DSRi1; Nikon, Tokyo, Japan). For three-dimensional (3D) reconstruction of the developing spiral intestine, sequential images of serial sections of the intestine were aligned using ImageJ (Fiji) (Schindelin et al., 2012) and the luminal space of intestine was filled using Photoshop (Adobe Systems, San Jose, CA, USA) before a 3D image was created using the 3D viewer of the ImageJ.

Scanning electron microscopy

For scanning electron microscopy observation, embryos of stages 27, 31E and 32, and juveniles, were examined. After dissection, spiral intestines of juveniles and embryos of stages 31E and 32 were pre-fixed in a fixative containing 2% paraformaldehyde and 2.5% glutaraldehyde in 0.05 mol l⁻¹ cacodylate buffer (CB, pH 7.4) (PG solution) for 3 min to harden the surface of the tissue. Tissue samples were cut using a razor blade and then fixed again in the PG solution for 2 h. After washing in 0.05 mol l⁻¹ CB for 5 min, samples were fixed in 1% osmium tetroxide for 1 h, washed in 0.05 mol l⁻¹ CB, dehydrated through a graded concentration of ethanol, immersed in butyl alcohol, and then dried in a vacuum freeze-dryer (JFD-300, JEOL Ltd, Tokyo, Japan) overnight. Tissues mounted on a sample holder were coated with platinum palladium using ion sputtering apparatus (E-1030, Hitachi High-Technologies Corporation, Tokyo, Japan) and were kept in a vacuum desiccator until use.

Due to the small size of the samples, the intestines from stage 27 embryos were cryosectioned to expose the gut cavity. The embryos were pre-fixed in the PG solution

for 30 min. After washing in 0.05 mol l⁻¹ CB, samples were immersed at 4°C in 10% glucose in 0.05 mol l⁻¹ CB for 10 min, 20% glucose for 30 min, 30% glucose for 40 min, optical cutting temperature (OCT) compound (Sakura Finetek Japan, Tokyo, Japan) for 30 min, and were then frozen in new OCT compound. Blocks were sliced at 5 µm using a cryostat until the intestinal lumen was exposed. After rinsing the residual OCT compound in 0.05 mol l⁻¹ CB and post-fixation in the PG solution for 2 h, tissues were processed for scanning electron microscopy as described above. All observations were made using a scanning electron microscope (s-4800, Hitachi High-Technologies Corporation) at a magnification of ×10,000 or ×20,000.

cDNA cloning

Complementary DNA cloning was performed as previously described in detail (Takagi et al., 2017) using whole spiral intestine dissected from juvenile cloudy catsharks. Total RNA was extracted using a commercially available kit (ISOGEN, Nippon Gene, Toyama, Japan). DNase-treated total RNA (1 µg) was reverse-transcribed to first-strand cDNA using an iScript cDNA Synthesis Kit (Bio-Rad, Hercules, CA, USA), following the manufacturer's instructions. Putative nucleotide sequences of mRNAs encoding catshark PepT1, Slc6a19 and β-actin were obtained by BLAST search on catshark transcriptome database Squalomix (<https://transcriptome.riken.jp/squalomix/>) (Hara et al., 2018). Partial cDNA fragments, which were amplified with Kapa Taq Extra DNA polymerase (Kapa Biosystems, Boston, MA, USA) and gene specific primer sets (Table 1), were ligated into pGEM-T Easy plasmid vector (Promega, Madison, WI, USA). The nucleotide sequences were determined by a DNA sequencer (ABI PRISM 3130, Life Technologies, Carlsbad, CA, USA).

Molecular phylogenetic analysis

Molecular phylogenetic analyses were conducted in MEGA7 (Kumar et al., 2016). The deduced amino acid sequences of catshark PepT1 and Slc6a19 were aligned with those of other animals using MUSCLE (Edgar, 2004). Molecular phylogenetic trees were inferred using the maximum likelihood method based on the Le_Gascuel_2008 model (Le and Gascuel, 2008). A discrete gamma distribution was used to model evolutionary rate differences among sites (five categories; +G parameter=0.4843). The bootstrap number was set to 1000.

Real-time quantitative PCR assay

Whole intestine was obtained from juveniles and embryos of stages 31E, 31L, 32, 33 and 34. Intestines were divided equally along the longitudinal axis into three parts: anterior, middle and posterior. Total RNA extraction and first-strand cDNA synthesis were conducted as described above. Quantitative PCR (qPCR) was performed using a 7900 HT Sequence Detection System (Life Technologies) with a Kapa SYBR Fast qPCR Kit (Kapa Biosystems), as previously described in detail (Hasegawa et al., 2016). The primers used for real-time qPCR were designed using PrimerQuest (<http://sg.idtdna.com/primerquest/home/index>) (Table 1). β -Actin mRNA was used as an internal control (Takagi et al., 2017). The plasmids containing cloned cDNA fragments were used as the known amounts of standard templates for absolute quantification in qPCR analyses.

***In situ* hybridization**

Digoxigenin (DIG)-labeled cRNA probes were synthesized from plasmids containing *PepT1* and *Slc6a19* coding sequences with DIG RNA Labeling Kit (Roche Applied Science, Mannheim, Germany). Tissue sections were mounted onto MAS-GP-coated glass slides (Matsunami Glass). Hybridization was conducted using a previously described protocol (Takabe et al., 2012). In brief, deparaffinized sections were treated with 5 $\mu\text{g ml}^{-1}$ proteinase K (Sigma-Aldrich) in PBS for 10 min at 37°C, immersed in pre-hybridization buffer (5×SSC: 0.75 mol l^{-1} NaCl and 83.3 mmol l^{-1} sodium citrate; pH 7.0; 50% formamide) at 58°C and hybridized with DIG-labeled cRNA probes in hybridization buffer (50% formamide, 5×SSC, 40 $\mu\text{g ml}^{-1}$ bovine calf thymus DNA) at 58°C for 40 h. Sections were then washed in 2×SSC for 30 min at room temperature, 2×SSC for 1 h at 65°C, and 0.1×SSC for 1 h at 65°C. After incubation with alkaline phosphatase-conjugated anti-DIG antibody (Roche) for 2 h at room temperature, signals were visualized with 4-nitro blue tetrazolium chloride (450 mg ml^{-1}) and X-phosphate/5-bromo-4-chloro-3-indolyl-phosphate (175 mg ml^{-1}) until sections were colored at 25°C in the dark. Sections were counterstained with Nuclear Fast Red (Vector Laboratories, Burlingame, CA, USA).

Statistical analysis

Data are expressed as means±s.e.m. Statistical analyses were conducted using Kyplot5.0 software (KyensLab Inc., Tokyo, Japan). Normality of data was checked by the Shapiro–Wilk test, followed by a Steel–Dwass or Tukey–Kramer multiple comparison test. P-values less than 0.05 were considered statistically significant.

RESULTS

Formation of spiral structure during development

Catshark embryos continued to develop inside the egg capsule for approximately 6 months prior to hatching (Fig. 1A–E). Histological investigation revealed that the spiral structure of intestine was fully formed prior to the pre-hatching period. At stage 23 of embryonic development (approximately one month post-fertilization), a straight intestinal tract was visible in the body cavity, which consisted of pseudostratified epithelium and mesenchyme (Fig. 1F). At stage 24, two separated intestinal lumens were observed in sagittal sections, showing the presence of one or two spiral turns (Fig. 1G, O). The number of turns continued to increase after stage 24 (Fig. 1H–J). At stage 31E, the number of spiral turns reached seven (Fig. 1K), which is equal to that of juveniles (Fig. 1L). The number of spiral turns was confirmed by 3D reconstruction using serial sections (Fig. 1M, N).

Yolk inflow into the intestine

At stage 23 in development, the yolk inside the external yolk sac (EYS) was black, and the embryo and the yolk stalk were transparent under transmitted light (Fig. 2A). At stage 24, sagittal sections revealed that the lumen of the yolk stalk was directly connected to the intestinal lumen (Fig. 2B, dotted line); however, a monolayer cellular membrane prevented yolk from flowing into the yolk stalk (Fig. 2C, arrows). At development stage 31E, yolk was not observed in the intestinal lumen (Fig. 2D); however, at stage 31L, white yolk was visible inside the yolk stalk (Fig. 2E, arrow) and eosinophilic yolk granules were observed in the intestine (Fig. 2F, arrow).

To determine the precise timing of yolk inflow into the embryonic intestine, I

further examined four individuals, the developmental stages of which were within 48 h after pre-hatching. Within 24 h after pre-hatching, one embryo had no yolk (Fig. 3A), while a second individual showed yolk granules inside the intestinal lumen (Fig. 3B). At 36–48 h after pre-hatching, two embryos had yolk granules inside the intestinal lumen (Fig. 3C, D), implying that yolk inflow into the intestine is likely to occur within 48 h after pre-hatching.

Formation of secondary folds and microvilli

Intestinal epithelium remained smooth without folding until pre-hatching (Fig. 4A, C), but in some individuals a slight protrusion of the intestinal epithelium was observed around the pre-hatching event, and obvious secondary folds were confirmed at stage 32 (Fig. 4E, arrows). The length of secondary folds gradually increased as the animal grew (Fig. 4E, G) and elongated secondary folds (Fig. 4G) and dense microvilli (Fig. 4H) were observed in the juvenile stage post-hatch. Microvillus formation began prior to secondary fold formation. Short microvilli were sparsely distributed in the stage 27 embryo (Fig. 4B, arrows). At stage 31E, microvilli covered the apical surface of the intestinal lumen (Fig. 4D) and both density and length of the microvilli increased in the juvenile stage (Fig. 4F, H).

Esophagus formation and opening

At stage 25, the esophagus was cylindrical in structure, filled with mesenchyme, and could be distinguished from the oral cavity and stomach (Fig. 5A, B). At stage 27, the luminal epithelium was differentiated, but the esophagus remained closed (Fig. 5C, D, arrowheads). By stage 33, the esophagus appeared closed by adhering the dorsal and

ventral sides of epithelia (Fig. 5E, F); however, this adhesion seemed not to be tight as some gaps were sparsely observed (Fig. 5F, arrows). The leaky but closed esophagus was observed also in the stage 34 embryo (Fig. 5H, arrows), and the closed portion became narrower longitudinally at this stage (Fig. 5G). We confirmed the opening of esophagus in fed juveniles (Fig. 5I, J).

Connection between spiral intestine and rectum

In the lesser spotted dogfish embryo, the rectum was shown to be closed until hatch (Mellinger et al., 1986, 1987). The serial transverse sections from the end of the spiral intestine to the rectum revealed that the lumen of the rectal canal, which forms the junction between the spiral intestine (Fig. 6C) and the rectum (Fig. 6E), was not fully developed and closed at stage 34 (Fig. 6D). In the hatched juvenile, formation of the rectal canal is completed, and the lumen was continuously formed from the spiral intestine to the rectum (Fig. 6H–J).

Spatiotemporal expression of *pept1* and *slc6a19* mRNAs

By searching the catshark transcriptome database, contigs showing high homology to *pept1* and *slc6a19* were found, and fragments of cDNAs encoding the catshark PepT1 and Slc6a19 were cloned. The accession numbers for the partial sequences of catshark *pept1* and *slc6a19* are LC507941 and LC507942, respectively. Maximum-likelihood analysis clearly shows that the catshark cDNAs belong to the vertebrate *pept1* (*slc15a1*) and *slc6a19* lineages, respectively (Fig. 7).

To evaluate nutrient absorptive function of embryonic intestine, expression of *pept1* and *slc6a19* mRNAs were examined by quantitative RT-PCR (qPCR) and *in situ*

hybridization (Figs 8–10). Low levels of *pept1* mRNA expression were detected at stages 31E and 31L (Fig. 8A). The expression levels significantly increased at stage 32, and thereafter remained high until the juvenile stage. *slc6a19* mRNA showed relatively low levels of expression during the embryonic period, and showed an increasing trend in expression in juveniles, although the changes between stages were statistically insignificant (Fig. 8B).

In the Mozambique tilapia, expression of *pept1* mRNA was shown to be rich in the anterior region of the intestine (Orozco et al., 2017), therefore I divided the spiral intestine into anterior, middle and posterior sections, and examined regional expression of *pept1* and *slc6a19* mRNA. *pept1* mRNA was uniformly distributed throughout the spiral intestine at and before stage 33, whereas from stage 34 onwards, expression of *pept1* mRNA was higher in the anterior region of the spiral intestine compared with the posterior region (Fig. 9A). Consistent with the results of qPCR, moderate signals were found in the entire region of intestine at stage 32 by *in situ* hybridization, and anteriorly biased signals were shown as developmental stage progressed (Fig. 10A, E, I). In the juvenile intestine, *pept1* mRNA showed intense signals in secondary folds constituting the first and second spiral turns (Fig. 10M) and moderate levels of *pept1* mRNA signals were observed in the epithelial cells of third to fifth spiral turns, but signals were faint in the posterior part of spiral intestine. The *pept1* mRNA signals were limited to the epithelial cells (Fig. 10B, F, J, N, arrowheads) and no expression was observed in submucosa.

Expression of *slc6a19* mRNA exhibited different patterns compared with *pept1* mRNA (Fig. 9B). At stage 32, mRNA levels of *slc6a19* in the anterior region were significantly higher compared with levels in the middle region. At stage 33, expression of

slc6a19 increased in the posterior region gradually and became significantly higher at stage 34. In the juvenile intestine, no difference was observed in *slc6a19* mRNA levels among the three regions. In agreement with the results of qPCR, the posterior-most region showed strong signals for *slc6a19* mRNA in the intestine of stage 34 embryos by *in situ* hybridization (Fig. 10K, arrow). Intense mRNA signals for *slc6a19* were shown in secondary folds throughout the juvenile intestine (Fig. 10O). The *slc6a19* mRNA signals were limited to the epithelial cells (Fig. 10D, H, L, P, arrowheads).

DISCUSSION

Here I demonstrated that spiral formation of the intestine was completed before pre-hatching in the cloudy catshark. I further revealed the presence of yolk in the intestine and expression of key nutrient transporters after pre-hatching. The present data suggest a switch from nutrient absorption via the yolk sac membrane to the intestine at the pre-hatching stage, which probably facilitates growth and development of the embryo inside the egg case.

Before the pre-hatching event: spiral intestine formation

The presence of a spiral intestine in developing embryos has been shown in several elasmobranch species including the round stingray (*Urobatis halleri*) (Babel, 1966), lesser spotted dogfish (Ballard et al., 1993) and tropical whitespotted bamboo shark (*Chiloscyllium plagiosum*) (Xu et al., 2015), but detailed spiral formation and functional relevance of the spiral intestine during embryonic development were unknown. Recently, detailed morphogenesis of the spiral intestine was reported in little skate (*Leucoraja erinacea*) using histology and micro-computed tomography scan (Theodosiou and Oppong, 2019). In the little skate, spiral formation began at stage 25, and the number of spiral turns reached 6.5 by stage 30. The number of spiral turns in embryos at the final developmental stage (stage 34; more than 14 weeks after stage 30) was eight, equivalent to that in adult individuals (Theodosiou and Oppong, 2019); however, the number of spiral turns at pre-hatching was not reported so it is unable to compare the exact timing of complete spiral formation between the cloudy catshark and little skate. Currently, the present study is the only study showing that spiral formation of the intestine is completed before pre-hatching in an elasmobranch. Further studies in other species are needed to

confirm whether our finding on the spiral formation is common in all cartilaginous fish.

In addition to spiral formation, microvillus formation was observed prior to pre-hatching. Short microvilli were sparsely distributed from stage 27, and microvilli covered the apical surface of the intestinal lumen at stage 31E, but intestinal epithelium remained smooth without folding until pre-hatching. In vertebrate intestines, it is generally accepted that three morphogenetic processes occur continuously to maximize surface area for nutrient absorption: (1) elongation of the gut tube, (2) microvilli formation, and (3) villi or secondary fold formation (Walton et al., 2016). In the zebrafish embryo, microvilli formation starts at 74 h post-fertilization (Wallace et al., 2005), whereas secondary folds formed around 96 h post-fertilization (Ng et al., 2005). Spiral formation in the cartilaginous fish intestine could be considered to be functionally equivalent to the elongation of gut tube in terms of an increase in luminal surface area. Therefore, it could be hypothesized that the described series of morphogenetic processes in the intestine may be common across jawed vertebrates.

After the pre-hatching event: nutritional absorption in the embryonic intestine

After the pre-hatching event, obvious secondary folds were found at stage 32, and the length of secondary folds, as well as the length and the density of microvilli, increased as the embryo grew. However, the most prominent change that occurred before and after the pre-hatching event was the presence of yolk in the embryonic intestine. Lechenault et al. (1993) reported that yolk transfer begins within 1 week of pre-hatching in the lesser spotted dogfish embryo. In my detailed observation, yolk transfer occurred within 48 h after pre-hatching. This variation may be due to a difference in incubation temperature of eggs (14°C in the previous study, and 16°C in the present study). Yolk transfer from the

EYS into the embryonic intestine is considered to be driven by cilia on the epithelium of EYS and the yolk stalk (Tewinkel, 1943); however, I identified a membrane preventing the movement of yolk into the intestine prior to pre-hatching (Lechenault and Mellinger, 1993). As the appearance of yolk occurs at pre-hatching, it can be assumed that the collapse of this membrane may be tightly regulated, possibly by signals released from the maturing intestine.

The present morphological findings are consistent with the previous histological observation showing that intestinal epithelial cells of elasmobranch embryos have the ability to absorb nutrients (Tewinkel, 1943; Okano et al., 1981; Teshima and Tomonaga, 2016). To further confirm nutrient absorption from the embryonic intestine, I examined expression of mRNAs encoding a peptide transporter (PepT1) and a neutral amino acid transporter (Slc6a19) as functional markers for nutrient absorption (Clements and Raubenheimer, 2006). The cDNA encoding PepT1 was previously cloned from the intestine of the bonnethead shark (*Sphyrna tiburo*) (Hart et al., 2016), and the present study showed the anterior-biased expression of *pept1* mRNA at stage 34 and juvenile spiral intestines of the cloudy catshark. This bias in expression is consistent with the distribution of *pept1* mRNAs in teleosts, such as European sea bass (*Dicentrarchus labrax*) (Terova et al., 2009), turbot (*Scophthalmus maximus*) (Xu et al., 2016) and tilapia (*Oreochromis mossambicus*) (Orozco et al., 2017). Zebrafish (*Danio rerio*) and grass carp (*Ctenopharyngodon idella*) show proximally restricted expression of *pept1* mRNA (Verri et al., 2003; Liu et al., 2013). These results imply that *pept1* mRNA in the intestine generally shows expression pattern in an anterior-biased fashion in fish. However, ubiquitous *pept1* mRNA expression has been shown in Atlantic cod (*Gadus morhua*) and killifish (*Fundulus heteroclitus macrolepidotus*) (Bucking and Schulte, 2012; Rønnestad

et al., 2007). In the present observations, *pept1* mRNA was initially expressed broadly throughout the entire intestine in early developmental stages, but the expression of *pept1* was restricted to the anterior intestine as development proceeded. A similar change in mRNA expression patterns (broader in larva) was also reported in the Japanese eel (*Anguilla japonica*) (Ahn et al., 2013). The expression pattern of *pept1* mRNA seems to be plastic depending on ontogeny, physiological condition or species.

Transporters contributing to amino acid absorption include a number of proteins that have distinct substrate specificities to neutral, basic and acidic amino acids (Bröer, 2008). In the present study, I selected a neutral amino acid transporter, Slc6a19, as the indicator of amino acid absorption due to the importance of neutral amino acids for maintaining body homeostasis (Sveier et al., 2001; Bröer et al., 2004; Craig and Moon, 2013; Belghit et al., 2014). Slc6a19 is a major neutral amino acid transporter expressed in the vertebrate intestine, and mutations in the *slc6a19* gene cause an inherited autosomal recessive defect known as Hartnup disorder (Kleta et al., 2004). Expression of *slc6a19* mRNA was found throughout the juvenile intestine in a pattern similar to that shown in European sea bass and turbot (Rimoldi et al., 2015; Xu et al., 2016). Aminopeptidase activity was shown to peak in the mid-spiral intestine of young adults or late juveniles of bonnethead sharks (Jhaveri et al., 2015), suggesting that peptides not absorbed in the anterior region may be digested by aminopeptidases and then absorbed in the form of free amino acids across the posterior region. In accordance with this notion, a remarkable expression of *slc6a19* mRNA was observed in the most posterior part of the intestine at stage 34. In the stage 34 embryo, the rectal canal that connects the spiral intestine to the rectum was closed, so the embryo will retain yolk digesta until hatching. This result was consistent with that reported in the lesser spotted dogfish, where the rectum of the embryo

was closed until hatching (Mellinger et al., 1986, 1987). It is possible that embryos may achieve maximum nutrient absorption from yolk digesta by up-regulating transport expression such as *Slc6a19* in the posterior region of spiral intestine. In Mozambique tilapia, the neutral amino acid transporter *slc6a18* mRNA was expressed in the posterior part of intestine to complete the absorption of neutral amino acids, supporting my notion (Orozco et al., 2018).

As yolk is directly transferred into the spiral intestine, it is assumed that anterior parts of the digestive tract, such as the esophagus and stomach, are not used during embryogenesis in the lecithotrophic cloudy catshark. The present histological observations revealed that the position equivalent to the esophagus was closed throughout the embryonic period. Consistent with our results, the digestive tract anterior to the spiral intestine appears to be inactive in the spiny dogfish embryo (Tewinkel, 1943). Immunoreactive signals for the gastric proton pump (H^+-K^+ -ATPase), which represents the functional marker of stomach activity, were first detected at stage 34 in lesser spotted dogfish embryos (Gonçalves et al., 2019). In contrast, embryos of many viviparous species drink or eat nutrient materials supplied from the mother (Fujita, 1981; Hamlett et al., 2011), meaning that their esophagus and stomach must be active even during the embryonic period. Collectively, cartilaginous fish embryos during the yolk-dependent period probably use only the posterior part of digestive tract, and may close a connection between spiral intestine and the oral cavity. This strategy may have an advantage to reduce the cost of innate immunity inside the digestive tract, as seawater, rich in microorganisms and pathogens, would not come into the digestive tract from the oral cavity. Indeed, it has been reported that gut-associated lymphomyeloid tissue develops before the onset of feeding in the lesser spotted dogfish embryo, which is much later compared with the

development of other immune systems (Lloyd-Evans, 1993).

Table 1. Primer sets used in the present study

Target		Amplicon (bp)
Primer sets for molecular cloning (5' to 3')		
<i>stpepT1</i>	Sense:	ATTCAGCCTGATCAGATGCAGA
	Antisense:	CCTGGAGCACTGATTTCATGTTG
<i>stslc6a19</i>	Sense:	TGGGCTGTGCTGTATGTATG
	Antisense:	AGAAAGTCCGAGGCAGAATAAC
<i>stactb</i>	Sense:	TGGTTGGTATGGGACAGAAAG
	Antisense:	ATCTGCTGGAAGGTGGAAAG
Primer sets for real-time qPCR assay (5' to 3')		
<i>stpepT1</i>	Sense:	ACCCTTCCTATCTTCCCTACC
	Antisense:	CCTCAGATGGTGCCAGTAAAT
<i>stslc6a19</i>	Sense:	TGGGCTGTGCTGTATGTATG
	Antisense:	TCTACCCTCCCTTATCTTGTCC
<i>stactb</i>	Sense:	CCTGGCATTGCAGACCGTAT
	Antisense:	GCAATGATCTTGATTTTCATGGTACT

Table 2. The accession numbers of genes used in the analysis

Gene name	Accession Number
<i>Anolis carolinensis</i> Slc6a19	XM_003219814.3
<i>Callorhinchus milii</i> B(0)AT1	XP_007887825
<i>Callorhinchus milii</i> Slc15a1	XM_007906296.1
<i>Chrysemy picta bellii</i> SLC15A1	XM_005303909.3
<i>Danio rerio</i> Slc15a1	AY300011.1
<i>Danio rerio</i> Slc6a19a.1	NM_001098178.1
<i>Gallus gallus</i> PEPT1	KF366603.1
<i>Gallus gallus</i> SLC6A19	XM_419056.6
<i>Homo sapiens</i> PepT2	NM_021082
<i>Homo sapiens</i> Slc6a18	NM_182632
<i>Homo sapiens</i> SLC6A19	NM_001003841.3
<i>Homo sapiens</i> solute carrier family 15, member 1	BC096329.3
<i>Latimeria chalumnae</i> SLC15A1	XM_005992304.1
<i>Latimeria chalumnae</i> SLC6A19	XM_014498080.1
<i>Lepisosteus oculatus</i> Slc15a1	XM_015363348.1
<i>Lepisosteus oculatus</i> Slc6a19	XM_006635651.2
<i>Meleagris gallopavo</i> PepT1	AY157977.1
<i>Meleagris gallopavo</i> SLC6A19	XM_010708607.2
<i>Mus musculus</i> Pept1	AF205540.1
<i>Mus musculus</i> Slc6a19	NM_028878.4
<i>Nanorana parkeri</i> SLC6A19	XM_018568852.1
<i>Oncorhynchus mykiss</i> SLC15A1	KY775396.1
<i>Pelodiscus sinensis</i> SLC6A19	XM_006137063.3
<i>Protothrops mucrosquamatus</i> SLC15A1	XM_015810135.1
<i>Rhinatrema bivittatum</i> SLC15A1	XM_029604484.1
<i>Rhincodon typus</i> B(0)AT1	XP_020367154
<i>Rhincodon typus</i> Slc15a1	XM_020512255.1
<i>Scyliorhinus torazame</i> Slc15a1	LC507941
<i>Scyliorhinus torazame</i> Slc6a19	LC507942
<i>Sphyrna tiburo</i> Slc15a1	KX216515.1
<i>Xenopus tropicalis</i> Slc15a1	XM_012957717.1
<i>Xenopus tropicalis</i> Slc6a19	NM_001127113.1

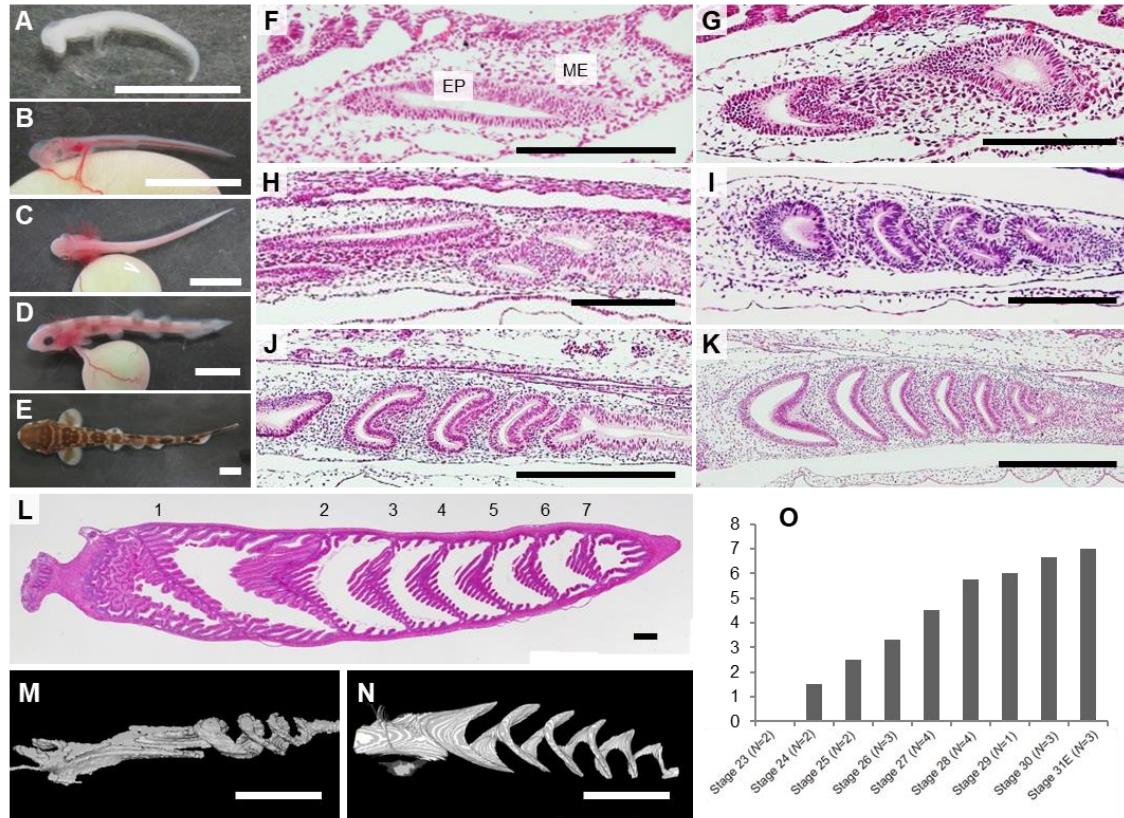


Figure 1. Developing spiral intestine of the cloudy catshark embryo. Representative developing embryos at stage 25 (A), stage 28 (B), stage 31L (C), stage 32 (D) and hatched fish (E) are shown. (F–L) Sections of developing spiral intestine stained with hematoxylin and eosin. Left side represents rostral region. (F) Stage 23. Pseudostratified epithelium (EP) composing a straight intestinal tract and mesenchyme (ME) were distinguishable. (G) Two separated luminal spaces indicating a spiral turn were observed in stage 24 embryo. (H–J) Spiral intestines of stages 25, 27 and 29, respectively. The numbers of turns increased along with the progress of development. (K) The number of spiral turns reached 7 at stage 31E, which is identical to that of juvenile intestine. (L) Juvenile. Numbers indicate number of spiral turns. (M, N) 3D reconstruction image of intestinal lumen of stage 27 (M) and stage 31E (N). (O) Developmental changes in the number of spiral turns. Scale bars: 1 cm (A–E), 250 μ m (F–I) and 500 μ m (J–N).

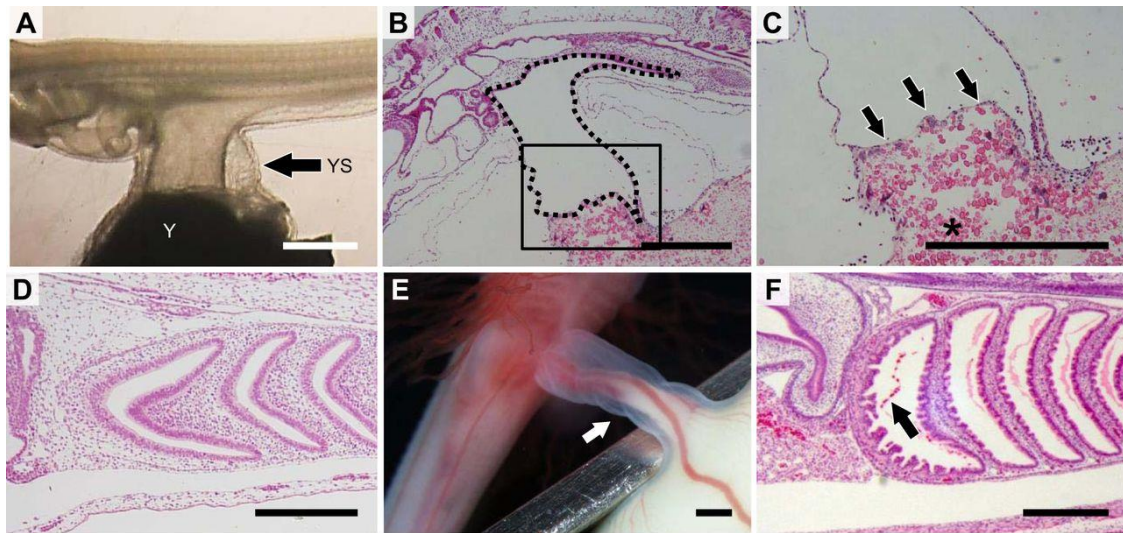


Figure 2. Yolk inflow into the intestine. (A) Stage 23 embryo (left side represents rostral region). The external yolk sac is connected to the embryo by the yolk stalk (YS); Y, yolk. (B) Hematoxylin and eosin staining section of stage 24 embryo. The dotted line indicates intestinal lumen directly connected to the YS. (C) Enlarged view of the boxed area in panel B; arrows indicate membranous lid preventing yolk (*) inflow into the embryonic intestine. (D) Sagittal section of stage 31E embryo intestine showing no eosinophilic yolk inside the intestine. (E) Light yellow-colored yolk was observed inside the YS in stage 31L embryo just after pre-hatching (arrow). (F) Section of the stage 31L embryo intestine. Eosinophilic yolk granules are visible in the intestinal lumen (arrow). Scale bars: 1 mm (A, B, D) and 500 μ m (C, E, F).

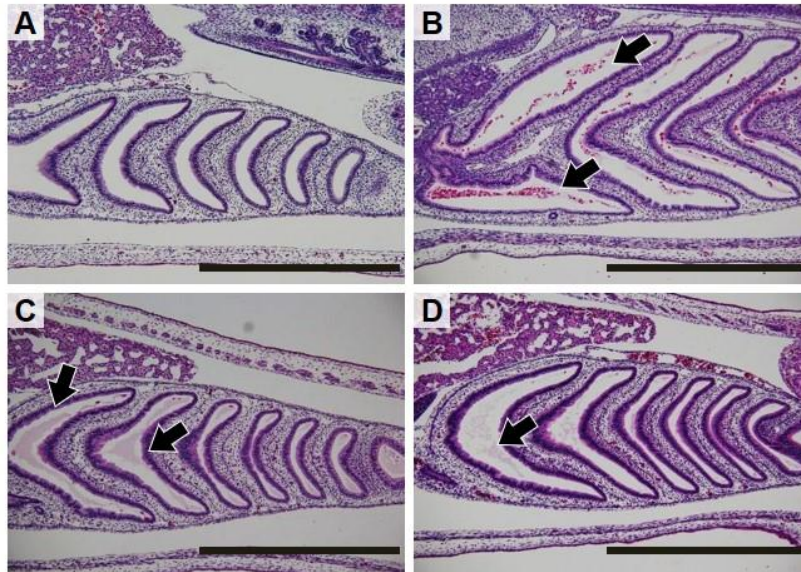


Figure 3. Yolk inflow occurred nearly pre hatching period. Sections of the intestine. (A) and (B) Sections of the intestine of stage 31L embryos within 24 hours after pre hatching. (C) and (D) Sections of the intestine of stage 31L embryos within 48 hours after pre hatching. Arrows indicate yolk inside the intestinal lumen. Bar = 1mm.

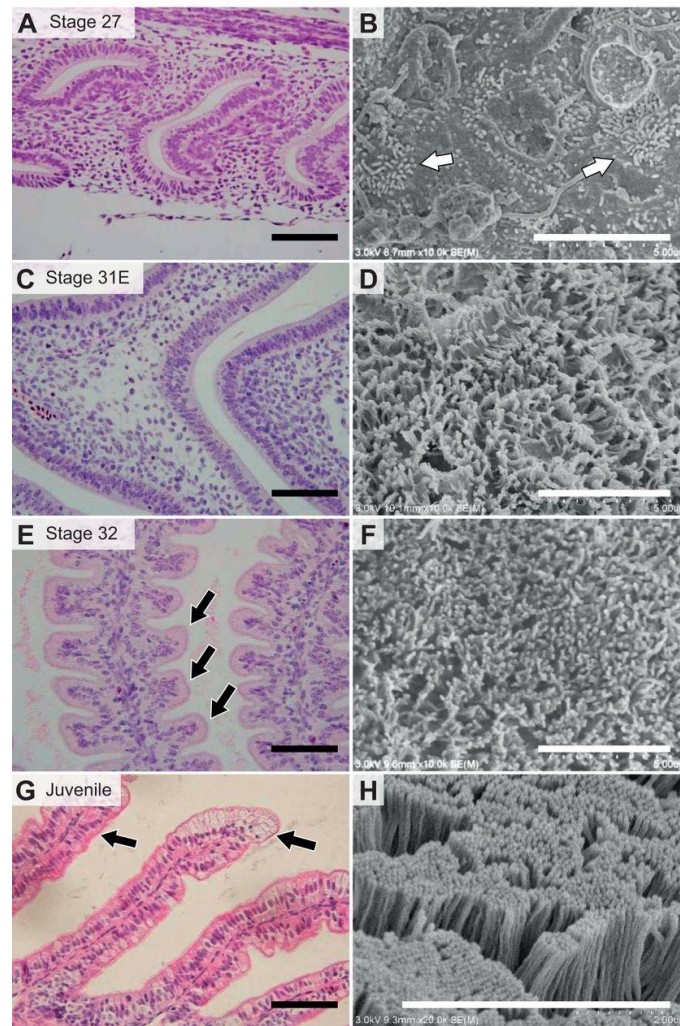


Figure 4. Formation of secondary folds and microvilli. (A, C, E, G) Sections of intestine of embryos and juveniles; black arrows indicate secondary folds. (B, D, F, H) Scanning electron micrographs of intestinal epithelium of embryos and juveniles; white arrows indicate emerging microvilli. Scale bars: 100 μm (A, C, E, G) and 5 μm (B, D, F, H).

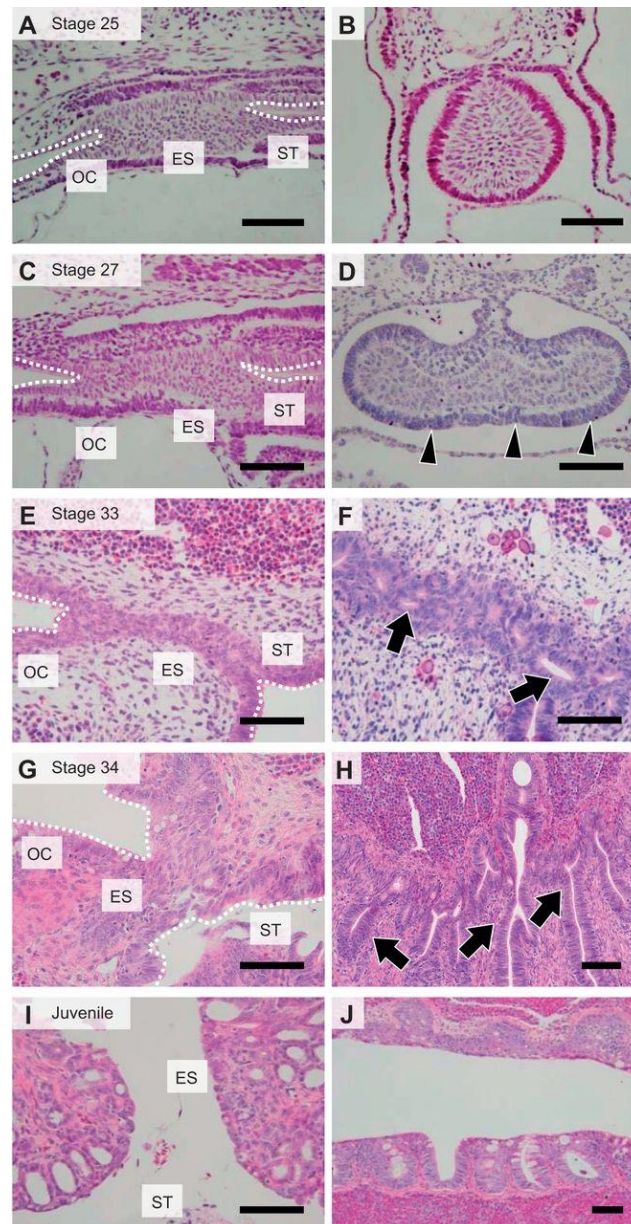


Figure 5. Opening of the esophagus. Sagittal (A, C, E, G, I) and cross-sections (B, D, F, H, J) of esophagus (ES) of embryos and juveniles. Left side represents rostral region in sagittal sections. Luminal surface of oral cavity (OC) and stomach (ST) are indicated by white dotted lines. Arrowheads indicate epithelium, while arrows represent gaps between dorsal and ventral sides of the esophagus. Scale bars, 100 μm.

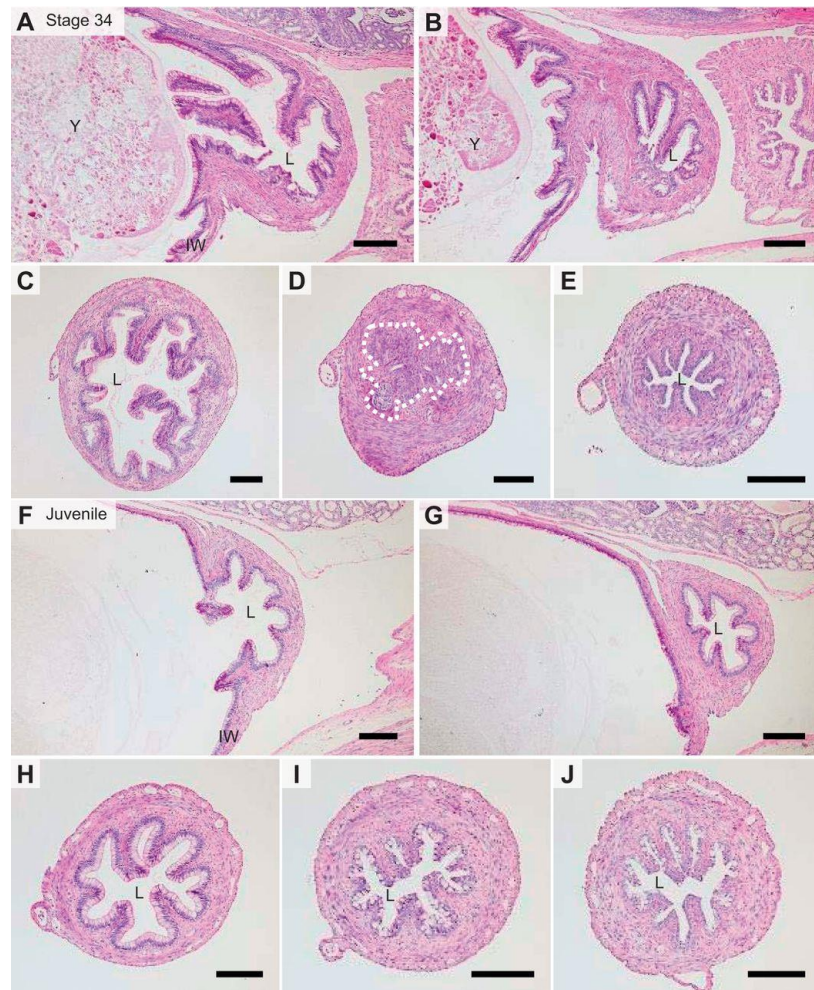


Figure 6. Connection between spiral intestine and rectum. Sagittal sections of posterior part of the spiral intestine (A, B, F, G) and transverse sections of the posterior-most portion of spiral intestine (C, H), the rectal canal (D, I) and the anterior-most portion of rectum (E, J). (A–E) Stage 34 embryo; (F–J) juvenile. The closed mucosal area in the rectal canal is indicated with a white dotted line. IW, intestinal wall; L, lumen; Y, yolk. Scale bars: 200 μm .

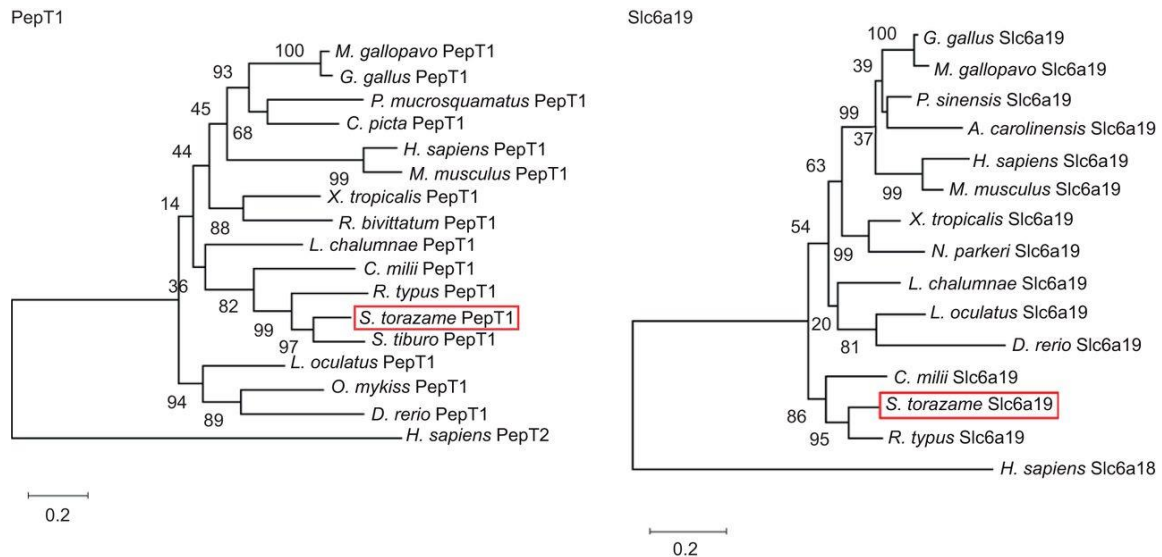


Figure 7. Molecular phylogenetic tree of vertebrate PepT1 and Slc6a19. Bootstrap probabilities are shown next to the branches. The accession numbers of genes used in the analysis are listed in Table 2. The cloudy catshark sequences are highlighted by the red boxes. *Homo sapiens* PepT2 and Slc6a18 were used as the outgroup.

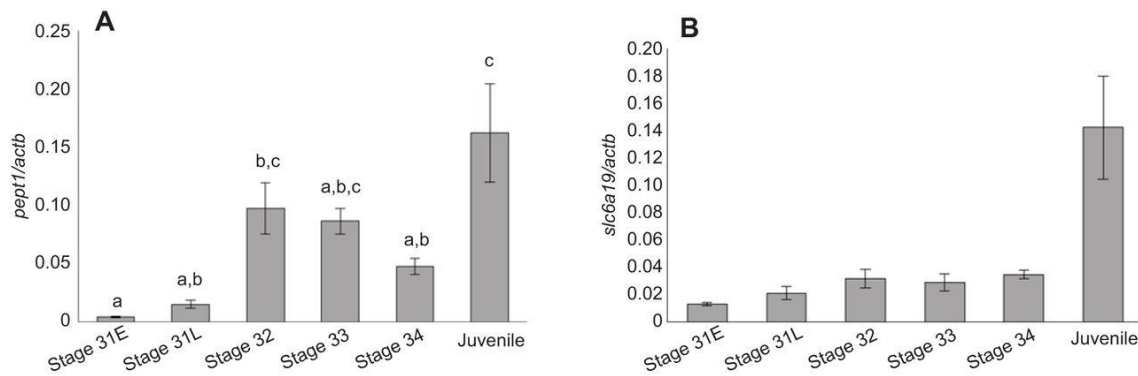


Figure 8. Changes in expression of *pept1* and *slc6a19* mRNAs in the developing spiral intestine. (A) *pept1*; (B) *slc6a19*. The mRNA levels are shown as the relative values to the mRNA levels of β -actin (*actb*). Data are presented as means \pm s.e.m. of N=5. Different lowercase letters indicate a significant difference ($P < 0.05$).

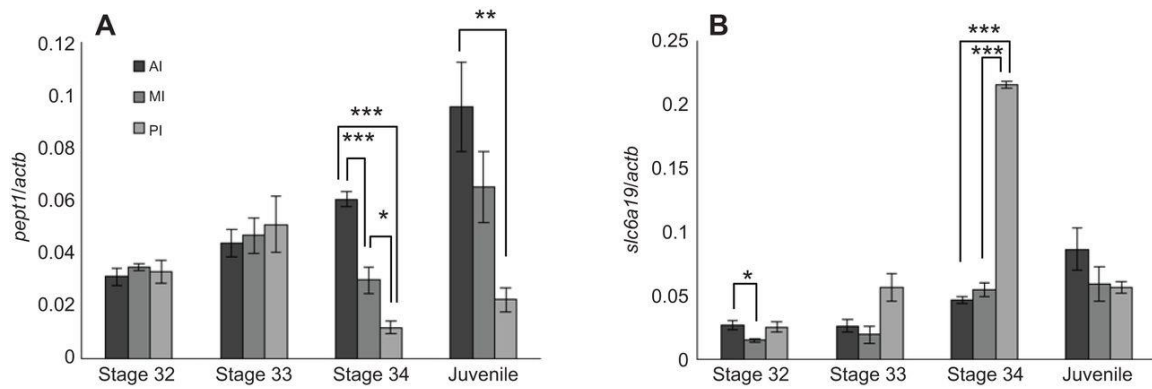


Figure 9. The mRNA levels of *pept1* and *slc6a19* in the developing spiral intestine. Developmental changes in the mRNA levels of *pept1* (A) and *slc6a19* (B) relative to those of β -actin (*actb*). Intestines were separated into the three segments, and mRNA levels in each segment were analysed. AI, anterior intestine; MI, middle intestine; PI, posterior intestine. Data are presented as means \pm s.e.m. of N=5. Statistically significant differences: *P<0.05, **P<0.01, ***P<0.001.

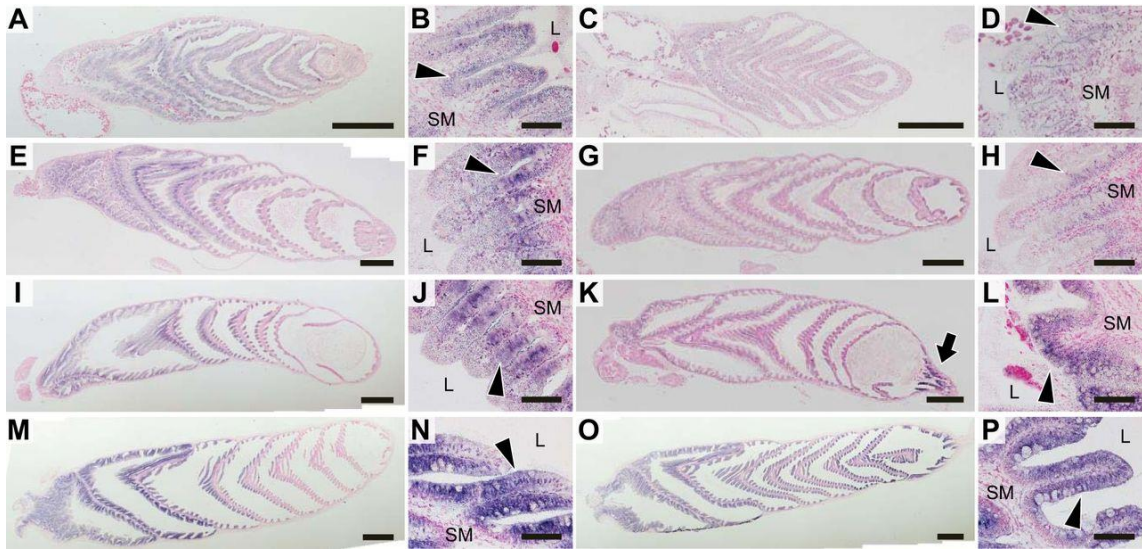


Figure 10. *In situ* hybridization analyses of *pept1* and *slc6a19* mRNA in the developing spiral intestine. The *pept1* (A, B, E, F, I, J, M, N) and *slc6a19* (C, D, G, H, K, L, O, P) mRNA signals in stage 32 (A–D), stage 33 (E–H), stage 34 (I–L) and juveniles (M–P). (B, D, F, H, J, L, N, P) Magnified views of A, C, E, G, I, K, M, O, respectively. Left side represents rostral region in sagittal sections. Sections were counterstained with Nuclear Fast Red. Arrow indicates signals in the posterior-most section of the intestine; arrowheads indicate signals in the epithelial cells. L, lumen; SM, submucosa. Scale bars, 1 mm (A, C, E, G, I, K, M, O) and 100 μ m (B, D, F, H, J, L, N, P).

Chapter 2

**Molecular investigation of nutrient absorption in the
yolk sac membrane and the intestine of the developing
embryo of cloudy catshark (*Scyliorhinus torazame*)**

ABSTRACT

As described in Chapter 1, the spiral intestine of cloudy catshark is completed at pre-hatching and function after pre-hatching to absorb nutrition from digested yolk. Therefore, I hypothesized that a functional shift of nutrition absorption should have occurred from the YSM to the intestine during embryonic development. To test this hypothesis, RNA-seq analysis was performed on YSM and the embryonic intestine, and candidate transcripts of genes involved in amino acid/peptide absorption, lipid absorption, and lysosomal digestion were identified. Subsequent qPCR analysis revealed that the expression of many identified genes such as *slc3a1*, *slc6a19*, *slc3a2*, *slc7a7* and *apoB* was increased in the intestine after the pre-hatching stage. Instead of a reciprocal decrease, expressions of many amino acid transporters, lipid absorption molecules, and lysosomal cathepsins were increased also in the YSM after the pre-hatching stage, which is in contrary to the above-mentioned hypothesis. Only a few transporters such as *slc7a3*, *slc7a6* and *slc38a5* and cathepsins were expressed at higher levels in early developmental stages before pre-hatching. These results imply that nutrient digestion and absorption in cloudy catshark embryo is more active in later developmental stages with both the intestine and YSM as nutrient absorptive surfaces. Embryonic body weight was markedly increased from stage 32, supporting the notion that active digestion and absorption of nutrients in the intestine and YSM for the rapid growth in later stages. The comprehensive analyses also suggest that the absorption mechanisms are different between the intestine and the YSM. While the intestine uptakes peptides/amino acids via specific transporters, the endodermal epithelial cells of YSM likely incorporate nutrient by endocytosis in addition to specific amino acid transporters.

INTRODUCTION

As mentioned in General Introduction, cartilaginous fish have many characteristics in their reproduction, such as, long developmental period and various reproductive modes including oviparity and viviparity (Musick and Ellis, 2005). In oviparous and yolk sac viviparous species, embryos depend on yolk as a sole nutrient source throughout development (Conrath and Musick, 2012). On the other hand, an embryo of matrotrophic species obtains additional nutrient inside uterus. For example, embryos ingest lipid-rich histotroph called uterine milk in the southern stingray (*Dasyatis americana*) (Hamlett et al., 1996), while embryos eat trophic eggs in the crocodile shark (*Pseudocarcharias kamoharai*) (Fujita, 1981). Embryos of placental viviparous species receive nutrition via placenta (Hamlett et al., 1985). These viviparous species also depend on yolk as a nutrient source in their early developmental period, implying that a shift of nutrition absorption site occurs from the extraembryonic yolk sac membrane to the embryonic gastrointestinal tract or placenta in viviparous species.

Oviparous embryos depend solely on yolk and do not ingest other nutrient such as uterine milk and trophic eggs. However, yolk in the external yolk sac was transferred into embryonic intestine in the middle of development in lesser spotted dogfish (*Scyliorhinus canicula*) (Ballard et al., 1993; Lechenault et al., 1993). In Chapter 1, I have established that the embryonic spiral intestine is completed and become functional at pre-hatching stage in cloudy catshark. I further found that yolk transfer to the embryonic intestine begins after pre-hatching, and the intestine absorbs nutrient thereafter (Chapter 1; Honda et al., 2020).

Yolk sac membrane (YSM) is a site for digestion and absorption of nutrient in the embryo before intestine becomes functional (Jollie and Jollie, 1967). Yolk sac membrane

consists of several layers including an ectodermal outer layer and an endodermal inner layer. Yolk platelets are degraded in the yolk syncytial layer and the resulting yolk granules are incorporated into the endodermal cells by endocytosis (Hamlett et al., 1987). Although lysosomal digestion of yolk droplet was suggested in the endodermal cells (Jollie and Jollie, 1967; Diez and Davenport, 1990), no apparent observation has supported the claim that yolk nutrient is transported into the vitelline circulation from the endodermal cells (Hamlett et al., 1987). Indeed, nutrient absorption function of YSM during embryonic development was controversial in literature. In the spiny dogfish (*Squalus acanthias*), nutrient absorption at the YSM was active in early period of development but became inactive at later stages (Jollie and Jollie, 1967). Meanwhile, nutrient absorptive function in the YSM became prominent in the late stage of development in the lesser spotted dogfish (Lechenault et al., 1993).

In this chapter, I aimed to clarify digestion and absorption function of yolk in YSM, and possible functional shift of nutrient absorption site from the YSM to the embryonic intestine in cloudy catshark. To this end, transcriptome analyses of embryonic intestine and YSM were conducted to identify candidate genes involved in amino acid and lipid absorption, because the main components of shark egg yolk are protein and lipid (Remme et al., 2005; Nishiguchi et al., 2017). Comprehensive search revealed that eighteen mRNAs encoding amino acid transporters were expressed either in the YSM or intestine. While transporters of both apical and basolateral localization were abundantly expressed in the intestine, the basolateral transporters were more prominent for amino acid transport in the YSM. In accord with the finding in Chapter 1, expression levels of many amino acid transporters and genes involved in lipid absorption increased after the pre-hatching in the embryonic intestine. Unexpectedly, many of candidate gene

expressions were also increased in the YSM at the stages after pre-hatching.

MATERIALS AND METHODS

Animals

Embryos and juveniles of catshark were maintained and sampled as described in Chapter 1. Embryonic body and the yolk sac were separated and then wet weight was measured when sampled. All animal experiments were conducted according to the Guidelines for Care and Use of Animals approved by the committee of The University of Tokyo (A16-13).

RNA-seq analysis

Intestine and YSM were used for RNA-seq analysis. The YSM of catshark can be divided into two layers: highly vascularized inner layer (YSMin), and ectodermal outer layer (YSMout). Two YSM layers (YSMin and YSMout) were separated and sampled from embryos of stages 31E and 32 (N=3). Intestines were sampled from stage 28 and stage 32 embryos (N=3). Total RNA was extracted from samples using a commercially available reagent (ISOGEN, Nippon Gene, Toyama, Japan). One μg (intestine) or 2 μg (YSM) of total RNA were treated with DNase I and purified with RNA Clean & Concentrator (Zymo Research, CA, USA). The concentration and quality of the extracted RNA were assessed using a Qubit 2.0 Fluorometer (Thermo Fisher Scientific, Waltham, MA, USA) and an Agilent 2100 Bioanalyzer (Agilent Technologies, Palo Alto, CA, USA), respectively. Libraries were prepared with 370 ng (intestine) or 1 μg (YSM) DNase I treated total RNA using a TruSeq total RNA sample preparation kit (Illumina, San Diego, CA, USA). Sequencing was performed on a Hiseq 1500 (Illumina) to obtain single end

80 bp reads (Tatsumi et al., 2015). The adaptor sequences and low-quality reads were discarded using Trim Galore! v0.3.1 (https://www.bioinformatics.babraham.ac.uk/projects/trim_galore/) and a fastq quality filter v0.10.0 (<https://www.bioinformatics.babraham.ac.uk/projects/fastqc/>).

De novo assembly was performed to obtain transcript contigs using Trinity version 2.4.0 (Grabherr et al., 2011). The contigs were annotated using ncbi-blast-2.6.0+ (McGinnis and Madden, 2004). The trimmed sequence reads were mapped to the contigs using bowtie2 v2.3.2 (Langmead and Salzberg, 2012) and the Transcripts Per Million (TPM) values were quantified using eXpress v1.5.1 (Cappé and Moulines, 2009).

cDNA cloning

Complementary DNA cloning was performed as described in Chapter 1, using gene specific primer sets (Table 3). Spiral intestine and pancreas were dissected from a juvenile cloudy catshark and YSMIn were obtained from embryos of stages 31E, 31L, 32 and 33. Total RNA extraction was conducted as described in Chapter 1. cDNA samples were prepared using a high-capacity cDNA reverse transcription kit (Life Technologies) following the manufacturer's instructions.

Amino acid transporters expressed in the intestine and the YSM were identified from transcriptome data. In addition, candidate transcripts of genes involved in lipid absorption and lysosomal digestion were selected as follows. Two major routes were known for lipid absorption: chylomicron and high-density lipoprotein (HDL) in the mammalian intestine (Hussain, 2014). Apolipoprotein B (ApoB) and apolipoprotein AI (ApoAI) are major components of chylomicron and HDL routes, respectively. In addition, microsomal triglyceride-transfer protein (MTP) and ATP-binding cassette sub-family A

member 1 (ABCA1) mediate the pathways of chylomicron and HDL, respectively (Hussain, 2014). In the YSM, lysosomal digestion of yolk droplet had been suggested in shark after the incorporation of yolk droplet by endocytosis (Jollie and Jollie, 1967; Hamlett et al., 1987; Diez and Davenport, 1990). As cathepsins are proteases localized in the lysosome (Stoka et al., 2016), cathepsins are defined as yolk protein digestion marker. Lysosomal acid lipase (LIPA) was selected as a lysosomal lipid digestion marker (Yadgary et al., 2014). Partial DNA sequences of candidate genes were obtained by cloning procedure described in Chapter 1. Putative nucleotide sequences of mRNAs were obtained from de novo assembled fasta file, or BLAST search on Squalomix (<https://transcriptome.riken.jp/squalomix/>) (Hara et al., 2018), and used for designing gene specific primers.

Molecular phylogenetic analysis

Molecular phylogenetic analyses were conducted in MEGA X (Kumar et al., 2018). The deduced amino acid sequence of catshark cathepsin L1 and cathepsin L2 were aligned with cathepsins of other animal using MUSCLE (Edgar, 2004). A model and parameters for making phylogenetic tree were same as Chapter 1.

Real-time quantitative PCR assay

Whole intestine was obtained from juveniles and embryos of stages 29, 30, 31E, 31L, 32, 33 and 34. As YSM could not be separated into YSM_{in} and YSM_{out} during early stages of development, whole YSM was sampled for stages 22-24 and 25-27. YSM_{in} was sampled from stages 28, 29, 30, 31E, 31L, 32, and 33. Pancreas was dissected out from juveniles and embryos of stages 31E, 31L, 32, 33, and 34. Total RNA extraction and first-

strand cDNA synthesis were conducted as described in Chapter 1. qPCR was performed using a 7900 HT Sequence Detection System (Life Technologies) with KAPA SYBR Fast qPCR Kit (Kapa Biosystems), as described in Chapter 1. The primers used for real-time qPCR were designed using PrimerQuest® program (IDT, Coralville, Iowa, USA) (<https://www.idtdna.com/SciTools>.) (Table 4).

***In situ* hybridization**

Intestine from embryos of stage 33 and YSM from stages 31E and 33 were used for *in situ* hybridization. Tissues were fixed in formalin with picric acid (saturated picric acid:formalin 3:1) at 4°C overnight. For the YSM, the whole yolk sac was fixed and then trimmed to remove the vast majority of yolk. Fixed tissues were processed for *in situ* hybridization as described in Chapter 1. Digoxigenin (DIG)-labeled cRNA probes were synthesized from plasmids containing cDNAs encoding partial slc43a2, ApoB, CTSL1 and CTSL2 as described in Chapter 1.

Transmission electron microscopy

For transmission electron microscopy observation, embryos of stage 29, 31E and 33 were examined. Inner layer of the YSM was dissected and fixed in fixative containing 2% paraformaldehyde and 2.5% glutaraldehyde in 0.05 mol l⁻¹ cacodylate buffer (CB, pH 7.4) for 2h. After washing in CB for 5 min, samples were fixed in 1% osmium tetroxide for 1 h. Fixed samples were dehydrated with a series of ethanol and propylene oxide, and then embedded in Epon812. Ultrathin sections were cut with a diamond knife and mounted on grids. The sections were stained with uranyl acetate and lead citrate, and were viewed on a transmission electron microscope (JEM-1400, JEOL Ltd) at 80kV.

Statistical analysis

Data are expressed as mean \pm s.e.m. Statistical analyses were conducted using Kyplot5.0 software (KyensLab Inc.). Normality of data was checked by Shapiro-Wilk test, followed by a Steel-Dwass or Tukey-Kramer's multiple comparison test. *P*-values less than 0.05 were considered statistically significant.

RESULTS

Expression profiles of amino acid transporters in the intestine and the YSM of the cloudy catshark embryo

Based on the knowledge of mammalian intestines (Bröer and Bröer, 2017), amino acid transporters were searched from transcriptomic data of the intestine and yolk sac membrane of catshark embryos. With the application of cut-off (contig with an TPM value of > 1 in either tissues), eighteen amino acid transporters, including *slc6a19* that was already examined in Chapter 1, were identified (Table. 5). Among them, *slc3a1* and *slc3a2* are ancillary subunits of *slc7* transporters so that they are not functional for amino acid absorption in themselves (Bröer and Fairweather, 2018). As transporters can be categorized in relation to their intracellular localization (Bröer, 2008), the identified transporters were classified into three groups as shown in Table 5: apical, basolateral and other (expressed in non-epithelial cells or localization was not determined) types. The TPM values of typical apical transporters (*slc3a1*, *slc6a19*, *slc7a9*) and basolateral transporters (*slc3a2*, *slc7a7*, *slc7a8*) were relatively high in the intestine of stage 32 embryos. On the other hand, TPM levels of apical transporters were low in YSM except for *slc7a9*. Basolateral and non-epithelial transporters such as *slc3a2*, *slc7a8*, *slc43a2*, and *slc7a2* have high TPM values (>10) in the YSM.

Changes in expression levels of amino acid transporters

To evaluate amino acid absorption activities, gene expressions of identified amino acid transporters were examined by quantitative RT-PCR (qPCR) in the intestine (from stage 29 to hatched juvenile) and the YSM (from stages 22 to 33) (Figs 11, 12, 13). After stage 28, YSM could be separated into inner and outer layers, and the inner layer of YSM

(YSMin) was used for measurement. On the other hand, as two layers of YSM could not be separated anatomically, whole YSM (YSMw) was used from stages 22 to 27.

Apical-type amino acid transporters (Fig. 11)

The mRNA levels of *slc3a1* were low before the pre-hatching stage (before 31E) in both the YSM and the intestine (Fig. 11A). The mRNA levels of *slc3a1* increased in the intestine from stage 32, and the increase became statistically significant at stage 34 and juveniles, whereas no changes were observed in the YSM. The mRNA levels of *slc6a19*, *slc7a9* and *pept1* have similar pattern of increased expression after pre-hatching in the intestine while they were expressed at low levels in the YSM (Fig. 11C, E, G). In the case of *slc7a9* in the YSM, moderate expression was detected from stages 29 to 33 compared to that of *slc6a19* and *pept1*. The mRNA levels of *slc6a20* and *slc36a1* were increased in the intestine after the pre-hatching stage (Fig. 11D, F). In the case of *slc6a20* and *slc36a1*, expression levels in the YSM also increased after pre-hatching. On the other hand, expression pattern of *slc6a18* was different from other transporters, where high expression was observed in the YSM before pre-hatching stage. The expression levels of *slc6a18* peaked at stage 29 and then decreased to stage 32, while expression levels remained low in the intestine throughout the embryonic development (Fig. 11B).

Basolateral-type amino acid transporters (Fig. 12)

Basolateral-type amino acid transporters shared a common expression pattern in the intestine; all the expression levels of transporters examined were increased after the pre-hatching stages (Fig. 12). Among them, the *slc3a2* mRNA levels continued to increase in the intestine until hatched juvenile (Fig. 12A). On the other hand, other basolateral transporters have peak expression levels at stage 33 and became lower at stage 34 (Fig. 12B-F). In the YSM, mRNA levels of *slc38a2* and *slc43a2* mRNAs showed

similar changes as those in the intestine, where the mRNA levels markedly increased after the pre-hatching stage (Fig. 12E, F). The levels of *slc7a7* and *slc7a8* mRNAs were slightly increased after the pre-hatching stage, but were constantly low in the YSM (Fig. 12C, D). Meanwhile, mRNAs of *slc3a2* and *slc7a6* were highly expressed in the YSM before the pre-hatching stage (Fig. 12A, B), which were expression profiles different from those of *slc7a7* and *slc7a8*. The mRNA levels of *slc3a2* remained high even after the pre-hatching, while the levels of *slc7a6* mRNA once decreased toward the pre-hatching stage, and somewhat increased at stage 33.

Other-type amino acid transporters (Fig. 13)

Amino acid transporters that subcellular localization is unknown or in non-epithelial cells are classified into this group in the present study (Fig. 13). In the intestine, *slc1a6* and *slc7a2* were not expressed or expressed constantly at low levels (Fig. 13A, B). On the other hand, mRNAs of *slc36a4*, *slc38a5* and *slc38a7* were increased after the pre-hatching stage and decreased at stage 34 (Fig. 13D-F), which is similar to the expression pattern of basolateral transporters. The mRNAs of this group exhibited distinct expression patterns in the YSM when compared to those of apical-type and basolateral-type amino acid transporters. The expression levels of *slc1a6*, *slc7a3*, *slc36a4*, *slc38a5* and *slc38a7* were high in the YSM of early developmental stages (stages 22-27), and were then decreased in the middle of development (stages 29-31E). The mRNA levels of these transporters increased again after the pre-hatching stage (Fig. 13A, C-F). Although the mRNA levels of *slc7a2* were low in the YSM of early stage embryos, the levels increased after the pre-hatching stage to the levels similar to those of *slc1a6*, *slc7a3*, *slc36a4*, *slc38a5* and *slc38a7* (Fig. 13).

Expression of candidate genes involved in lipid absorption

Candidate genes were identified from the RNA-seq data as markers of lipid absorption (Table. 6). The *apoB* expression in the YSM was increased from stage 29, and further increased after the pre-hatching stage (Fig. 14A). The *mtp* mRNA was also increased after the pre-hatching stage in the YSM, but no increase was observed before the pre-hatching period (Fig. 14B). In the intestine, expression of both *apoB* and *mtp* was largely increased after the pre-hatching stage. However, after reaching the peak level at stage 33, the levels of both mRNAs were decreased at stage 34 (Fig. 14A, B). The expression pattern of *abca1* mRNA resembled to that of *mtp* mRNA in both the intestine and the YSM (Fig. 14D). On the other hand, mRNA levels of *apoAI* were gradually increased from stage 28 to stage 31L in the YSM and then decreased (Fig. 14C). In the intestine, *apoAI* expression was conspicuously increased after the pre-hatching stage and peaked at stage 34.

Gene expression of lysosomal digestive enzymes

To evaluate protein digestion capacity in the YSM, putative cathepsin genes were searched in the transcriptomic data (Table. 7). We narrowed down the candidate genes by the TPM value (>100) and information in the previous studies: six genes were identified as cathepsin L1 (*ctsl1*), cathepsin L2 (*ctsl2*), cathepsin F1 (*ctsf1*), cathepsin F2 (*ctsf2*), cathepsin A (*ctsa*), and cathepsin B (*ctsb*). Cloudy catshark cathepsin F1, F2, L1 and L2 were named based on sequence similarity and the molecular phylogenetic analysis with other vertebrate cathepsin proteins (Fig. 15). Molecular phylogenetic tree showed that catshark cathepsin L1 was clustered in the clade with cathepsin L1 of other vertebrates. Catshark cathepsin L2 was branched outside of the clade of cathepsin L1, cathepsin K,

and cathepsin S. Catshark cathepsin F1 and cathepsin F2 were clustered in the clade of cathepsin F.

The *ctsa* mRNA level was low in early developmental stages and increased after the pre-hatching stage (Fig. 16A). The mRNA levels of *ctsb* and *ctsl1* were high in the early stages examined (stages 22-24), gradually decreased until stage 28, and then continuously increased until stage 33 (Fig. 16B, E). The *ctsl2* expression was increased at stage 29 and was maintained at high levels during the embryonic development (Fig. 16F). The levels of *ctsl2* mRNA were 10 to 1000 times higher than those of other cathepsin mRNAs. The *ctsf1* and *ctsf2* mRNAs increased at stage 28 and 29, maintained at high levels, and then decreased at stage 32 (Fig. 16C, D), an expression pattern that is different from those of other cathepsin genes. The expression of lysosomal lipid digestion marker *lipa* was detectable during the whole developmental period and increased after stage 32 (Fig. 16G).

Localization of *slc43a2* and *apoB* mRNAs in YSM and intestine

In situ hybridization was performed to localize *slc43a2* and *apoB* mRNAs in the YSM and intestine, because *slc43a2* and *apoB* were abundantly expressed in the YSM among amino acid transporters (Fig. 12F) and lipid transporting proteins (Fig. 14A), respectively. In the YSM, both *slc43a2* and *apoB* mRNA signals were detected in the endodermal cells that are in contact with yolk platelets (Fig. 17A-F). No signal was observed in hematopoietic cells or fibrous connective layer (Fig. 17D, E). In the intestine, *slc43a2* mRNA signals were detected in epithelial cells of stage 33 embryos (Fig. 17G). The *apoB* mRNA signals were also found in the epithelial cells, but signals were restricted just below the apical membrane of epithelial cells (Fig. 17H).

Localization of *ctsl1* and *ctsl2* mRNAs in the YSM

Among the cathepsin mRNAs, localization of *ctsl1* and *ctsl2* mRNAs were investigated (Fig. 18). The *ctsl1* mRNA signals were detected in the endodermal cells (Fig. 18A, D). On the other hand, *ctsl2* mRNA signals were observed in the hematopoietic cells (Fig. 18B, E). No signals for *ctsl2* mRNA were observed in endodermal cells or blood cells.

Endocytosis of yolk droplets into the endodermal cells

To investigate endocytosis of yolk granules, TEM observation was performed (Fig. 19). Small yolk granules enveloped in a membrane structure were observed in the YSL near the boundary with the endodermal cell at stage 29 (Fig. 19B, arrows). Both the number of membrane packets containing yolk droplets and the density of yolk droplets inside the packets increased at stage 31E (Fig. 19D, arrows). Membrane packets containing yolk granules were also abundant at stage 33 (Fig. 19F, arrows).

Expression levels of mRNAs encoding pancreatic digestive enzymes

In order to investigate digestive capacity of the embryonic pancreas, mRNA levels of three digestive enzymes were quantified: trypsin, bile salt-activated lipase (BSDL), and phospholipase A2 (*pla2g1b*) (Fig. 20). The *trypsin* and *pla2g1b* mRNA levels were low in stages 31E and 31L, and then increased after stage 32 until hatched juvenile stage (Fig. 20A, B). The *bsdl* mRNA expression was low during the entire embryonic period, although a slight increase was observed at stage 34 (Fig. 20C). The *bsdl* mRNA levels were conspicuously increased in hatched juveniles.

Developmental changes in the wet weight of embryo and yolk sac

To determine when the growth is active, wet weight of the embryonic body and the yolk sac were measured (Fig. 21). The weight of the body and the YSM did not change from stages 27 to stage 31E, before pre-hatching. From stage 32, the body weight increased while the yolk sac weight decreased significantly.

DISCUSSION

In this chapter, expression of genes involved in nutrient digestion and absorption was examined in the YSM and intestine during embryonic development of cloudy catshark. I have determined that the yolk is directed to the embryonic intestine at pre-hatching, which coincide the beginning of a functional intestine for nutrient absorption (Chapter 1; Honda et al., 2020). Therefore, I focused on a possible shift of nutrition absorption site from the extraembryonic yolk sac membrane to the embryonic intestine. Indeed, expression of genes encoding for nutrient transporters and digestion enzymes increased in the embryonic intestine after the pre-hatching stage. However, the present study also revealed an increase in mRNA levels of amino acid transporters, lipid absorption molecules, and lysosomal digestive enzymes in the YSM after the pre-hatching stage. The combined observation suggested that the embryo obtains nutrient from both YSM and intestine, allowing an increased growth rate after the pre-hatching stage.

Previous reports suggested that the YSM contributes to nutrient absorption during the early stages of development, while the embryonic intestine plays the role in absorbing nutrients during the later embryonic periods in oviparous and aplacental viviparous cartilaginous fishes (Tewinkel, 1943; Jollie and Jollie, 1967). This notion was supported by the results of embryonic cloudy catshark, where yolk in the extraembryonic yolk sac is transferred into the embryonic intestine after the pre-hatching period (Chapter 1; Honda et al., 2020). However, most amino acid transporters and lipid absorption molecules in the YSM were expressed at low levels during the early developmental stages, and their expressions were increased after the pre-hatching stage (Figs 11-14, 16, 22). In addition, endocytosis of yolk droplets in the YSM seemed to be active in later stages (Fig. 19).

These results imply that activity of nutrient absorption is not high in the YSM before the pre-hatching stage. The present results coincided with the results by Lechenault and colleagues (1993), where the digestion and absorption in the YSM were active in stage 33 embryo of lesser spotted dogfish. On the other hand, in yolk sac viviparous spiny dogfish, YSM was not active in later stages of embryonic development (Jollie and Jollie, 1967). Activity of nutrient absorption in the YSM may vary depending on species and/or reproductive modes. In the cloudy catshark embryo, embryonic body weight markedly increased from stage 32 (Fig. 21). High nutrient absorption from both intestine and YSM may contribute to the rapid growth after the pre-hatching stage. Different yolk consumption rate during embryonic period (slow in early period and fast in later period) is also known in avian species such as Japanese quail (*Coturnix japonica*) (Yoshizaki et al., 2004) and teleost species such as European plaice (*Pleuronectes platessa*) (Skjærven et al., 2003).

In addition to amino acid transporters and apolipoproteins expressed in the embryonic intestine, expression of digestive enzymes such as trypsin and phospholipase A2 in the pancreas were increased after the pre-hatching stage. These results further support that the embryonic intestine actively digest protein and phospholipid to facilitate absorption. These findings are in agreement with the results in spiny dogfish, where zymogen granules were observed in the pancreas of 65 mm embryos (presumably correspond to stage 32) (Tewinkel, 1943). On the other hand, expression of cholesterol esterase (*bsdl*) in the pancreas was maintained at the low level during embryonic development, but the expression became high in hatched juveniles feeding on squid. These results are probably related to the composition of egg yolk. For example, egg yolk of lesser spotted dogfish contains approximately 20% lipid dry weight. The lipid is

composed of 30-60% phospholipid, while cholesterol accounts for only 5% of the total lipid in the egg yolk (Wrisez et al., 1993).

I observed an intriguing finding where the expressions of many genes responsible for nutrient absorption were decreased in the intestine at stage 34. This pattern was common in many basolateral-type and other-type amino acid transporters, and lipid absorption molecules (Figs 12-14). Contrary to this decrease, four out of seven apical-type amino acid transporters were continuously expressed at increasing rate until juveniles (Fig. 11), implying that nutrients are actively absorbed into epithelial cells, but transfer of amino acids into blood vessels are not remarkable at the peri-hatching period (stage 34). Since ApoB and MTP are essential for chylomicron assembly (Wang et al., 2013; Hussain, 2014), the basolateral transport of endocytosed lipids would also be lowered in the intestinal epithelial cells. Teshima and Tomonaga (2016) observed that yolk like substance is accumulated in the intestinal epithelial cells of larger embryos of aplacental viviparity freshwater stingrays (*Disceus thayeri*, *Potamotrygon magdalenae*, and *Potamotrygon motoro*). Catshark embryos of stage 34 had transferred all yolk from the external yolk sac into the intestine and the internal yolk sac, thus the stored yolk in the intestine could be an immediate nutrient reserve for the juvenile after hatch.

When the gene expression profiles were compared between apical-type and basolateral-type amino acid/peptide transporters (Fig. 22A), both types of transporters were abundantly expressed in the embryonic intestine (such as *slc3a1*, *slc6a19*, *slc6a20*, *slc7a9*, and *pept1* are apical-type while *slc3a2*, *slc7a6*, *slc7a7*, *slc7a8*, and *slc38a2* are basolateral-type). These transporters were also known as major transporters expressed in the mammalian intestinal epithelial cells (Bröer, 2008; Bröer and Fairweather, 2018), implying that the nutrient absorption mechanisms are relatively conserved between

cartilaginous fishes and mammals. On the other hand, the number of apical-type transporters (*slc3a1*, *slc6a19*, and *pept1*) were less in the YSM than that identified in the intestine. In other words, the basolateral-type amino acid transporters were expressed abundantly both in the intestine and YSM, while expressions of the apical-type transporters were more prominent in the intestine. In particular, PepT1 and Slc6a19 are transporters having high capacity and broad substrate specificity including di- and tri-peptides (PepT1) and all neutral amino acids (Slc6a19) (Bröer et al., 2004; Daniel, 2004). These results suggest that an alternative mechanism should be present for the absorption of amino acids/peptides from yolk. Indeed, membrane packets containing yolk droplets were observed in the YSM (Fig. 19), suggesting that endocytosis from yolk syncytial layer to the endodermal cell occurred. Similar phenomenon was reported in Atlantic sharpnose shark (*Rhizoprionodon terraenovae*) that yolk platelets were degraded in the yolk syncytial layer and the resulting yolk granules were incorporated into endodermal cells by endocytosis (Hamlett et al., 1987). In the YSM of cloudy catshark embryo, amino acids/peptides are likely transported by both endocytosis and amino acid transporters into the endodermal cells, while the incorporated amino acids are likely to be transferred to the blood vessels (Fig. 23). Among the basolateral-type transporters, *slc43a2* was the most abundantly expressed transporter in the YSM, which is important for the intrauterine growth of embryos in the mammalian placenta (Cleal et al., 2011; Guetg et al., 2015). Therefore, it is likely that *slc43a2* is an important amino acid transporter commonly expressed in the extraembryonic tissues.

Currently, distribution and function of “other”-type amino acid transporters remain to be clarified. In cloudy catshark embryos, the other-type transporters were highly expressed in the YSM (Fig. 22A). The prominent feature of this category was their

abundant expression in the YSM at early developmental stages (stages 22-27). The expression of *slc7a3* and *slc38a5* was at higher levels among this category. In the mammalian hepatocytes, Slc38a5 uptakes glutamine for urea synthesis (Bhutia and Ganapathy, 2016). On the other hand, Slc7a3 absorbs arginine and was expressed in most peripheral tissues in mouse (Closs et al., 2006). Glutamine and arginine are required for urea synthesis in elasmobranch, which actively produce urea for osmoregulation in marine environment (Ballantyne, 1997, 2015). Ornithine urea cycle enzymes are expressed in the YSM of early developmental embryos in cloudy catshark, implying that the YSM produces urea for osmoregulation of embryo (Takagi et al., 2017). Taken together, Slc7a3 and Slc38a5 could have a role in supplying substrates for urea synthesis in catshark embryos. On the other hand, expression of *slc7a2* was at low levels during early stages and was increased from stage 31E, just before the pre-hatching stage. Slc7a2 was reported to have a role in providing the arginine for nitric oxide synthesis in macrophage (Closs et al., 2000). If the Slc7a2 has a similar role in cartilaginous fish, the increase in expression may be related to an increase of immunity before hatching.

Cathepsins are proteases localized in the lysosome. Four (*ctsa*, *ctsb*, *ctsl1*, *ctsl2*) out of six cathepsins examined have increased expression along the development, particularly after the pre-hatching stage (Figs. 16 and 22C). The high expressions levels of cathepsins in late developmental stages are consistent with the results of basolateral-type amino acid transporters, implying that active digestion and transfer of amino acids to the blood vessels. Yolk digestion by CTSA in sea bass (*Dicentrarchus labrax*) (Carnevali et al., 2001) and by CTSB in killifish (*Fundulus heteroclitus*) (Tingaud-Sequeira et al., 2011) was reported, supporting their roles in obtaining nutrient from yolk storage. In addition, CTSL is reported to be involved in yolk protein digestion in rainbow

trout (*Oncorhynchus mykiss*) (Sire et al., 1994), sea bass (Carnevali et al., 2001), zebrafish (*Danio rerio*) (Tingaud-Sequeira and Cerdà, 2007), and killifish (Tingaud-Sequeira et al., 2011). Therefore, these cathepsins are possible proteases for yolk digestion in cloudy catshark embryo. In this study, as *ctsl1* mRNA was detected in the endodermal cells, yolk protein digestion likely occurs in the endodermal cells. On the other hand, *ctsl2* mRNA was detected in the hematopoietic cells, implying that *ctsl2* may have different functions other than nutrient digestion (Fig. 18). Cathepsin K may be involved in hematopoiesis because the number of hematopoietic stem cells increased in cathepsin K-knockout mouse (Jacome-Galarza et al., 2014). Catshark CTSL2 clustered in the clades with CTSK, CTSS and CTSL1 (Fig. 15). It is assumed that catshark CTSL2 may possess similar characteristics as of CTSK, which may play a role in the hematopoietic process of catshark YSM. On the other hand, *ctsf1* and *ctsf2* exhibited different expression pattern when compared to other cathepsins. The *ctsf* mRNA levels increased in the gill when the fish was exposed to bacteria, suggesting that CTSF has a role on immune responses in olive flounder (*Paralichthys olivaceus*) (Kim et al., 2008; Ahn et al., 2009) and turbot (*Scophthalmus maximus* L.) (Gao et al., 2017). Therefore, CTSF in the YSM of cloudy catshark may be involved in the innate immunity starting from pre-hatching stage.

In summary, expression of genes related to protein/lipid digestion and absorption increased levels after pre-hatching in both the intestine and the YSM. The high mRNA levels in the YSM of later stages were unanticipated, because egg yolk begin to flow into the embryonic intestine, and the YSM gradually shrinks toward stage 34. Therefore, nutrient absorption in cloudy catshark embryo is more active among late developmental stages, when both the intestine and the YSM were used as nutrient absorptive surfaces. A

marked increase in embryonic body weight from stage 32 supports the notion.

Table 3. Primer sets for molecular cloning used in the present chapter

Target		Amplicon (bp)	
Primer sets for molecular cloning (5' to 3')			
stSlc1a6	Sense:	CTACATCGGGAGGGAAAGATTG	590
	Antisense:	GGATTCTTGCGGGTGACTATAA	
stSlc3a1	Sense:	CAAGTGGGCCTACACGATATT	631
	Antisense:	GTTCACGGTACAGGGTCAAA	
stSlc3a2	Sense:	GCAGGAGTGGTTTGGGATTA	810
	Antisense:	ACGAGGAATCGGTCACTTTG	
stSlc6a18	Sense:	GGAGACCAAAGTGGGACAATAA	891
	Antisense:	AGCCAAGCAAGGAGAAGATG	
stSlc6a20	Sense:	CCTTGGCTCTTCTGGTGATAG	796
	Antisense:	GACCAGAGGGAATGATGGTAAA	
stSlc7a2	Sense:	CGCTGTTTGTCCACCATAGA	874
	Antisense:	TTGCATCCAGCAGGTAGTAAG	
stSlc7a3	Sense:	TGTGGCCTACTTTGGTGTATC	561
	Antisense:	GGAGATTGTTTCGTCTGGGTAAA	
stSlc7a6	Sense:	GCCTACATACTGGAGTCCTTTG	503
	Antisense:	CACGTCACAACAGGCATAGA	
stSlc7a7	Sense:	CTTGACCAACGTGGCCTATTA	835
	Antisense:	GGGATGAAAGCCTAACCTGTAG	
stSlc7a8	Sense:	CATCATCATGGGCTTTGTTTCAG	816
	Antisense:	GGCTTGTTGCTCCAGTAGAT	
stSlc7a9	Sense:	ACCCTCTTCCTTTGCGATAAT	921
	Antisense:	GGAGCGAGAACCAAGTAGATAG	
stSlc36a1	Sense:	GCTCTTCGCCTGATGTTTCT	920
	Antisense:	CGCTGGCAAATTGAGTGTTATG	
stSlc36a4	Sense:	GACGAAGAGGGTATCTCGTTTAC	618
	Antisense:	GTGAGGCATGTCCCTCATAAT	
stSlc38a2	Sense:	GCTGGCGATAACCATGACTATAA	946
	Antisense:	TCAGAATTGGCACAGCATAGA	
stSlc38a5	Sense:	GGCCTTCCTTGCCTCATTTA	754
	Antisense:	CGATCATTGACAGGTGGGTATC	
stSlc38a7	Sense:	CAGTCAAAGGCCACTGGTATAG	521
	Antisense:	GTGAAGGATTGGGTAGGATGTG	
stSlc43a2	Sense:	ATCGCCATGGACAAGTATGG	782
	Antisense:	ACTCCGAAGATTGAGGAGTAGA	

stApoA1	Sense:	CCTCTGTCCGATGAGATTCAAG	950
	Antisense:	GTCCTGGTGATCGGCAAATA	
stApoB	Sense:	ACACCTCTGCTAAGGGATCTA	905
	Antisense:	GCTGAGAACTTCCTGCATTTG	
stABCA1	Sense:	AACATCACCACCTCCATCATC	585
	Antisense:	CTGCTCCACCTCCATCTTTAC	
stMTP	Sense:	CTGGGTGCTGTTGATCCTAAT	932
	Antisense:	TCTTGGGCTCCAGTTCTTTC	
stCTSA	Sense:	ACCCAGCTTTAGGCAGTATTC	850
	Antisense:	GTGGCTCTGTTGTGTCTCTT	
stCTSB	Sense:	CTCTCAGGACATGGTCAACTTC	570
	Antisense:	GTGTAACCAGCCTCACATCTC	
stCTSF1	Sense:	GAGGAGGACAGGTTCCAAATC	771
	Antisense:	GGAGTTCTTCACGGTCCAATAA	
stCTSF2	Sense:	CGGTCCCAGTTCAAGGATTT	291
	Antisense:	CTTGCTGGGTATGGACAGATTAG	
stCTSL1	Sense:	GCTCCACTAACTCTCCTCAAAC	598
	Antisense:	GGTCCATCAGTCCACCATTAC	
stCTSL2	Sense:	CCTCCCAATCGAAGCTGATAAC	586
	Antisense:	GTGGTTCTTGCACCGACTATAC	
stLIPA	Sense:	GGAGGCGTTCTGGACATTTA	799
	Antisense:	CGCAGCTCACTCATACTTTCT	
stTrypsin	Sense:	AAACACCCAGCCTACAACCTAC	524
	Antisense:	GGACACGGAGCTGAGATTTATT	
stBSDL	Sense:	CACCAGGTAACCAAGGTCTATG	760
	Antisense:	CCCTGAGTATGTCGAGAATGAAG	
stPla2g1b	Sense:	AAATGCGATCCTTGGTCCTC	436
	Antisense:	CAACAGTAACGATCCCTGTCAA	

Table 4. Primer sets for real-time qPCR assay used in the present chapter

Target		Amplicon (bp)	
Primer sets for real-time qPCR assay (5' to 3')			
stSlc1a6	Sense:	CGTCGTCACCCATCAATCTTAC	102
	Antisense:	CCTCCTCATCAAGCATCAACTC	
stSlc3a1	Sense:	CTTGGA ACTCCGACCACTTAC	113
	Antisense:	TCTCGATTGCTGTTGGATCA	
stSlc3a2	Sense:	GCTTCATCGCTGGAACAGTA	104
	Antisense:	TCCTCCAGTCCAATCTCATCT	
stSlc6a18	Sense:	GATGCAGCCACCCAGATATT	97
	Antisense:	CCACCTCGCAGTTGTTCTT	
stSlc6a20	Sense:	GGCTCTTCTGGTGATAGTTCTG	103
	Antisense:	TGGCTTGTGTCCTATCATCTTT	
stSlc7a2	Sense:	(same with the cloning primer)	82
	Antisense:	CCTCACCAGCTAGAACGTAAAC	
stSlc7a3	Sense:	GTGGCCTACTTTGGTGTATCT	107
	Antisense:	GGTCCCAGCCAACATACT	
stSlc7a6	Sense:	ACTCCGGTTGGGATACTCTTA	100
	Antisense:	(same with the cloning primer)	
stSlc7a7	Sense:	CCACCTGCCAGAACATAAGA	91
	Antisense:	CAGGACACAGTAGCAGATCAA	
stSlc7a8	Sense:	GGGAGTGATGTCCTGGATTATG	88
	Antisense:	CAACCTTGAGGAGGTGAAGAG	
stSlc7a9	Sense:	GTCATCATTGTGGCTGGAATTG	105
	Antisense:	CGCCAAACCAATAGAACCAAAG	
stSlc36a1	Sense:	CTGGAAATACCTGGCACCTT	121
	Antisense:	AGCCACTGGTGGTAGATTATTG	
stSlc36a4	Sense:	TGCTCAGCTTGCTTCCTTT	102
	Antisense:	GACTGACAGCCATTGAGAGATT	
stSlc38a2	Sense:	GAGCTACATCAAGCTACCTCTAC	97
	Antisense:	AGGTACCAATGCCCAGTATTT	
stSlc38a5	Sense:	CGGTTGAAAGCTGCCTATTTATT	126
	Antisense:	CCAAGAGCGTCTTCCATTCT	
stSlc38a7	Sense:	(same with the cloning primer)	123
	Antisense:	CACTCAGGGTACTGGCATATTT	
stSlc43a2	Sense:	TCTCCTGCTTACTGATTGCTTAC	118
	Antisense:	GTCAGTGAGGTGAAGGTCATAC	

stApoA1	Sense:	GGTTGAAGCTGGAAGAGAAGAT	104
	Antisense:	CTCAACACTCTGATTGACCCTAC	
stApoB	Sense:	GGGCTTCAGACGATTTCAGATT	102
	Antisense:	AAAGTAAGCGGGTAGGTGTTC	
stABCA1	Sense:	CTGGTACATCGAGGCAGTTT	92
	Antisense:	CCGTGTCTCCACACCAATAG	
stMTP	Sense:	(same with the cloning primer)	110
	Antisense:	CCTCCGCGGTATAACTGTATTT	
stCTSA	Sense:	(same with the cloning primer)	109
	Antisense:	CAGAACCACAGGATCATTCTCA	
stCTSB	Sense:	(same with the cloning primer)	85
	Antisense:	GTAAGTGGCCGGAACATTCT	
stCTSF1	Sense:	CTCAACCCAGTGATCAGTAACA	103
	Antisense:	CCCAATGAGAAGGACAAGACA	
stCTSF2	Sense:	GAGAAGAGGTTCCAGATCTTTGT	142
	Antisense:	TTGGGTTGAGGTAGAAGTTAGC	
stCTSL1	Sense:	(same with the cloning primer)	82
	Antisense:	AGACTCCAACCAGGCATAAAG	
stCTSL2	Sense:	ACGAAGCGCACGGTATTT	127
	Antisense:	GTGGTTCTTGCACCGACTAT	
stLIPA	Sense:	GGCCATTCTCAGGGAACAA	95
	Antisense:	ACAGGAGCCAAGGCAATAAA	
stTrypsin	Sense:	GGTCTGCAATTCGTCTCCT	117
	Antisense:	(same with the cloning primer)	
stBSDL	Sense:	CCTACCCGAGCGATCTGTATAA	101
	Antisense:	AGGCCAGTCTTTGGTGTATTG	
stPla2g1b	Sense:	AGACAAGTGCTGCCTAAATCA	117
	Antisense:	GTCTTCCCAGAGCAAGAATAGG	

Table 5. Amino acid transporters expressed in yolk sac membrane and intestine identified in transcriptome analysis

putative localization	Transcript contig ID	SLC number	putative gene product	TPM value		
				31E YSMin	32 YSMin	32 intestine
apical	TRINITY_DN68157_c9_g2	Slc3a1	Neutral and basic amino acid transport protein rBAT	3.72	0.25	10.40
	TRINITY_DN35499_c0_g1	Slc6a18	Sodium-dependent neutral amino acid transporter B(0)AT3	2.73	0.45	0.58
	TRINITY_DN60712_c0_g1	Slc6a19	Sodium-dependent neutral amino acid transporter B(0)AT1	0.12	0.17	45.51
	TRINITY_DN61159_c0_g1	Slc6a20	Sodium- and chloride-dependent transporter XTRP3	1.16	4.59	6.20
	TRINITY_DN66656_c0_g1	Slc7a9	b(0,+)-type amino acid transporter 1	20.51	30.83	14.49
	TRINITY_DN143119_c0_g1	Slc36a1	Proton-coupled amino acid transporter 1	0.37	2.08	0.57
basolateral	TRINITY_DN67547_c1_g1	Slc3a2	4F2 cell-surface antigen heavy chain	44.99	39.72	71.33
	TRINITY_DN68243_c0_g1	Slc7a6	Y+L amino acid transporter 2	0.66	1.20	2.67
	TRINITY_DN70063_c17_g1	Slc7a7	Y+L amino acid transporter 1	0.23	0.42	14.82
	TRINITY_DN57982_c0_g1	Slc7a8	Large neutral amino acids transporter small subunit 2	13.53	14.56	36.94
	TRINITY_DN58066_c0_g1	Slc38a2	Sodium-coupled neutral amino acid transporter 2	3.75	2.49	4.12
	TRINITY_DN37134_c0_g1	Slc43a2	Large neutral amino acids transporter small subunit 4	1.03	18.60	7.51
other	TRINITY_DN53217_c0_g1	Slc1a6	Excitatory amino acid transporter 4	1.26	1.58	0.52
	TRINITY_DN70444_c0_g1	Slc7a2	Cationic amino acid transporter 2	31.37	50.50	0.10
	TRINITY_DN53940_c0_g1	Slc7a3	Cationic amino acid transporter 3	3.51	5.33	3.24
	TRINITY_DN52522_c0_g1	Slc36a4	Proton-coupled amino acid transporter 4	0.54	1.73	2.96
	TRINITY_DN64338_c0_g1	Slc38a5	Sodium-coupled neutral amino acid transporter 5	0.33	1.09	0.65
	TRINITY_DN62704_c1_g1	Slc38a7	Putative sodium-coupled neutral amino acid transporter 7	1.64	2.73	7.51

TPM, transcripts per kilobase million.

Table 6. Lipid absorption genes expressed in yolk sac membrane and intestine identified in transcriptome analysis

Transcript contig ID	putative gene product	TPM value		
		31E YSM	32 YSM	32 intestine
TRINITY_DN70098_c4_g1	Apolipoprotein B	3089.08	4146.9	4838.06
TRINITY_DN64661_c0_g1	Microsomal triglyceride transfer protein	5.77	9.73	35.97
TRINITY_DN69420_c0_g2	Apolipoprotein A-I	551.29	601.18	1678.74
TRINITY_DN70132_c0_g1	ATP-binding cassette sub-family A member 1	11.00	8.41	34.92

TPM, transcripts per kilobase million.

Table 7. Cathepsins expressed in yolk sac membrane and intestine identified in transcriptome analysis

Transcript contig ID	putative gene product	TPM value	
		31E YSMin	32 YSMin
TRINITY_DN69767_c3_g3	Cathepsin L2	4496.82	3469.43
TRINITY_DN68938_c0_g1	Cathepsin F1	450.02	97.06
TRINITY_DN65741_c0_g1	Cathepsin L1	125.03	147.09
TRINITY_DN68938_c0_g2	Cathepsin F2	164.92	38.07
TRINITY_DN64326_c0_g1	Cathepsin B	25.11	61.85
TRINITY_DN61889_c0_g1	Dipeptidyl peptidase 1	34.46	40.40
TRINITY_DN65869_c2_g1	Pro-cathepsin H	13.76	12.12
TRINITY_DN62813_c0_g1	Cathepsin L1	12.34	12.68
TRINITY_DN51919_c0_g1	Cathepsin D	7.33	17.10
TRINITY_DN69202_c20_g1	Lysosomal protective protein	7.62	12.98
TRINITY_DN56465_c0_g1	Cathepsin Z	4.70	7.96
TRINITY_DN68672_c0_g2	Cathepsin L1	4.09	4.19
TRINITY_DN67109_c5_g1	Cathepsin D	3.00	4.09
TRINITY_DN64173_c0_g1	Cathepsin O	2.49	2.70
TRINITY_DN148559_c0_g1	Cathepsin L	0.80	1.31
TRINITY_DN128969_c0_g1	Cathepsin L	0.14	1.09

TPM, transcripts per kilobase million.

Table. 8 The accession numbers of genes used in the analysis

Gene name	Accession number
Catshark <i>CTSF1</i>	PE TRINITY DN74700 c13 g
Catshark <i>CTSF2</i>	PE TRINITY DN74700 c13 g
Catshark <i>CTSL1</i>	TRINITY_DN65741_c0_g1
Catshark <i>CTSL2</i>	PE_TRINITY_DN70779_c0_g1
Chicken <i>CTSH</i>	NP_001305336.1
Chicken <i>CTSK</i>	NP_990302.2
Chicken <i>CTSS</i>	NP_001026516.1
Elephant fish <i>CTSH</i>	XP_007903522.1
Elephant fish <i>CTSL1</i>	A0A4W3K499
Finch <i>CTSL1</i>	XP_021386814.1
Frog <i>CTSF</i>	NP_001106423.1
Frog <i>CTSK</i>	NP_001072435.1
Frog <i>CTSS</i>	NP_001005695.1
Human <i>CTSF</i>	NP_003784.2
Human <i>CTSH</i>	NP_001306066.1
Human <i>CTSK</i>	NP_000387.1
Human <i>CTSL1</i>	NP_001244900.1
Human <i>CTSS</i>	NP_001186668.1
Lizard <i>CTSF</i>	XP_034954775.1
Medaka <i>CTSS</i>	NP_001098157.1
Zebrafish <i>CTSF</i>	NP_001071036.1
Zebrafish <i>CTSH</i>	NP_997853.1
Zebrafish <i>CTSK</i>	NP_001017778.1
Zebrafish <i>CTSL1</i>	BC066490

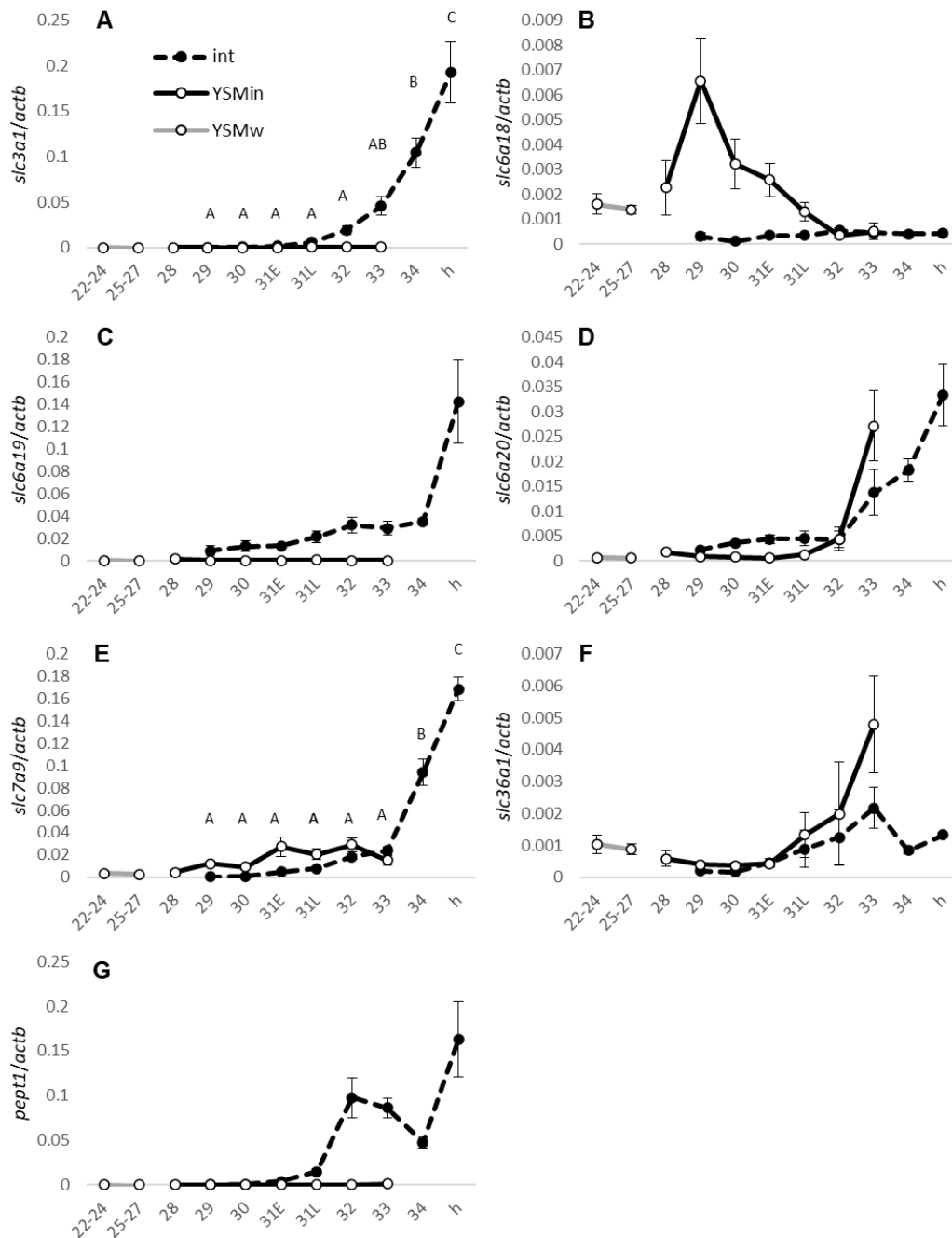


Figure 11. Developmental changes in levels of apical-type amino acid transporter mRNAs in the YSM and intestine. (A) *slc3a1*; (B) *slc6a18*; (C) *slc6a19*; (D) *slc6a20*; (E) *slc7a9*; (F) *slc36a1*; (G) *pept1*. The mRNA levels are shown as the relative values to the mRNA levels of β -actin (*actb*). The values of intestine for *slc6a19* and *pept1* from stages 31E to hatched juvenile were quoted from Chapter 1. Data are presented as means \pm s.e.m. of N=5. Different uppercase letters indicate a significant difference between stages in the intestine ($P < 0.05$). int, intestine; YSMMin, inner YSM; YSMw, whole YSM.

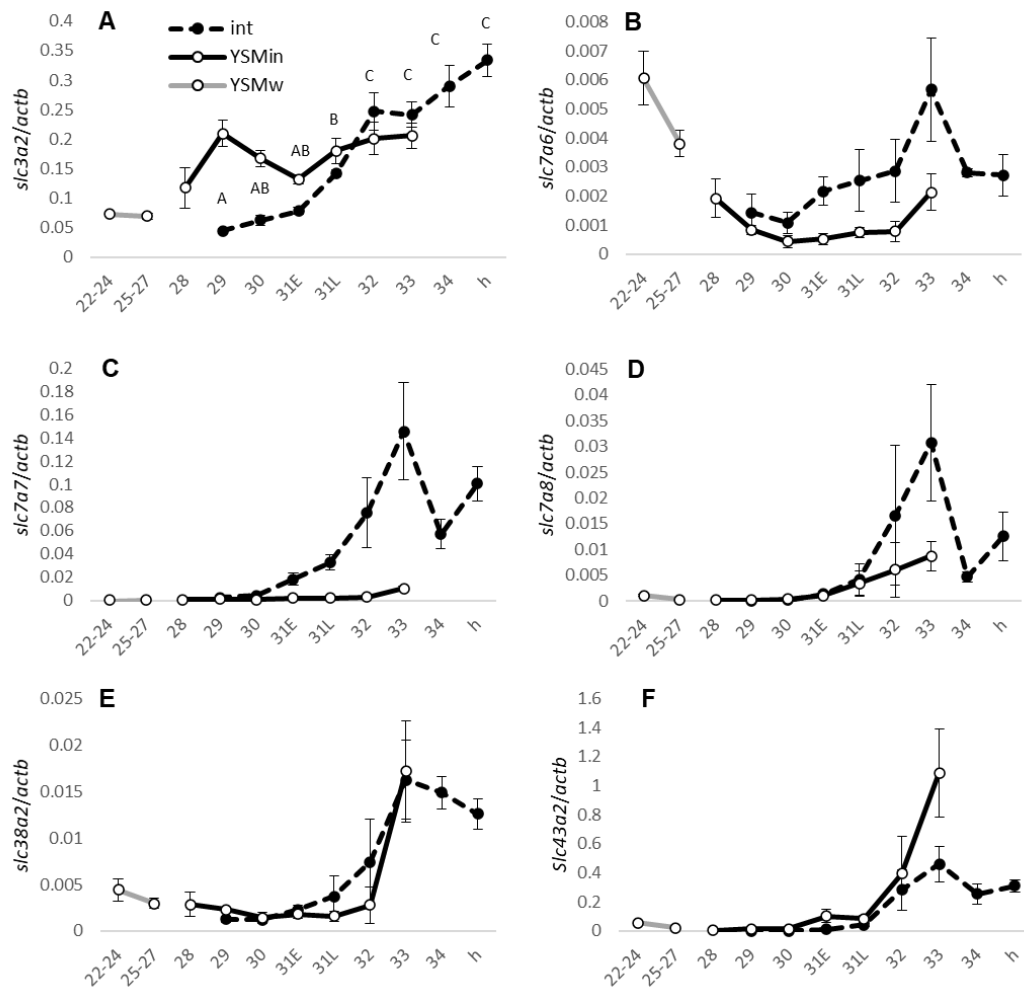


Figure 12. Developmental changes in levels of basolateral-type amino acid transporter mRNAs in the YSM and intestine. (A) *slc3a2*; (B) *slc7a6*; (C) *slc7a7*; (D) *slc7a8*; (E) *slc38a2*; (F) *slc43a2*. The mRNA levels are shown as the relative values to the mRNA levels of β -actin (*actb*). Data are presented as means \pm s.e.m. of N=5. Different uppercase letters indicate a significant difference between stages in the intestine (P<0.05). int, intestine; YSM_{in}, inner YSM; YSM_w, whole YSM.

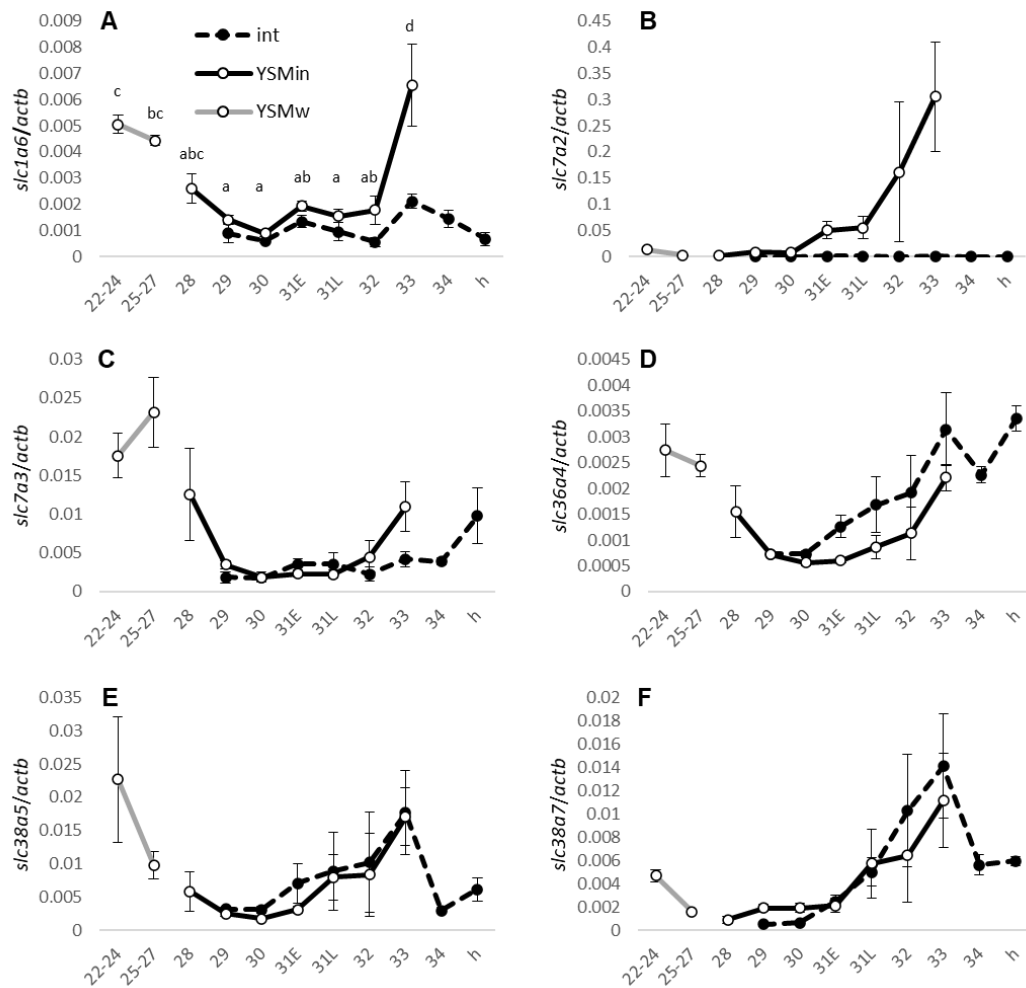


Figure 13. Developmental changes in levels of other-type amino acid transporter mRNAs in the YSM and intestine. (A) *slc1a6*; (B) *slc7a2*; (C) *slc7a3*; (D) *slc36a4*; (E) *slc38a5*; (F) *slc38a7*. The mRNA levels are shown as the relative values to the mRNA levels of β -actin ($actb$). Data are presented as means \pm s.e.m. of N=5. Different lowercase letters indicate a significant difference between stages in the YSM (P<0.05). int, intestine; YSMIn, inner YSM; YSMw, whole YSM.

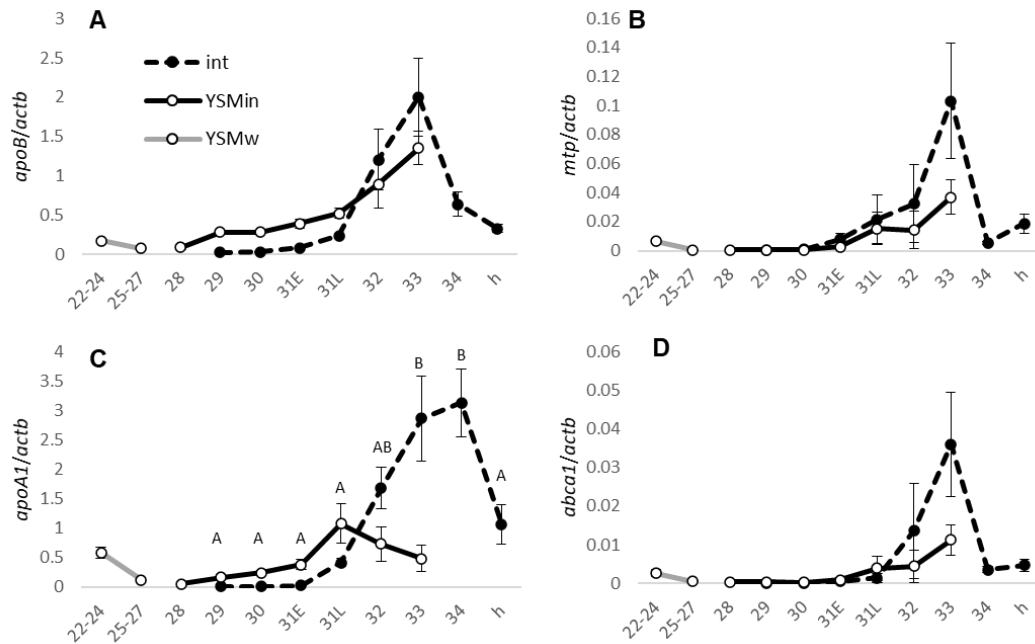


Figure 14. Developmental changes in mRNA levels of genes involved in lipid absorption in the YSM and intestine. (A) *apoB*; (B) *mtp*; (C) *apoA1*; (D) *abca1*. The mRNA levels are shown as the relative values to the mRNA levels of β -actin (*actb*). Data are presented as means \pm s.e.m. of N=5. Different uppercase letters indicate a significant difference between stages in the intestine ($P < 0.05$). int, intestine; YSMMin, inner YSM; YSMw, whole YSM.

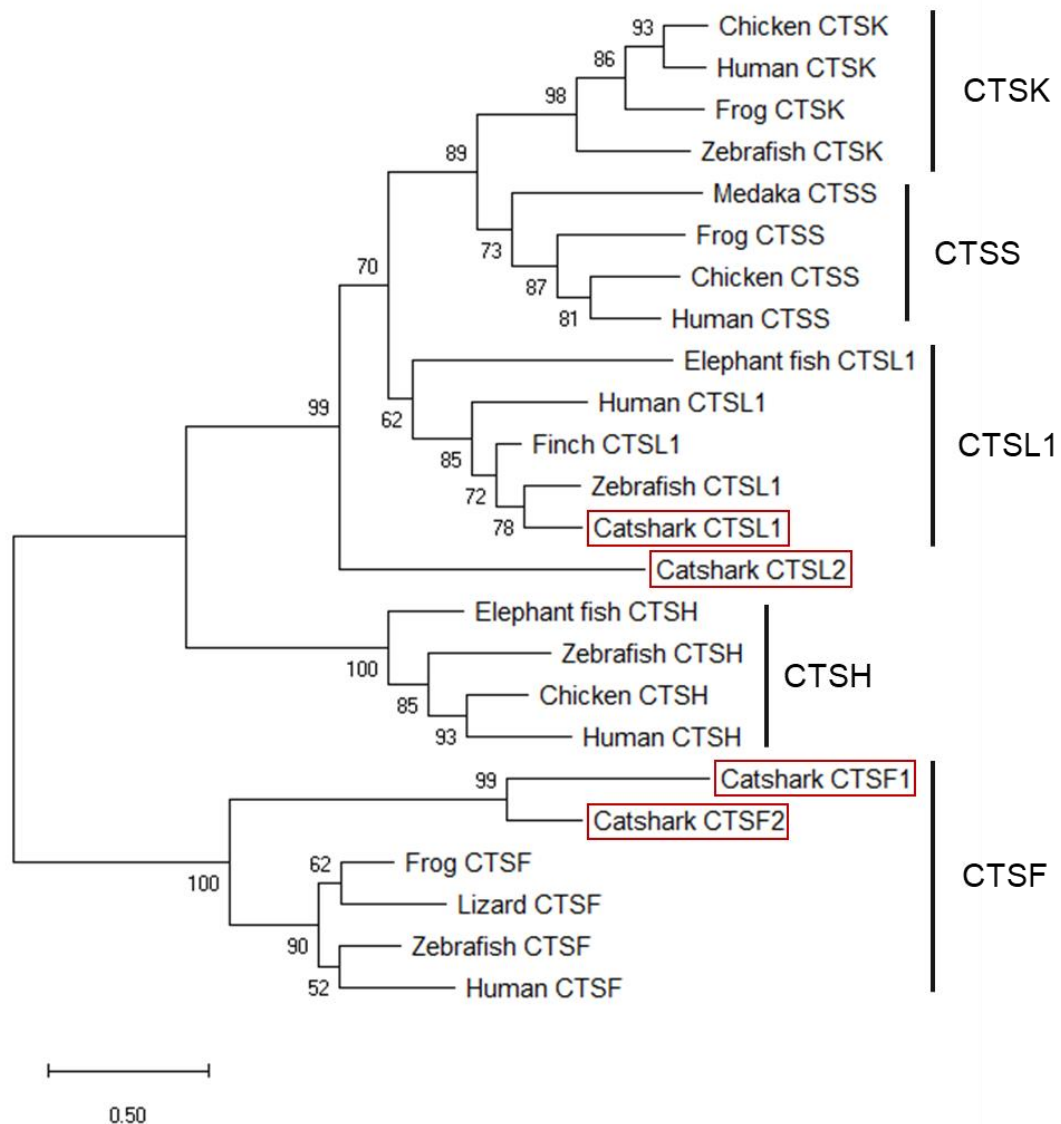


Figure 15. Molecular phylogenetic tree of vertebrate cathepsins. Bootstrap probabilities are shown next to the branches. The accession numbers of genes used in the analysis are listed in Table 8. The cloudy catshark sequences are highlighted by the red boxes.

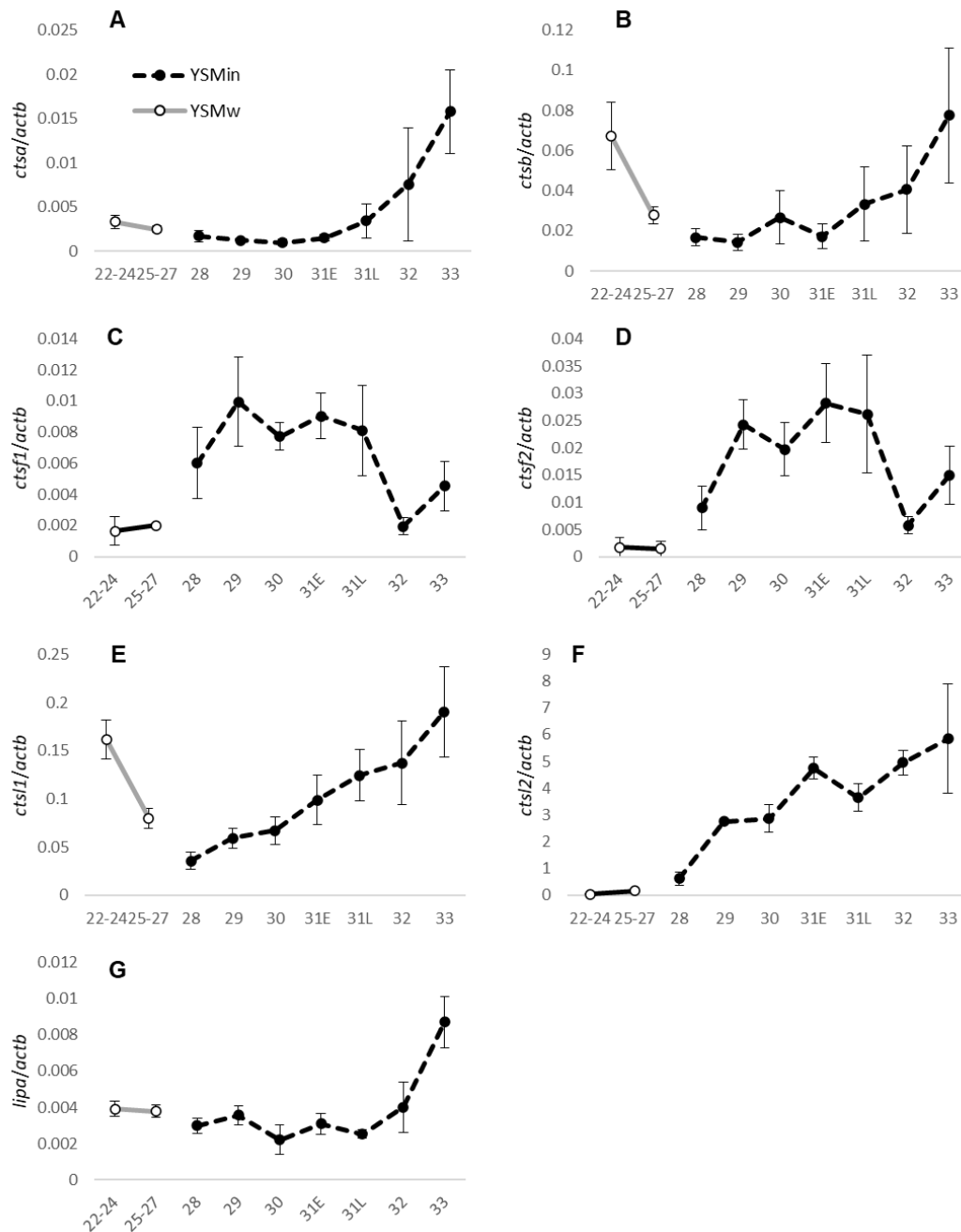


Figure 16. Developmental changes in mRNA levels of lysosomal digestive enzymes in the YSM. (A) *ctsa*; (B) *ctsb*; (C) *ctsf1*; (D) *ctsf2*. (E) *ctsl1*; (F) *ctsl2*; (G) *lipa*. The mRNA levels are shown as the relative values to the mRNA levels of β -actin (*actb*). Data are presented as means \pm s.e.m. of N=5. YSMIn, inner YSM; YSMw, whole YSM.

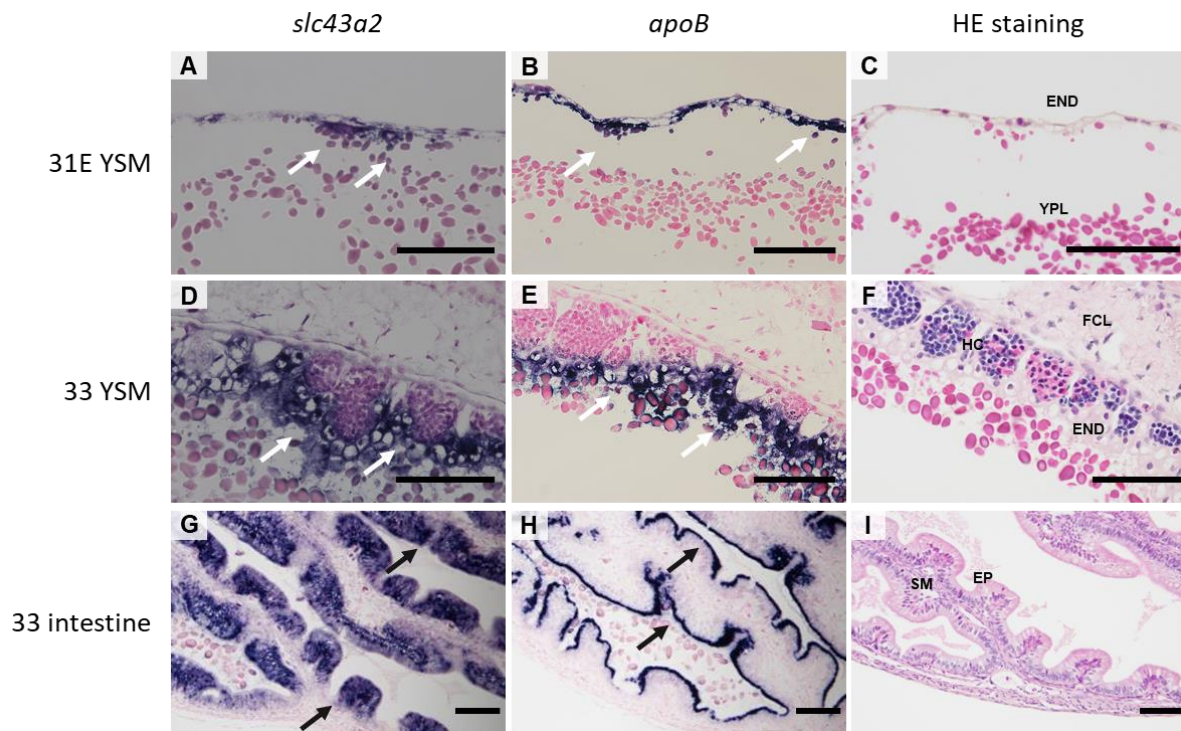


Figure 17. *In situ* hybridization analyses of *slc43a2* and *apoB* mRNA in the YSM and intestine. The *slc43a2* (A, D, G), *apoB* (B, E, H) mRNA signals and HE staining (C, F, I) in the YSM of stage 31E (A–C), YSM of stage 33 (D–F) and intestine of stage 33 (G–I). White arrows indicate signals in the endodermal cells. Black arrows indicate signals in the epithelial cells. END, endoderm; EP; epithelial cell; FCL, fibrous connective layer; HC, hematopoietic cell SM, submucosa. Scale bars, 100 μ m.

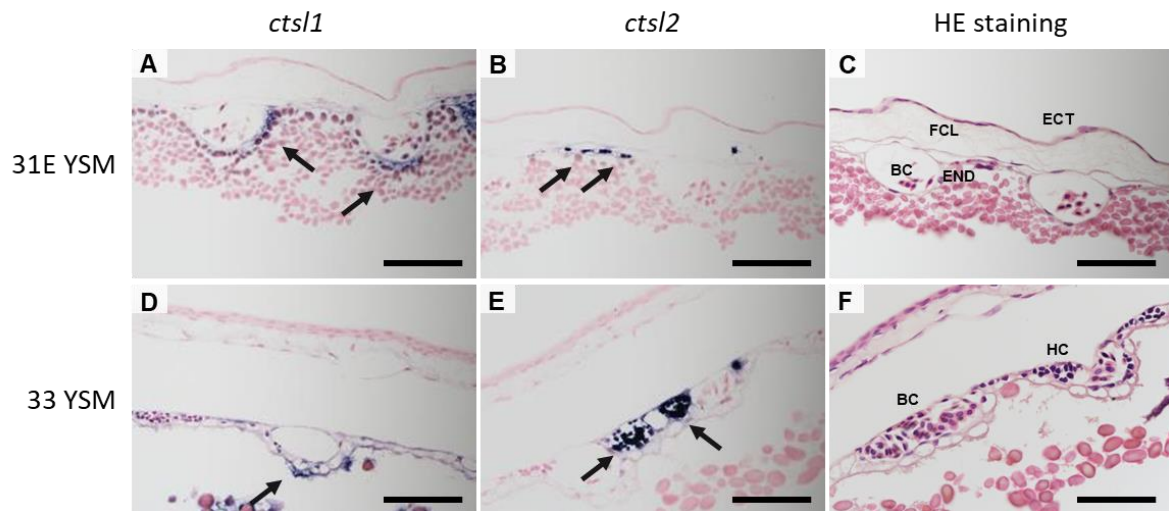


Figure 18. *In situ* hybridization analyses of *ctsl1* and *ctsl2* mRNA in the YSM. The *ctsl1* (A, D), *ctsl2* (B, E,) mRNA signals and HE staining (C, F) in the YSM of stage 31E (A–C) and YSM of stage 33 (D–F). Black arrows indicate signals in the endodermal cells (A, D) and hematopoietic cells (B, E), respectively. BC, blood cell; END, endoderm; ECT ectoderm; FCL, fibrous connective layer; HC, hematopoietic cell. Scale bars, 100 μ m.

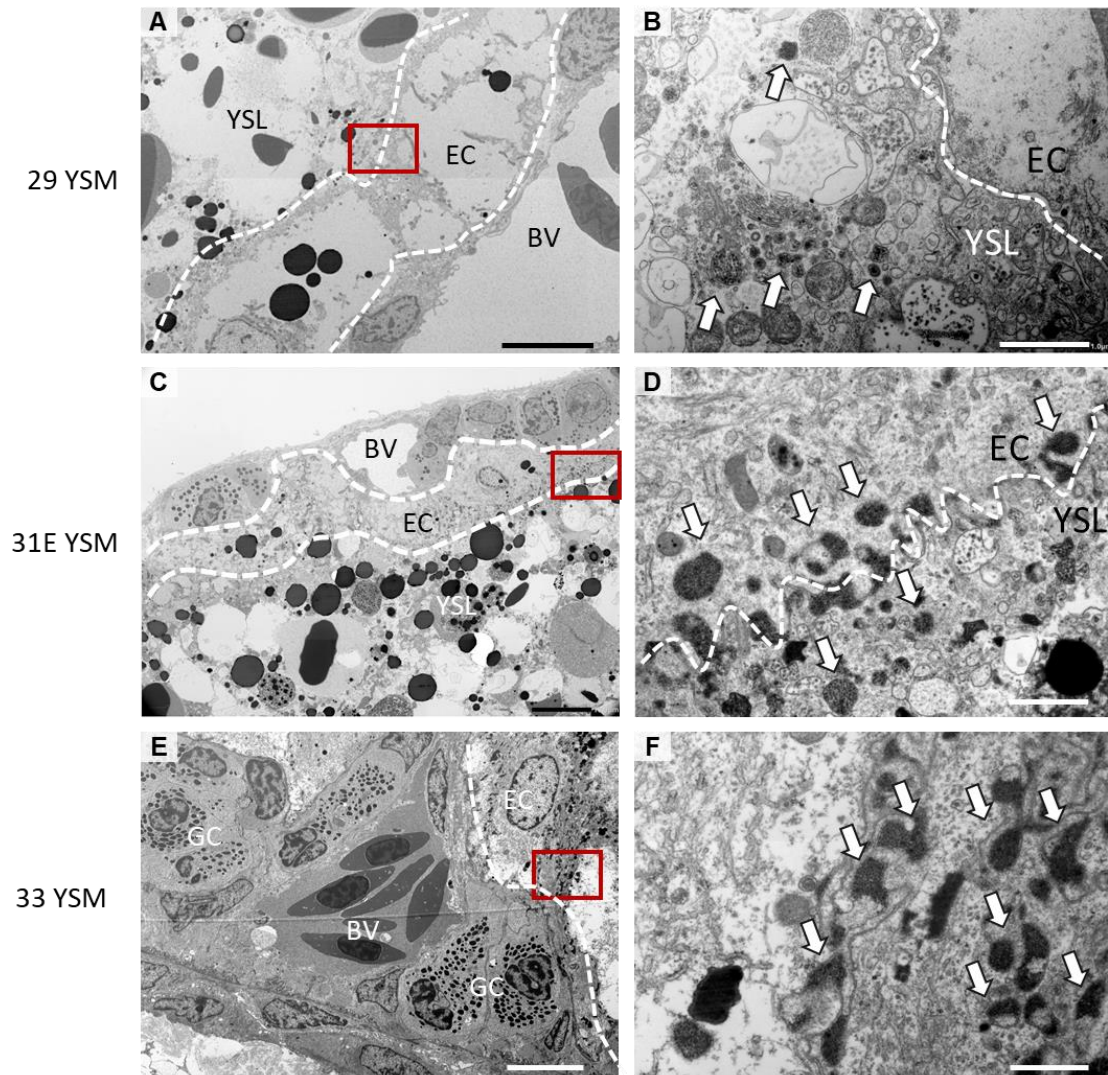


Figure 19. Endocytosis of yolk droplets in the YSM. TEM observation of the inner layer of the YSM at stage 29 (A, B), stage 31E (C, D) and stage 33 (E, F). (B, D, E) Magnified views of red box in A, C, E, respectively. Boundary between endodermal cell layer and other layers is indicated with a white dotted line. Arrows indicate membrane packets containing yolk droplets. BV, Blood vessel; EC, Endodermal cell; GC, granular cell; YSL, yolk syncytial layer. Scale bars: 10µm (A, C, E) and 1µm (B, D, E).

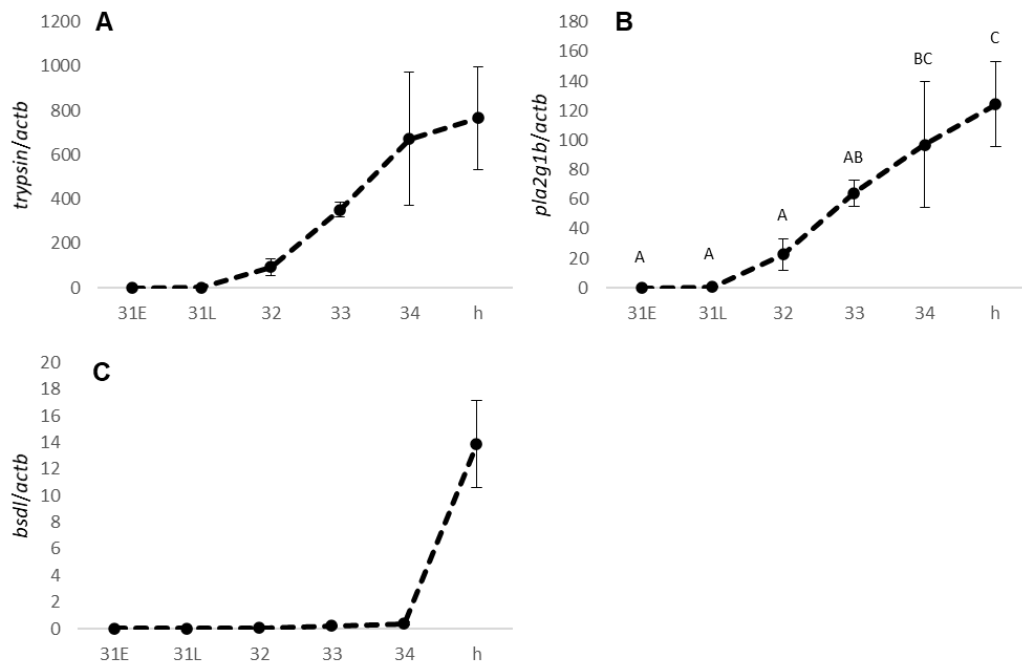


Figure 20. Developmental changes in mRNA levels of digestive enzymes in the pancreas. (A) *trypsin*; (B) *pla2g1b*; (C) *bsd1*. The mRNA levels are shown as the relative values to the mRNA levels of β -actin (*actb*). Data are presented as means \pm s.e.m. of N=5. Different uppercase letters indicate a significant difference between stages ($P < 0.05$).

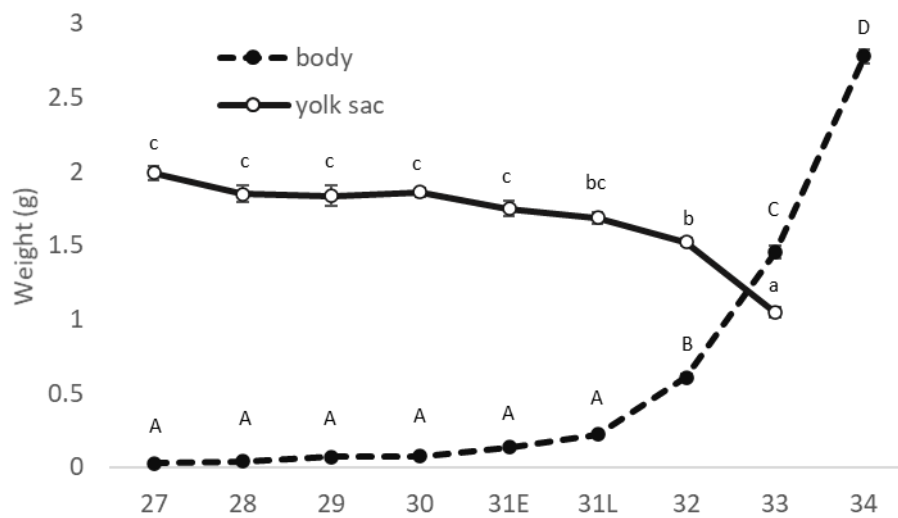


Figure 21. Developmental changes in the wet weight of embryos and yolk sac. Data are presented as means \pm s.e.m. N= 5 (stage 27); 15 (stage 28); 11 (stage 29); 20 (stage 30); 25 (stage 31E); 22 (stage 31L); 66 (stage 32); 77 (stage 33); 44 (stage 34) for embryonic body, 6 (stage 27); 16 (stage 28); 17 (stage 29); 24 (stage 30); 29 (stage 31E); 21 (stage 31L); 67 (stage 32); 88 (stage 33) for yolk sac.

A

localization	Slc	substrate	YSM			Intestine	
			22-27	28-31L	32-33	29-31L	32-h
Apical	Slc3a1	subunit					
	Slc6a18	G, A					
	Slc6a19	All neutral					
	Slc6a20	P					
	Slc7a9	R,K					
	Slc36a1	G,P,A					
Basolateral	Slc3a2	subunit					
	Slc7a6	K,R,Q,H,M,L					
	Slc7a7	K,R,Q,H,M,L,A,C					
	Slc7a8	All neutral except P					
	Slc38a2	G,P,A,S,C,Q,N,H,M					
	Slc43a2	L,I,M,F,V					
Other	Slc1a6	D,E					
	Slc7a2	K,R,O					
	Slc7a3	K,R,O					
	Slc36a4	P,W					
	Slc38a5	Q,N,H,A					
	Slc38a7	Q,N,H,A,S,D					

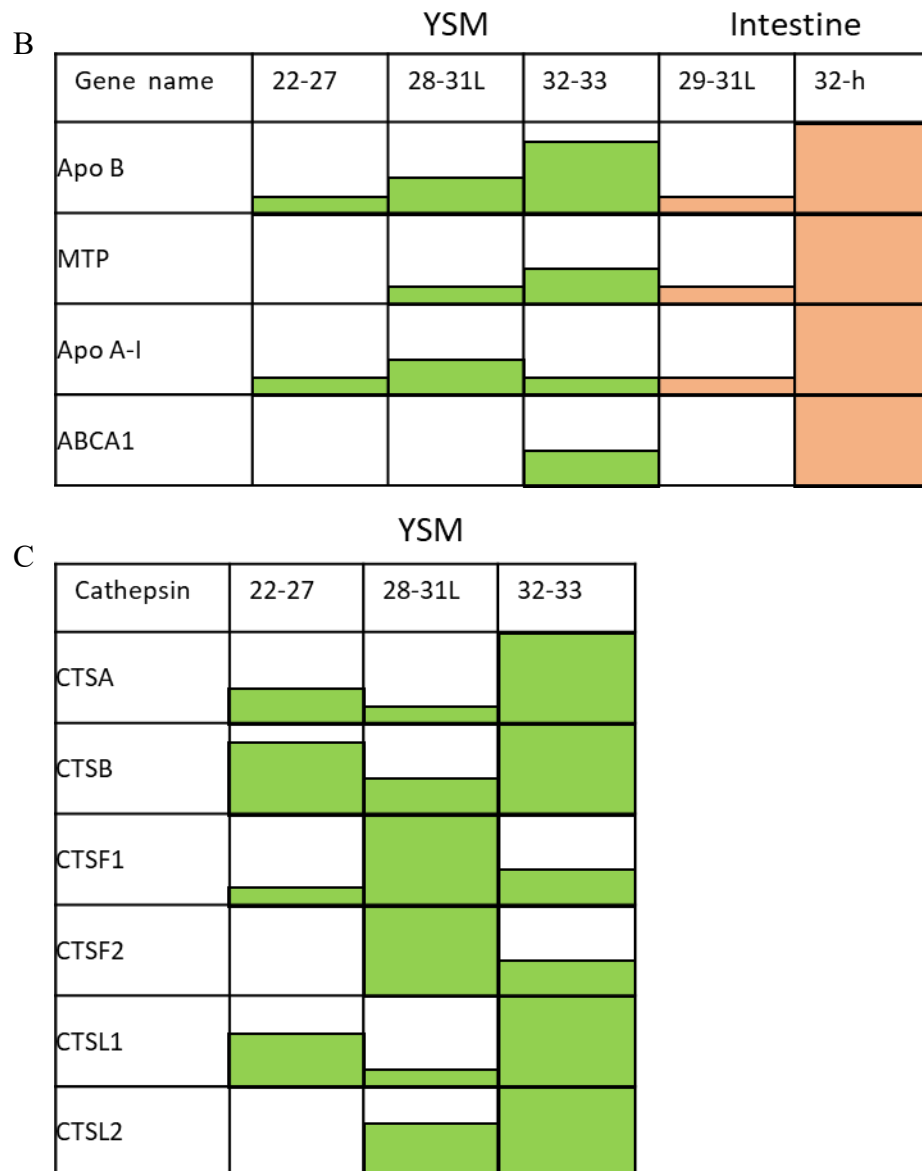


Figure 22. (A) Schematic diagram exhibiting expression levels of amino acid transporters. Green bars indicate mRNA expression in the YSM, while orange bars represent mRNA expression in the intestine. amino acid abbreviations are as follows: Alanine, A; Leucine, L; Arginine, R; Lysine, K; Asparagine, N; Methionine, M; Aspartic Acid, D; Phenylalanine, F; Cysteine, C; Proline, P; Glutamine, Q; Serine, S; Glutamic Acid, E; Threonine, T; Glycine, G; Tryptophan, W; Histidine, H; Tyrosine, Y; Isoleucine, I; Valine, V. (B) Schematic diagram exhibiting expression levels of lipid absorption molecules. Green bars indicate mRNA expression in the YSM, while orange bars represent mRNA expression in the intestine. (C) Schematic diagram exhibiting expression levels of cathepsins in the YSM.

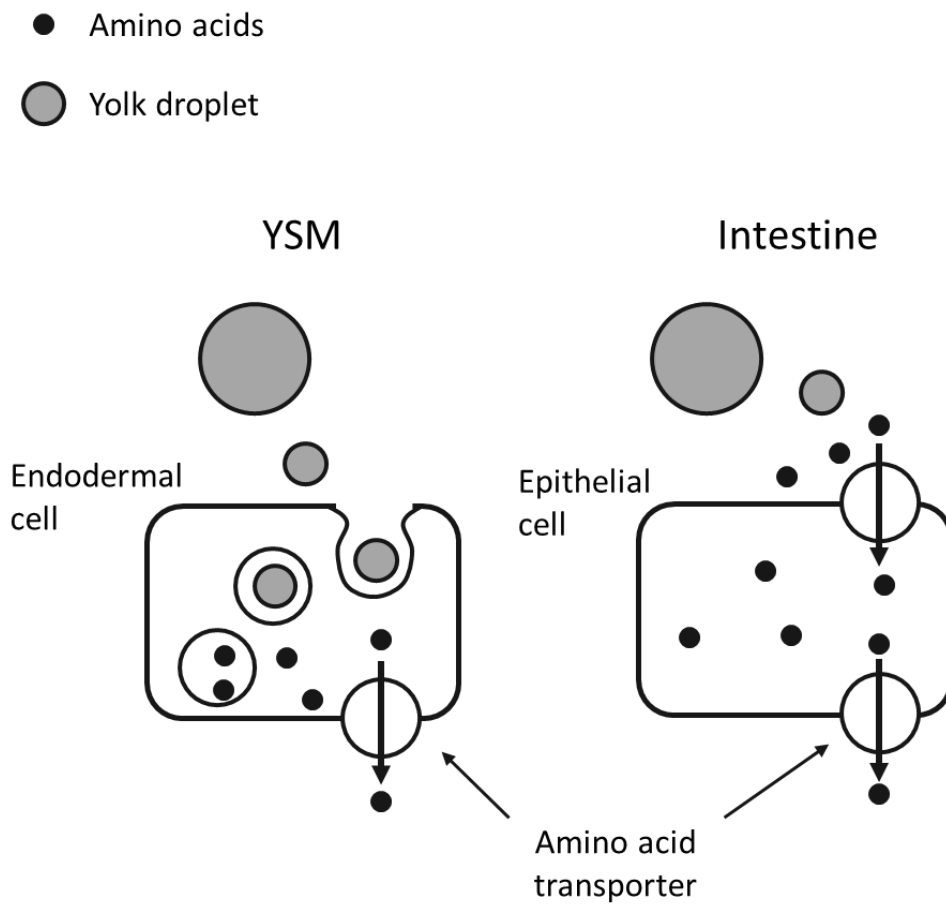


Figure 23. Schematic diagram representing possible uptake mechanisms of amino acids in the YSM and the intestine. In the YSM, yolk droplets are likely endocytosed into the endodermal cells and then digested amino acids are transported by basolateral amino acid transporters into blood vessels. In the intestine, on the other hand, yolk droplets are digested in the lumen and then amino acids are transported via apical and basolateral amino acid transporters into blood vessels.

General Discussion

Needless to say, nutrient absorption by embryos is essential for proper ontogenic processes. However, most vertebrate embryos do not have functional gastrointestinal systems until late developmental stages, and thus development of nutrient absorption surface (where? when? and how?) is an important topic in the developmental physiology field. Cartilaginous fishes have various reproductive modes such as oviparity and placental and aplacental viviparities (Musick and Ellis, 2005; Buddle et al., 2019). The modes of nutrition absorption are also unique depending on their reproductive modes. Embryos of all cartilaginous fishes depend on yolk as nutrient source during their early developmental period, while viviparous embryos are provided with trophic eggs (oophagy), uterine milk (histotroph) or nutrient directly through placenta. These features suggest that nutrient absorption mechanism changes during the embryonic development in cartilaginous fishes. Even in oviparous species, which depend solely on yolk, the yolk from the external yolk sac is directed into the embryonic intestine in the mid-embryonic stage, suggesting a shift of nutrition absorption surfaces. Various modes of nutrition absorption in oviparous cartilaginous fish are good research models for the comparative studies of embryonic nutrition. In the present study, nutrient absorption was investigated using oviparous cloudy catshark as a model animal. In Chapter 1, I focused on the morphological and functional development of the spiral intestine. Nutrient absorptive function of the YSM was investigated in Chapter 2 by examining genes discovered from transcriptome data, which are involved in digestion and absorption. In General Discussion, I summarize and discuss the findings from the integrative perspectives on developmental events, reproductive strategies in fishes, and reproductive modes in cartilaginous fishes.

The pre-hatching event: a physiological turning point in embryonic development of cartilaginous fish

The development of spiral intestine was reported in the embryos of the round stingray (*Urobatis halleri*) (Babel, 1966), lesser spotted dogfish (Ballard et al., 1993) and tropical whitespotted bamboo shark (*Chiloscyllium plagiosum*) (Xu et al., 2015). However, these studies focused on general development of digestive systems or whole embryos and lack detailed observation focusing on the intestinal morphogenesis. Recently, Theodosiou and Oppong, (2019) showed that spiral formation begins at stage 25 and completes before hatch (stage 34) in little skate (*Leucoraja erinacea*). The number of spirals in the embryos of little skate was 0.5 at stage 25, 4.5 at stage 27, 6.5 at stage 30, and 8 at stage 34 (final stage), which is equal to the number of spirals present in adult. In the little skate study, no information was available between stages 30 and 34, despite a long interval (more than 14 weeks) between stages 30 to 34. Since the spiral valve is a structure for nutrient absorption, the timing when spiral formation completes and when intestine begins absorption is assumed to be related. In the present study, I performed a detailed morphological investigation and revealed that spiral formation is completed at stage 31E, before the pre-hatching event in cloudy catshark embryos. At the pre-hatching, yolk begins to flow into the intestine. Furthermore, after the start of yolk inflow, various features including formation of secondary folds and microvilli, and expressions of amino acid transporters, lipid absorption molecules, and digestive enzymes, were found, suggesting active absorption of nutrient by the intestine. It is likely that spiral valve formation before intestinal absorption is necessary because spiral valve contains blood vessels and nerves which contribute to nutrient transport and regulate intestinal function, respectively. These results strongly imply that the “pre-hatching” event marks a

developmental switch for active growth to begin.

The pre-hatching was thought to be a physical event, where the eggshell opens to expose the embryos to the external environment. This event is unique in cartilaginous fish, and it may facilitate seawater circulation to improve respiration (Diez and Davenport, 1987) and/or increase the space for the growing embryo inside the egg case (Mellinger et al., 1986, 1989). In addition, recent studies have demonstrated that the pre-hatched embryos are endowed with several physiological functions: respiration using buccal pumping and the internal gill (Rodda and Seymour, 2008; Tomita et al., 2014), urea synthesis in the liver (Takagi et al., 2014, 2017), enhanced immune system with immunoglobulin-positive cell production in the lymphomyeloid tissues (Lloyd-Evans, 1993), and nutrient absorption in the intestine (Chapter 1; Honda et al., 2020). Therefore, the pre-hatching is likely a developmental turning point for the embryos instead of a trivial physical event.

After the pre-hatching event, the catshark embryo is exposed to outer environment, and is endowed with physiological abilities that enable them to survive outside the eggshell. These features strongly imply that the pre-hatching of oviparous cartilaginous fish is equivalent to the hatching in teleosts. Lechenault et al. (1993) previously reached the same conclusion that pre-hatching is comparable to hatching of anamniotes because pre-hatching occurs as a result of the degradation of a solid layer of eggshell. In vertebrates, individuals that have not yet reached adult form can be classified into “larvae” and “juvenile”. The newly hatched oviparous teleosts are called larvae and they still attach to a large yolk sac. According to the definition, the embryos after the pre-hatching stage correspond to the “hatched larvae” in oviparous cartilaginous fish (Fig. 24). If so, why does “hatched larvae” of oviparous cartilaginous fish stay inside egg case? Teleosts lay

large numbers of small size eggs into open water. The larval period of teleost fish is generally short and they rapidly grow into juveniles. Nevertheless, the larval stage of teleost fish confronts a problem of high mortality largely due to starvation and predation (high birth rate but high infant mortality, r-selection) (MacArthur and Wilson, 1967). On the other hand, oviparous cartilaginous fish adopt a separate strategy of “low birth and premature death rates, K-selection” (MacArthur and Wilson, 1967). For this strategy, it would be reasonable for the hatched larvae to stay inside the egg case to increase survival by reducing predation risk (Fig. 24).

Nutrient absorption after pre-hatching stage: mechanisms for rapid growth in “hatched larvae”

Based on the results of the morphological and functional development of the embryonic intestine, I hypothesized that an ontogenic shift of nutrient absorptive surfaces from the YSM to the embryonic intestine occurs after the pre-hatching event. Prior to the functional development of embryonic intestine, the YSM must be the only absorptive surface for nutrient. Mechanisms for yolk absorption in the YSM have been described in teleosts and birds. The teleost YSM have no endodermal cellular layer (Heming and Buddington, 1988) and yolk digestion and absorption occur at the yolk syncytial layer (YSL) (Shimizu and Yamada, 1980; Sire et al., 1994; Krieger and Fleig, 1999). On the other hand, YSL is absent in the YSM of avian embryos (Mobbs and McMillan, 1979), and the yolk is phagocytosed into endodermal cells in chick YSM (Lambson, 1970; Mobbs and McMillan, 1981), and is further processed into yolk metabolites that are secreted into vitelline circulation (Kanai et al., 1996). The mRNAs encoding peptide transporter, amino acid transporters, and sugar transporters were present in the chick YSM,

suggesting that these transporters contribute to the nutrient absorption in the YSM (Yadgary et al., 2011; Speier et al., 2012; Yadgary et al., 2014). In cloudy catshark, many transporter mRNAs were detected in the transcriptome data of YSM, and subsequently confirmed by qPCR and *in situ* hybridization analyses. In Atlantic sharpnose shark (*Rhizoprionodon terraenovae*), yolk platelets are degraded in the YSL and the resulting yolk granules are incorporated into the endodermal cells by endocytosis (Hamlett et al., 1987), as seen in cloudy catshark in the present study. In the YSM of cloudy catshark embryos, apical-type amino acid transporters were relatively less than those of basolateral-type transporters expressed in the YSM and of apical-type transporters in the embryonic intestine. These results support the uptake of yolk in the YSM is mainly by endocytosis.

A striking feature of yolk utilization in the cartilaginous fish embryo is the direct transfer of yolk from the external yolk sac into the embryonic intestine. Although it is difficult to estimate the proportion of yolk consumption between the YSM and the intestine, intestine is considered to be a dominant organ to absorb yolk (Lechenault et al., 1993). In contrast, the whole yolk is absorbed inside the yolk sac membrane in teleosts because no luminal connection was found between the yolk sac and the gastrointestinal tract (Ng et al., 2005). In chick embryo, yolk does not move into the intestine due to a loop structure of intestinal tract, which closes the lumen between yolk sac and the intestine, during most of embryonic period (Speake et al., 1998). During the final phase of embryonic period, yolk is transferred into the intestine via yolk stalk in chicken (Romanoff, 1960; van der Wagt et al., 2020). Collectively, both cartilaginous fishes and birds initially absorb yolk in the YSM and the inflow of yolk from the yolk sac into the intestine is blocked by a cellular membrane in the cloudy catshark and the intestinal loop

in the chick embryo. After certain stage, these structures are dissolved to allow the inflow of yolk into intestine for digestion and absorption. Both cartilaginous fishes and birds have a telolecithal egg that may have different origins, but could have shared common features due to similar nutrient absorption modes.

The most unanticipated result in the present study was the high expression levels of nutrient transporting proteins in the YSM even after the pre-hatching period. These results imply that activity of nutrient absorption increased in the YSM along with intestine. Active digestion and absorption in the YSM of stage 33 embryo was also reported in lesser spotted dogfish (Lechenault et al., 1993). In the cloudy catshark embryos, embryonic body weight markedly increased from stage 32. High nutrient absorption rates in both intestine and YSM probably facilitate the rapid growth after the pre-hatching stage. Again, rapid growth is a feature of the “larval period”, supporting my idea that the hatched larvae stays inside the egg case to increase survival and avoid danger in oviparous cartilaginous fishes (Fig. 24).

Morphogenesis and functional regionalization of spiral intestine

Morphogenesis of the spiral structure of cartilaginous fish intestine is also an interesting topic. Theodosiou and Oppong (2019) suggested that asymmetric protrusion of the intestinal lumen causes the spiral valves. In birds, a mechanical force derived from asymmetric cellular proliferation and growth provokes the morphogenesis of the chick intestinal tract (Savin et al., 2011). Therefore, it is possible that such factors may also affect morphogenesis of spiral intestine in cartilaginous fishes.

Spiral intestine is a plesiomorphic feature in vertebrates. However, most of existing vertebrates possess intestinal tract without spiral valves. It was considered that

the disappearance of the spiral valves has evolved twice independently in teleosts and tetrapods. In gar and bowfin, only small portion of their intestine has spiral structure (Argyriou et al., 2016), suggesting that their intestines exhibit intermediate phenotypes between spiral- and straight-types. The spiral intestine is advantageous as a large surface area for absorption is possible with limited abdominal space (Budker, 1971) in animals that possess large liver or intrauterine embryos (Moss, 1984). The *cdx1* and *cdx2* were expressed in the prospective intestine in the lesser spotted dogfish embryo, suggested that these transcription factors maintained intestinal epithelium (Gonçalves et al., 2019). Further studies, in particular on molecular mechanism of spiral formation, will clarify the evolutionary aspect of spiral intestine in vertebrates.

Feeding habits of elasmobranchs have been extensively studied because they are important top predators in marine ecosystem (Wetherbee et al., 1990). Activity of digestive enzymes including pancreatic lipases in spiny dogfish (Rasco and Hultin, 1988), bile salt-dependent triacylglycerol lipase (Patton et al., 1997) and gastric pepsin (Papastamatiou, 2007) in leopard sharks (*Triakis semifasciata*), and pepsin, trypsin and lipase in shortfin mako shark (*Isurus oxyrinchus*) (Newton et al., 2015) were measured. On the other hand, functional specialization at different regions of the spiral intestine has not been studied in cartilaginous fishes. As most vertebrate intestine can be divided into several distinct segments according to morphology and functions, I was interested in whether the spiral intestine could have region-specific functions. The only report concerning a nutrient absorption molecule, PepT1, did not examine the transporter distribution in the intestine of bonnethead shark (Hart et al., 2016). In the present study, I revealed that *pepT1* mRNA was dominate at the anterior region while the *slc6a19* mRNA was ubiquitously distributed in the spiral intestine of juveniles. The *pepT1* expression

pattern is consistent to those found in teleosts (Teroval et al., 2009; Xu et al., 2016; Orozco et al., 2017). In addition to nutrient absorption, the end-distal part of the spiral intestine was suggested to have a role in water absorption in little skate (*Leucoraja erinacea*) (Theodosiou and Simeone, 2012). Taken together, the present study clearly revealed that the spiral intestine is a sophisticated organ with function-specific regionalization. Although the mRNA of *slc6a19* was found ubiquitously in the spiral intestine, a remarkable increase in expression was observed in the end-posterior part of the intestine only at stage 34, implying that the embryos may maximize nutrient absorption from yolk digesta just before hatching. The plasticity of transporter expression of nutrient absorption proteins can be flexibly controlled according to physiological and developmental conditions.

Reproductive modes and the use of digestive tract: existence of functional triggers?

In this thesis, I described nutrient absorption during developmental period in the oviparous cloudy catshark. As mentioned in General Introduction, cartilaginous fish have various reproductive modes. In matrotrophic viviparous species, embryos obtain nutrient from mother inside the uterus, in addition to yolk (Musick and Ellis, 2005). It appears that the portion of the digestive tract involved and the stage when it becomes functional are different among reproductive modes. Embryos ingest nutrient substances secreted by uterine wall in histotrophic species (Hamlett et al., 1996; Hamlett et al., 2005). In oophagy and adelphagy, embryos eat eggs and siblings, respectively (Fujita, 1981; Gilmore et al., 1983). It is obvious that embryos of these reproductive modes should have a complete digestive tract including mouth, esophagus, stomach, and spiral intestine. However, oviparous species incorporate yolk directly from the yolk sac into the spiral intestine, and

thus only the spiral intestine was active during embryonic period. Oophagic porbeagle shark (*Lamna nasus*) embryos have embryonic teeth specific for hatching and consumption of egg case (Francis, 2000). In oophagic crocodile shark, stomach of 401~428 mm embryo (equal to or larger than stage 34) was filled with yolk material while stomach of 37.9~40.8 mm embryo (equal to stage 31L) was yolk-free (Fujita, 1981). Fujita (1981) suggested that the stomach was not functional when embryos absorb yolk through external yolk sac membrane. These results imply that embryos initially depend on the YSM, subsequently involve the spiral intestine, and then utilize the whole digestive tract among oophagy and adelphagy species (Fig. 25). Surprisingly, embryos of false catshark (*Pseudotriakis microdon*) transfer ingested yolk material (oophagy) to the external yolk sac for storage (Yano, 1992). Even in the placental viviparous species, embryos before placental formation follow the above-mentioned developmental shift in nutrient absorption: yolk absorption at the YSM, yolk absorption in the intestine, and then histotroph ingestion. (Hamlett, 1989) (Fig. 25). After the yolk sac placenta is formed, embryos obtain nutrients from mother via substance exchange at the placenta (Hamlett et al., 1985). Collectively, embryos of lecithotrophic species only use their spiral intestine while embryos of matrotrophic species use the whole digestive tract (Fig. 25). Digestive tracts are developed in both types, but functional trigger must be separately regulated in each portion at relevant developmental stages. I am deeply interested in the transcription and/or hormonal regulation of the development and functions in the digestive tract of cartilaginous fish after this doctoral study.

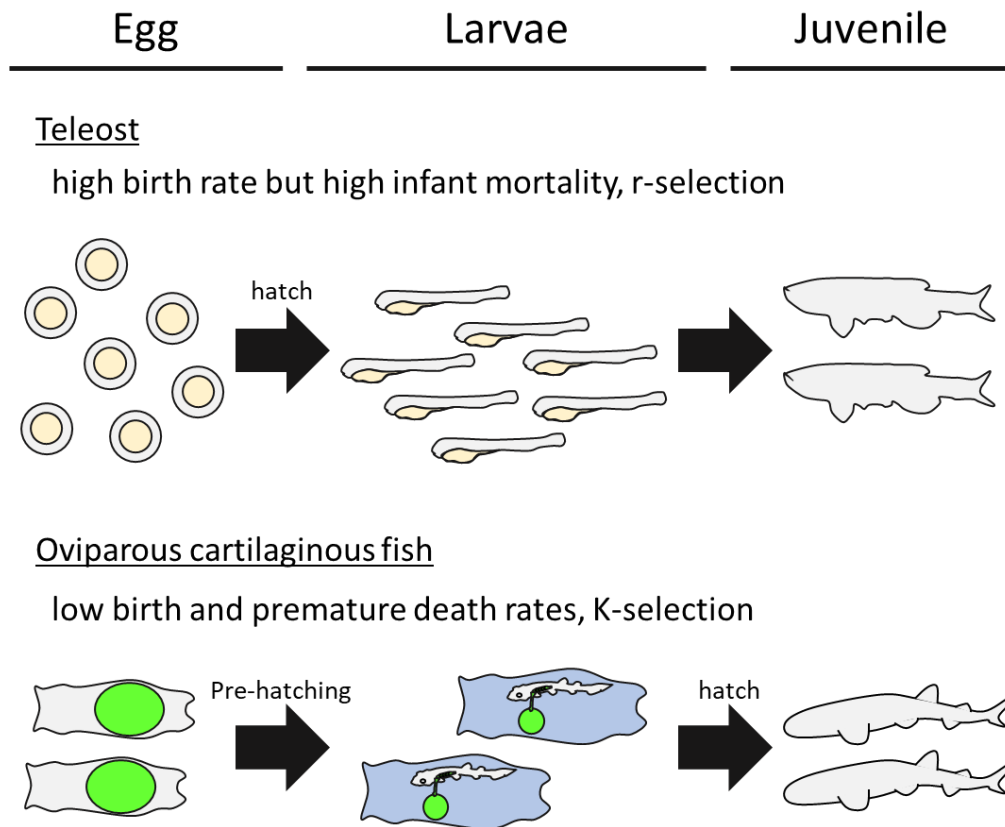


Figure 24. Reproductive strategy of early period in life history of teleosts and oviparous cartilaginous fish.

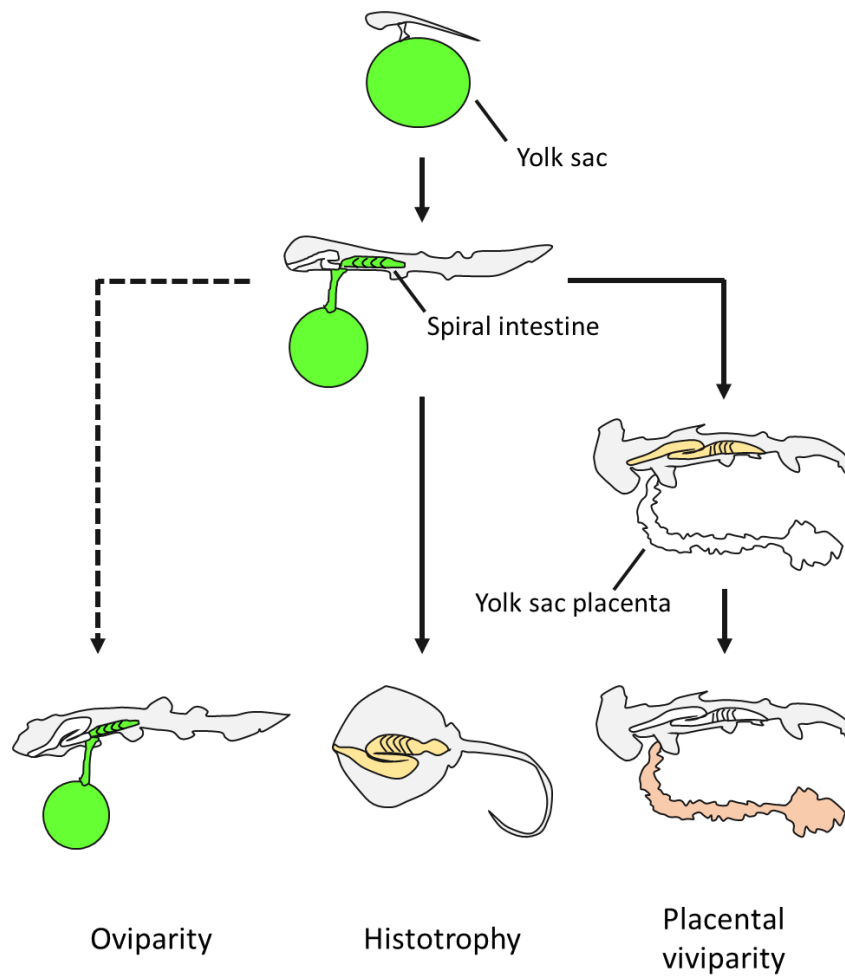


Figure 25. The use of digestive tracts during embryonic period in different reproductive modes. Solid arrows indicate the change of the site for nutrient absorption. Dashed arrow indicates no change for nutrient absorption. Colored area is functional for nutrient absorption.

Acknowledgements

First of all, I would like to express my deepest gratitude to my academic supervisor, Prof. Susumu Hyodo, professor of the Laboratory of Physiology in the Atmosphere and Ocean Research Institute (AORI), The University of Tokyo. I have learned attitude to science, way of thinking, essences of experimental technique, and importance to work with others, from him. He has been encouraging me for any time in my master's and PhD course. Without his guidance and persistent help this thesis would not have been possible. I am proud to be a PhD student of him.

I am sincerely grateful to Asst. Prof. Wataru Takagi. He always gave me helpful advice whatever I asked. I was impressed with his extensive knowledge and strict interpretation on data. I appreciate for teaching me experimental techniques and RNA-seq analysis, and for driving me to Oarai Aquarium to obtaining shark eggs.

I would like to express my sincere gratitude to Assoc. Prof. Shinji Kanda, who has provided many invaluable comments on my research. He has set up a better environment for the experiment.

I am grateful to Emer. Prof. Yoshio Takei for his incisive comments on my research. He kindly encouraged me when I was a master's student.

I am grateful to Makoto Kusakabe, the Associate Professor of Shizuoka University, for his supports, valuable comments and warm encouragement.

I am grateful to Mrs. Sanae Ogasawara for supporting me maintenance of aquarium and how to take care of shark.

I would like to extend my gratitude to Dr. Shigehiro Kuraku (RIKEN BDR) for

collaborating on RNA-seq analysis of catshark. I feel grateful to Dr. Kazuaki Yamaguchi (RIKEN BDR) for practical advice on RNA-seq analysis pipeline. I am also grateful to staffs of Laboratory for Phyloinformatics, for performing RNA-seq experiment. Moreover, I am grateful to Mr. Kazuya Kofuji, Mr. Kotaro Tokunaga and other aquarium staffs of the Aqua World Oarai, for helping me to keep adult catshark and collecting the eggs.

I am deeply grateful to Mrs. Catherine P. Loretz and Dr. Christopher A. Loretz (University at Buffalo), and Dr. Cunming Duan (University of Michigan) for their kind encouragement and valuable discussion. I am also grateful to Dr. W. Gary Anderson (University of Manitoba) for critical comments on my manuscript.

I am grateful to Dr. Taro Watanabe, who has maintained laboratory instruments and rearing facility. I have been able to do experiments smoothly thanks to him. I am also grateful to Dr. Nobuhiro Ogawa, for his invaluable assistance in the electron microscopy observation. I owe my special gratitude to Dr. Marty K.S. Wong for teaching me experiments of molecular biology, scientific writing, and philosophy. He kindly corrected the manuscript of my thesis. I am grateful to Dr. Chika Fujimori for her warm encouragement any time. I am grateful to Dr. Shiegenori Nobata. He told me attitude of doing research. I am grateful to Dr. Mayu Inokuchi (Toyo University), who taught me experimental data analysis when she was a member of Laboratory of Physiology. I am really grateful to Mrs. Kiriko Ikeba, Mrs. Miwako Ebihara, and Mrs. Yoko Nakamura for their invaluable support and warm encouragement.

I would like to express my gratitude to senior laboratory members, for teaching me experimental techniques and discussing with me. I am grateful to Dr. Kumi Hasegawa, Dr. Yukitoshi Katayama, Dr. Itaru Imaseki, and Mr. Shuntaro Ogawa. I learned a lot and

obtained ideas through discussing with them. I would like to thank Ms. Ayuko Iki, Ms. Natsuki Inoue, Mr. Takuya Shimada, Ms. Masayo Nomoto, Mr. Satoru Ozaki, Ms. Tomomi Kashiwabara, Ms. Mako Nakao, Mr. Takuto Inoue, Ms. Ayaka Fukuda, Ms. Momoko Saito, Mr. Naotaka Aburatani, Mr. Takashi Horie, Mr. Katsumi Yokota, Mr. Kazuki Maeda, Mr. Koya Shimoyama for their kind support and for providing a nice atmosphere in laboratory.

Finally, I would like to express my special gratitude to my family for their kind support and many encouragements.

References

- Ahn, H., Yamada, Y., Okamura, A., Tsukamoto, K., Kaneko, T., and Watanabe, S.** (2013). Intestinal expression of peptide transporter 1 (PEPT1) at different life stages of Japanese eel, *Anguilla japonica*. *Comp. Biochem. Physiol. B Biochem. Mol. Biol.*, **166**, 157-164.
- Ahn, S. J., Kim, N. Y., Seo, J. S., Je, J. E., Sung, J. H., Lee, S. H., ... and Lee, H. H.** (2009). Molecular cloning, mRNA expression and enzymatic characterization of cathepsin F from olive flounder (*Paralichthys olivaceus*). *Comp. Biochem. Physiol. B, Biochem. Mol. Biol.*, **154**(2), 211-220.
- Argyriou, T., Clauss, M., Maxwell, E. E., Furrer, H., and Sánchez-Villagra, M. R.** (2016). Exceptional preservation reveals gastrointestinal anatomy and evolution in early actinopterygian fishes. **Sci. Rep.**, **6**, 1-10.
- Babel, J. S.** (1966). Reproduction, life history, and ecology of the round stingray, *Urolophus halleri* Cooper. *Fish Bull.*, **137**, 1-104.
- Balfour, F. M.** (1878). A monograph on the development of elasmobranch fishes. London, UK: MacMillan and Co.
- Ballantyne, J. S.** (1997). Jaws: the inside story. The metabolism of elasmobranch fishes. *Comp. Biochem. Physiol. B, Biochem. Mol. Biol.*, **118**(4), 703-742.
- Ballantyne, J. S.** (2015). Metabolism of elasmobranchs (Jaws II). In *Fish Physiology* (Vol. 34, pp. 395-456). Academic Press.
- Ballard, W. W., Mellinger, J., and Lechenault, H.** (1993). A series of normal stages for development of *Scyliorhinus canicula*, the lesser spotted dogfish (Chondrichthyes: Scyliorhinidae). *J. Exp. Zool.*, **267**, 318-336.
- Beard, J.** (1896) The yolk-sac, yolk and merocytes in Scyllium and Lepidostew. *Anat. Anz.*, **12**, 334-347.
- Belghit, I., Skiba-Cassy, S., Geurden, I., Dias, K., Surget, A., Kaushik, S., Panserat,**

- S., and Seiliez, I.** (2014). Dietary methionine availability affects the main factors involved in muscle protein turnover in rainbow trout (*Oncorhynchus mykiss*). *Br. J. Nutr.*, **112**, 493-503.
- Bertin, L.** (1958). Appareil digestif. In *Traité de zoologie*, Vol. **13** (ed. P. P. Grassé), pp. 1248-1302. Paris: Masson et Cie Éditeurs.
- Bhutia, Y. D., and Ganapathy, V.** (2016). Glutamine transporters in mammalian cells and their functions in physiology and cancer. *Biochim Biophys Acta Mol Cell Res*, **1863**(10), 2531-2539.
- Blackburn, D. G.** (1999). Viviparity and oviparity: evolution and reproductive strategies. In *Encyclopedia of Reproduction* (eds E. Knobil and J. D. Neill), pp. 994–1003. Academic Press, New York.
- Brett, K. E., Ferraro, Z. M., Yockell-Lelievre, J., Gruslin, A., and Adamo, K. B.** (2014). Maternal–fetal nutrient transport in pregnancy pathologies: the role of the placenta. *Int. J. Mol. Sci.*, **15**(9), 16153-16185.
- Bröer, A., Klingel, K., Kowalczuk, S., Rasko, J. E. J., Cavanaugh, J., and Bröer, S.** (2004). Molecular cloning of mouse amino acid transport system B⁰, a neutral amino acid transporter related to Hartnup disorder. *J. Biol. Chem.*, **279**, 24467-24476.
- Bröer, S.** (2008). Amino acid transport across mammalian intestinal and renal epithelia. *Physiol. Rev.*, **88**(1), 249-286.
- Bröer, S., and Bröer, A.** (2017). Amino acid homeostasis and signalling in mammalian cells and organisms. *Biochem. J.*, **474**(12), 1935-1963.
- Bröer, S., and Fairweather, S. J.** (2018). Amino acid transport across the mammalian intestine. *Compr. Physiol.*, **9**(1), 343-373.
- Bucking, C., and Schulte, P. M.** (2012). Environmental and nutritional regulation of expression and function of two peptide transporter (PepT1) isoforms in a euryhaline teleost. *Comp. Biochem. Physiol. A Mol. Integr. Physiol.*, **161**, 379-387.
- Bucking, C.** (2015). Feeding and digestion in elasmobranchs: tying diet and physiology

- together. In *Fish Physiology* (Vol. 34, pp. 347-394). Academic Press.
- Buddle, A. L., Van Dyke, J. U., Thompson, M. B., Simpfendorfer, C. A., and Whittington, C. M.** (2019). Evolution of placentotrophy: using viviparous sharks as a model to understand vertebrate placental evolution. *Mar. Freshw. Res.*, **70**(7), 908-924.
- Budker, P.** (1971). *The Life of Sharks*. New York: Columbia University Press.
- Canan, B., Nascimento, W. S. D., Silva, N. B. D., and Chellappa, S.** (2012). Morphohistology of the digestive tract of the damselfish *Stegastes fuscus* (Osteichthyes: Pomacentridae). *Sci. World J.*, **2012**, 787316.
- Cappé, O., and Moulines, E.** (2009). On-line expectation–maximization algorithm for latent data models. *J R Stat Soc Series B Stat Methodol*, **71**(3), 593-613.
- Carnevali, O., Mosconi, G., Cambi, A., Ridolfi, S., Zanuy, S., and Polzonetti-Magni, A. M.** (2001). Changes of lysosomal enzyme activities in sea bass (*Dicentrarchus labrax*) eggs and developing embryos. *Aquaculture*, **202**(3-4), 249-256.
- Carvalho, L., and Heisenberg, C. P.** (2010). The yolk syncytial layer in early zebrafish development. *Trends Cell Biol.*, **20**(10), 586-592.
- Castro, J. I., Sato, K., and Bodine, A. B.** (2016). A novel mode of embryonic nutrition in the tiger shark, *Galeocerdo cuvier*. *Mar. Biol. Res.*, **12**(2), 200-205.
- Chatchavalvanich, K., Marcos, R., Poonpirom, J., Thongpan, A., and Rocha, E.** (2006). Histology of the digestive tract of the freshwater stingray *Himantura signifer* Compagno and Roberts, 1982 (Elasmobranchii, Dasyatidae). *Anat. Embryol.*, **211**, 507-518.
- Cleal, J. K., Glazier, J. D., Ntani, G., Crozier, S. R., Day, P. E., Harvey, N. C., ... and Lewis, R. M.** (2011). Facilitated transporters mediate net efflux of amino acids to the fetus across the basal membrane of the placental syncytiotrophoblast. *J. Physiol.*, **589**(4), 987-997.
- Clements, K. D., and Raubenheimer, D.** (2006). Feeding and nutrition. In *The*

- Physiology of Fishes* (ed. D. H. Evans, J. B. Claiborne and S. Currie), pp. 47-82. Florida: CRC Press.
- Closs, E. I., Scheld, J. S., Sharafi, M., and Förstermann, U.** (2000). Substrate supply for nitric-oxide synthase in macrophages and endothelial cells: role of cationic amino acid transporters. *Mol. Pharmacol.*, **57**(1), 68-74.
- Closs, E. I., Boissel, J. P., Habermeier, A., and Rotmann, A.** (2006). Structure and function of cationic amino acid transporters (CATs). *J. Membr. Biol.*, **213**(2), 67-77.
- Compagno, L.J.V.** (1988). *Sharks of the Order Carcharhiniformes*. Princeton University Press, Princeton, NJ.
- Compagno, L.J.V.** (1990). Alternative life-history styles of cartilaginous fishes in time and space. *Environ. Biol. Fish.*, **28**, 33-75.
- Compagno, L.J.V.** (2001). *Sharks of the World: An Annotated and Illustrated Catalogue of Shark Species Known to Date. Vol. 2. Bullhead, Mackerel and Carpet Sharks (Heterodontiformes, Lamniformes and Orectolobiformes)*. Food and Agriculture Organization of the United Nations, Rome.
- Compagno, L., Dando, M., and Fowler, S.** (2005). A field guide to the sharks of the world. pp. 34-37. London: Harper Collins
- Conrath, C. L., and Musick, J. A.** (2012). Reproductive biology of elasmobranchs. In *Biology of Sharks and Their Relatives*, 2nd edn (ed. J. C. Carrier J. A. Musick and M. R. Heithaus), pp. 291-311. Florida: CRC Press.
- Craig, P. M., and Moon, T. W.** (2013). Methionine restriction affects the phenotypic and transcriptional response of rainbow trout (*Oncorhynchus mykiss*) to carbohydrate-enriched diets. *Br. J. Nutr.*, **109**, 402-412.
- Daniel, H.** (2004). Molecular and integrative physiology of intestinal peptide transport. *Annu. Rev. Physiol.*, **66**, 361-384.
- Diez, J. M., and Davenport, J.** (1987). Embryonic respiration in the dogfish (*Scyliorhinus canicula* L.). *J. Mar. Biol. Assoc. UK*, **67**, 249-261.

- Diez, J. M., and Davenport, J.** (1990). Embryonic fatty acid composition as a function of yolk fatty acid composition in eggs of the lesser spotted dogfish (*Scyliorhinus canicula* L.). *Lipids*, **25**(11), 724.
- Drozdowski, L. A., and Thomson, A. B.** (2006). Intestinal sugar transport. *World J Gastroenterol*, **12**(11), 1657.
- Edgar, R. C.** (2004). MUSCLE: multiple sequence alignment with high accuracy and high throughput. *Nucleic Acids Res.*, **32**, 1792-1797.
- Fange, R., and Grove, D.** (1979). Digestion. pp. 161–260. In: W.S. Hoar, D.J. Randall and J.R. Brett (ed.) *Fish Physiology*, Volume 8, Academic Press, New York.
- Francis, M. P.** (2000). Reproduction, embryonic development, and growth of the porbeagle shark, *Lamna nasus*, in the southwest Pacific Ocean. *Fish. Bull.*, **98**, 41-63.
- Fujita, K.** (1981). Oviparous embryos of the pseudocarchariid shark, *Pseudocarcharias kamoharui*, from the Central Pacific. *Jpn. J. Ichthyol.*, **28**, 37-44.
- Gao, C., Fu, Q., Su, B., Song, H., Zhou, S., Tan, F., and Li, C.** (2017). The involvement of cathepsin F gene (CTSF) in turbot (*Scophthalmus maximus* L.) mucosal immunity. *Fish Shellfish Immunol.*, **66**, 270-279.
- Gerhartz, B., Auerswald, E. A., Mentele, R., Fritz, H., Machleidt, W., Kolb, H. J., and Wittmann, J.** (1997). Proteolytic enzymes in yolk-sac membrane of quail egg. Purification and enzymatic characterisation. *Comp. Biochem. Physiol. B, Biochem. Mol. Biol.*, **118**(1), 159-166.
- Gerhartz, B., Kolb, H. J., and Wittmann, J.** (1999). Proteolytic activity in the yolk sac membrane of quail eggs. *Comp. Biochem. Physiol. A Mol. Integr. Physiol.*, **123**(1), 1-8.
- Gilmore, R.G., Dodrill, J., and Linley, P. A.** (1983). Reproduction and embryonic development of the sand tiger shark, *Odontaspis taurus* (Rafinesque). *U.S. Fish. Bull.*, **81**, 201–225.
- Gonçalves, O., Freitas, R., Ferreira, P., Araújo, M., Zhang, G. J., Mazan, S., Cohn,**

- M. J., Castro, L. F. C., and Wilson, J. M.** (2019). Molecular ontogeny of the stomach in the catshark *Scyliorhinus canicula*. *Sci. Rep.*, **9**, 586.
- Goto, T.** (2001). Comparative anatomy, phylogeny and cladistic classification of the order Orectolobiformes (Chondrichthyes, Elasmobranchii). *Mem. Grad. Sch. Fish. Sci. Hokkaido Univ.*, **48**, 1–100.
- Grabherr, M. G., Haas, B. J., Yassour, M., Levin, J. Z., Thompson, D. A., Amit, I., ... and Chen, Z.** (2011). Full-length transcriptome assembly from RNA-Seq data without a reference genome. *Nat. Biotechnol.*, **29**(7), 644-652.
- Guetg, A., Mariotta, L., Bock, L., Herzog, B., Fingerhut, R., Camargo, S. M., and Verrey, F.** (2015). Essential amino acid transporter Lat4 (*Slc43a2*) is required for mouse development. *J. Physiol.*, **593**(5), 1273-1289.
- Hadley, C. E.** (1929). The Dissection of the Spiral Valve of *Squalus Acanthias*. *Science*, **69**(1793), 500-500.
- Haines, A. N., Flajnik, M. F., Rumfelt, L. L. and Wourms, J. P.** (2005). Immunoglobulins in the eggs of the nurse shark, *Ginglymostoma cirratum*. *Dev. Comp. Immunol.*, **29**, 417-430.
- Hamlett, W. C., and Wourms, J. P.** (1984). Ultrastructure of the pre-implantation shark yolk sac placenta. *Tissue Cell*, **16**(4), 613-625.
- Hamlett, W. C., Allen, D. J., Stribling, M. D., Schwartz, F. J., and Didio, L. J.** (1985). Permeability of external gill filaments in the embryonic shark. Electron microscopic observations using horseradish peroxidase as a macromolecular tracer. *J. Submicrosc. Cytol.*, **17**(1), 31-40.
- Hamlett, W. C.** (1986). Prenatal nutrient absorptive structures in selachians. In Indo-Pacific Fish Biology: *Proceedings of the second International Conference on Indo-Pacific Fishes*, eds. T. Uyeno, R., Arai, T. Taniuchi, and K. Matsuura (pp. 333-344).
- Hamlett, W. C., Schwartz, F. J., and DiDio, L. J.** (1987). Subcellular organization of the yolk syncytial-endoderm complex in the preimplantation yolk sac of the shark,

- Rhizoprionodon terraenovae*. *Cell Tissue Res.*, **247**(2), 275-285.
- Hamlett, W. C.** (1989). Evolution and morphogenesis of the placenta in sharks. *J. Exp. Zool.*, **252**(S2), 35-52.
- Hamlett, W. C., Musick, J. A., Eulitt, A. M., Jarrell, R. L., and Kelly, M. A.** (1996). Ultrastructure of uterine trophonemata, accommodation for uterolactation, and gas exchange in the southern stingray, *Dasyatis americana*. *Can. J. Zool.* **74**, 1417-1430.
- Hamlett, W. C., Kormanik, G., Storrie, M., Stevens, B., and Walker, T. I.** (2005). Chondrichthyan parity, lecithotrophy and matrotrophy. In *Reproductive biology and phylogeny of Chondrichthyes: sharks, batoids, and chimaeras*, 3, pp. 395-434.
- Hamlett, W. C., Kormanik, G., Storrie, M., Stevens, B., and Walker, T. I.** (2011). Chondrichthyan parity, lecithotrophy and matrotrophy. In *Reproductive Biology and Phylogeny of Chondrichthyes: Sharks, Batoids, and Chimaeras* (ed. W. C. Hamlett), pp. 405-421. Florida: CRC Press.
- Hara, Y., Yamaguchi, K., Onimaru, K., Kadota, M., Koyanagi, M., Keeley, S. D., Tatsumi, K., Tanaka, K., Motone, F., Kageyama, Y., ... and Kuraku, S.** (2018). Shark genomes provide insights into elasmobranch evolution and the origin of vertebrates. *Nat. Ecol. Evol.*, **2**, 1761-1771.
- Harahush, B. K., Fischer, A. B. P., and Collin, S. P.** (2007). Captive breeding and embryonic development of *Chiloscyllium punctatum* Muller and Henle, 1838 (Elasmobranchii: Hemiscyllidae). *J. Fish Biol.*, **71**(4), 1007-1022.
- Hart, H. R., Evans, A. N., Gelsleichter, J., and Ahearn, G. A.** (2016). Molecular identification and functional characteristics of peptide transporters in the bonnethead shark (*Sphyrna tiburo*). *J. Comp. Physiol. B Biochem. Syst. Environ. Physiol.*, **186**, 855-866.
- Hasegawa, K., Kato, A., Watanabe, T., Takagi, W., Romero, M. F., Bell, J. D., Toop, T., Donald, J. A., and Hyodo, S.** (2016). Sulfate transporters involved in sulfate secretion in the kidney are localized in the renal proximal tubule II of the elephant

- fish (*Callorhinchus milii*). *Am. J. Physiol. Regul. Integr. Comp. Physiol.*, **311**, R66-R78.
- Heming, T. A., and Buddington, R. K.** (1988). 6 yolk absorption in embryonic and larval fishes. In *Fish physiology* (Vol. 11, pp. 407-446). Academic Press.
- Holmgren, S., and Nilsson, S.** (1999) Digestive system. In: Hamlett WC (ed) *Sharks, skates, and rays: the biology of shark fishes*. The Johns Hopkins University Press, Baltimore, pp 144–173.
- Honda, Y., Takagi, W., Wong, M. K., Ogawa, N., Tokunaga, K., Kofuji, K., and Hyodo, S.** (2020). Morphological and functional development of the spiral intestine in cloudy catshark (*Scyliorhinus torazame*). *J. Exp. Biol.*, **223**, jeb225557.
- Hussain, M. M.** (2014). Intestinal lipid absorption and lipoprotein formation. *Curr Opin Lipidol*, **25**(3), 200.
- Hyodo, S., Kakumura, K., Takagi, W., Hasegawa, K., and Yamaguchi, Y.** (2014). Morphological and functional characteristics of the kidney of cartilaginous fishes: with special reference to urea reabsorption. *Am. J. Physiol. Regul. Integr. Comp. Physiol.*, **307**, R1381-R1395.
- Imamura, S., Yabu, T., and Yamashita, M.** (2008). Autophagy-mediated yolk absorption during fish embryogenesis. *Bull. Fish. Res. Agen.*, **26**, pp. 29-34
- Iwai, T.** (1957). The sequence of yolk absorption in the embryo of the deep-sea luminous shark, *Etmopterus lucifer* Jordan et Snyder. *Bull. Jap. Soc. Sci. Fish*, **23**(6), 295-301.
- Jacome-Galarza, C., Soung, D. Y., Adapala, N. S., Pickarski, M., Sanjay, A., Duong, L. T., ... and Drissi, H.** (2014). Altered hematopoietic stem cell and osteoclast precursor frequency in cathepsin K null mice. *J. Cell. Biochem.*, **115**(8), 1449-1457.
- Jhaveri, P., Papastamatiou, Y. P., and German, D. P.** (2015). Digestive enzyme activities in the guts of bonnethead sharks (*Sphyrna tiburo*) provide insight into their digestive strategy and evidence for microbial digestion in their hindguts. *Comp. Biochem. Physiol. A, Mol. Integr. Physiol.*, **189**, 76-83.

- Jollie, W. P., and Jollie, L. G.** (1967). Electron microscopic observations on accommodations to pregnancy in the uterus of the spiny dogfish, *Squalus acanthias*. *J. Ultrastruct. Res.*, **20**, 161-178.
- Jones, C. J. P., and Hamlett, W. C.** (2004). Structure and glycosylation of the term yolk sac placenta and uterine attachment site in the viviparous shark *Mustelus canis*. *Placenta*, **25**(10), 820-828.
- Jorgensen, P., Steen, J. A., Steen, H., and Kirschner, M. W.** (2009). The mechanism and pattern of yolk consumption provide insight into embryonic nutrition in *Xenopus*. *Development*, **136**(9), 1539-1548.
- Kanai, M., Soji, T., Sugawara, E., Watari, N., Oguchi, H., Matsubara, M., and Herbert, D. C.** (1996). Participation of endodermal epithelial cells on the synthesis of plasma LDL and HDL in the chick yolk sac. *Microsc. Res. Tech.*, **35**(4), 340-348.
- Kararli, T. T.** (1995). Comparison of the gastrointestinal anatomy, physiology, and biochemistry of humans and commonly used laboratory animals. *Biopharm. Drug Dispos.*, **16**(5), 351-380.
- Khanna, D. R.** (2004). *Biology of Fishes*, pp. 56-63. Delhi, India: Discovery Publishing House.
- Kiela, P. R., and Ghishan, F. K.** (2016). Physiology of intestinal absorption and secretion. *Best Pract Res Clin Gastroenterol.*, **30**(2), 145-159.
- Kim, Y. O., Park, E. M., Nam, B. H., Kong, H. J., Kim, W. J., Lee, S. J., and Choi, T. J.** (2008). Molecular cloning and characterization of cathepsin F from olive flounder *Paralichthys olivaceus*. *FASEB J.*, **22**, 199-199.
- Kleta, R., Romeo, E., Ristic, Z., Ohura, T., Stuart, C., Arcos-Burgos, M., Dave, M. H., Wagner, C. A., Camargo, S. R. M., Inoue, S., ... and Matsuura, N.** (2004). Mutations in SLC6A19, encoding B⁰AT1, cause Hartnup disorder. *Nat. Genet.*, **36**, 999-1002.
- Knight, D. P., and Hunt, S.** (1976). Fine structure of the dogfish egg case: a unique

- collagenous material. *Tissue Cell*, **8**(1), 183-193.
- Knupp, C., and Squire, J.** (1998). X-ray diffraction analysis of the 3D organization of collagen fibrils in the wall of the dogfish egg case. *Proc. Royal Soc. B.*, **265**(1411), 2177-2186.
- Komazaki, S., and Hiruma, T.** (1999). Degradation of yolk platelets in the early amphibian embryo is regulated by fusion with late endosomes. *Dev. Growth Differ.*, **41**(2), 173-181.
- Komazaki, S., Tanaka, N., and Nakamura, H.** (2002). Regional differences in yolk platelet degradation activity and in types of yolk platelets degraded during early amphibian embryogenesis. *Cells Tissues Organs*, **172**(1), 13-20.
- Krieger, J., and Fleig, R.** (1999). Yolk mobilization in perch, *Perca fluviatilis* L., embryos. *Fish Physiol. Biochem.*, **21**(2), 157-165.
- Kumar, S., Stecher, G., and Tamura, K.** (2016). MEGA7: molecular evolutionary genetics analysis version 7.0 for bigger datasets. *Mol. Biol. Evol.*, **33**, 1870-1874.
- Kumar, S., Stecher, G., Li, M., Knyaz, C., and Tamura, K.** (2018). MEGA X: molecular evolutionary genetics analysis across computing platforms. *Mol. Biol. Evol.*, **35**(6), 1547-1549.
- Lager, S., and Powell, T. L.** (2012). Regulation of nutrient transport across the placenta. *J. Pregnancy*, **2012**.
- Lambson, R. O.** (1970). An electron microscopic study of the entodermal cells of the yolk sac of the chick during incubation and after hatching. *Am. J. Anat.*, **129**(1), 1-19.
- Lane, T. H., and Jackson, H. M.** (1969). Voidance time for 23 species of fish. U.S. Fish and Wildlife Service. Washington, D.C. *Invest. fish control.*, **33**. 4 pp.
- Langmead, B., and Salzberg, S. L.** (2012). Fast gapped-read alignment with Bowtie 2. *Nat. Methods*, **9**(4), 357.
- Le, S. Q., and Gascuel, O.** (2008). An improved general amino acid replacement matrix. *Mol. Biol. Evol.*, **25**, 1307-1320.

- Lechenault, H., and Mellinger, J.** (1993). Dual origin of yolk nuclei in the lesser spotted dogfish, *Scyliorhinus canicula* (Chondrichthyes). *J. Exp. Zool.*, **265**(6), 669-678.
- Lechenault, H., Wriesez, F., and Mellinger, J.** (1993). Yolk utilization in *Scyliorhinus canicula*, an oviparous dogfish. *Environ. Biol. Fish.*, **38**, 241-252.
- Leigh, S. C., Papastamatiou, Y., and German, D. P.** (2017). The nutritional physiology of sharks. *Rev. Fish Biol. Fish.*, **27**, 561-585.
- Liu, Z., Zhou, Y., Feng, J., Lu, S., Zhao, Q., and Zhang, J.** (2013). Characterization of oligopeptide transporter (PepT1) in grass carp (*Ctenopharyngodon idella*). *Comp. Biochem. Physiol. B Biochem. Mol. Biol.*, **164**, 194-200.
- Lloyd-Evans, P.** (1993). Development of the lymphomyeloid system in the dogfish, *Scyliorhinus canicula*. *Dev. Comp. Immunol.*, **17**, 501-514.
- MacArthur, R. H., and Wilson, E. O.** (1967). The theory of island biogeography. Princeton university press, Princeton, NJ.
- McGinnis, S., and Madden, T. L.** (2004). BLAST: at the core of a powerful and diverse set of sequence analysis tools. *Nucleic Acids Res.*, **32** (Web Server issue), W20-5.
- Mellinger, J., Wriesez, F. and Alluchon-Gerard, M. J.** (1986). Developmental biology of an oviparous shark, *Scyliorhinus canicula*. In *Indo-Pacific Fish Biology: Proceedings of the Second International Conference on Indo-Pacific Fishes* (ed. T. Uyeno, R. Arai, T. Taniuchi and K. Matsuura), pp. 310-332. Tokyo: Ichthyological Society of Japan.
- Mellinger, J., Wriesez, F., and Desselle, J. C.** (1987). Transitory closures of esophagus and rectum during elasmobranch development: models for human congenital anomalies? *Arch. Biol.*, **98**, 209-230.
- Mellinger, J., Wriesez, F., Leray, C. and Haye, B.** (1989). A comparison of egg and newborn lipids in the oviparous dogfishes, *Scyliorhinus canicula* and *S. stellaris* (Chondrichthyes). Preliminary data. *Biol. Struct. Morphol.*, **2**, 44.
- Mobbs, I. G., and McMillan, D. B.** (1979). Structure of the endodermal epithelium of

- the chick yolk sac during early stages of development. *Am. J. Anat.*, **155**(3), 287-309.
- Mobbs, I. G., and McMillan, D. B.** (1981). Transport across endodermal cells of the chick yolk sac during early stages of development. *Am. J. Anat.*, **160**(3), 285-308.
- Moss, S. A.** (1984). *Sharks: An Introduction for the Amateur Naturalist*. Englewood, NJ: Prentice-Hall.
- Musa, S. M., Czachur, M. V., and Shiels, H. A.** (2018). Oviparous elasmobranch development inside the egg case in 7 key stages. *PloS one*, **13**(11), e0206984.
- Musick, J. A., and Ellis, J. K.** (2005). Reproductive evolution of chondrichthyans. In *Reproductive Biology and Phylogeny of Chondrichthyes: Sharks, Batoids, and Chimaeras*, Vol. 3 (ed. W. C. Hamlett), pp. 45-80. CRC Press.
- Nakaya, K., White, W. T., and Ho, H. C.** (2020). Discovery of a new mode of oviparous reproduction in sharks and its evolutionary implications. *Sci. Rep.*, **10**(1), 1-12.
- Newton, K. C., Wraith, J., and Dickson, K. A.** (2015). Digestive enzyme activities are higher in the shortfin mako shark, *Isurus oxyrinchus*, than in ectothermic sharks as a result of visceral endothermy. *Fish Physiol. Biochem.*, **41**(4), 887-898.
- Ng, A. N. Y., De Jong-Curtain, T. A., Mawdsley, D. J., White, S. J., Shin, J., Appel, B., Dong, P. D. S., Stainier, D. Y. R., and Heath, J. K.** (2005). Formation of the digestive system in zebrafish: III. Intestinal epithelium morphogenesis. *Dev. Biol.*, **286**, 114-135.
- Nishiguchi, Y., Tomita, T., Ihara, H., Kiuchi, S., Tani, A., and Okada, M.** (2017). Chemical composition of eggs from *Deania hystricosa*. *Int J Anal Bio-Sci*, **5**(4).
- Okano, T., Otake, K., Teshima, K., and Mizue, S.** (1981). Epithelial cells of the intestine in *Mustelus manazo* and *M. griseus* embryos. Studies on Sharks – XX. *Bull. Off Fac. Fish.*, **51**, 23-28.
- Onimaru, K., Motone, F., Kiyatake, I., Nishida, K., and Kuraku, S.** (2018). A staging table for the embryonic development of the brownbanded bamboo shark (*Chiloscyllium punctatum*). *Dev. Dyn.*, **247**(5), 712-723.

- Orozco, Z. G. A., Soma, S., Kaneko, T., and Watanabe, S.** (2017). Effects of fasting and refeeding on gene expression of *slc15a1a*, a gene encoding an oligopeptide transporter (PepT1), in the intestine of Mozambique tilapia. *Comp. Biochem. Physiol. B Biochem. Mol. Biol.*, **203**, 76-83.
- Orozco, Z. G. A., Soma, S., Kaneko, T., and Watanabe, S.** (2018). Spatial mRNA expression and response to fasting and refeeding of neutral amino acid transporters *slc6a18* and *slc6a19a* in the intestinal epithelium of Mozambique tilapia. *Front. Physiol.*, **9**, 212.
- Papastamatiou, Y. P.** (2007). The potential influence of gastric acid secretion during fasting on digestion time in leopard sharks (*Triakis semifasciata*). *Comp. Biochem. Physiol. A Mol. Integr. Physiol.*, **147**(1), 37-42.
- Parker, T. J.** (1880). On the intestinal spiral valve in the genus *Raia*. *Trans. Zool. Soc. London*, **11**, 49-61.
- Patton, J. S., Warner, T. G., and Benson, A. A.** (1977). Partial characterization of the bile salt-dependent triacylglycerol lipase from the leopard shark pancreas. *Biochim. Biophys. Acta, Lipids Lipid Metab.*, **486**(2), 322-330.
- Perrault, C.** (1671). Mémoires pour servir à l'histoire naturelle des animaux. Académie des sciences, pp. 54-58. Paris: Imprimerie royale.
- Rasco, B. A., and Hultin, H. O.** (1988). A comparison of dogfish and porcine pancreatic lipases. *Comp. Biochem. Physiol. B, Biochem. Mol. Biol.*, **89**(4), 671-677.
- Remme, J. F., Synnes, M., and Stoknes, I. S.** (2005). Chemical characterisation of eggs from deep-sea sharks. *Comp. Biochem. Physiol. B, Biochem. Mol. Biol.*, **141**(2), 140-146.
- Rimoldi, S., Bossi, E., Harpaz, S., Cattaneo, A. G., Bernardini, G., Saroglia, M., and Terova, G.** (2015). Intestinal B0AT1 (SLC6A19) and PEPT1 (SLC15A1) mRNA levels in European sea bass (*Dicentrarchus labrax*) reared in fresh water and fed fish and plant protein sources. *J. Nutr. Sci.*, **4**, 1-13.

- Rodda, K. R., and Seymour, R. S.** (2008). Functional morphology of embryonic development in the Port Jackson shark *Heterodontus portusjacksoni* (Meyer). *J. Fish Biol.*, **72**, 961-984.
- Romanoff, A. L.** (1960). The avian embryo. Structural and functional development. pp.1041-1078. New York, Macmillan Co.
- Romer A. S., and Parsons T. S.** (2007). Digestive system. In: The vertebrate body. 5th ed. Tokyo: Hosei University Press. pp. 306–325.
- Rønnestad, I., Gavaia, P. J., Viegas, C. S. B., Verri, T., Romano, A., Nilsen, T. O., Jordal, A.-E. O., Kamisaka, Y., and Cancela, M. L.** (2007). Oligopeptide transporter PepT1 in Atlantic cod (*Gadus morhua* L.): cloning, tissue expression and comparative aspects. *J. Exp. Biol.*, **210**, 3883-3896.
- Rusaouën, M., Pujol, J. P., Bocquet, J., Veillard, A., and Borel, J. P.** (1976). Evidence of collagen in the egg capsule of the dogfish, *Scyliorhinus canicula*. *Comp. Biochem. Physiol. B, Biochem. Mol. Biol.*, **53**(4), 539-543.
- Savin, T., Kurpios, N. A., Shyer, A. E., Florescu, P., Liang, H., Mahadevan, L., and Tabin, C. J.** (2011). On the growth and form of the gut. *Nature*, **476**(7358), 57-62.
- Schindelin, J., Arganda-Carreras, I., Frise, E., Kaynig, V., Longair, M., Pietzsch, T., Preibisch, S., Rueden, C., Saalfeld, S., Schmid, B., ... and Cardona, A.** (2012). Fiji: an open-source platform for biological-image analysis. *Nat. Methods.*, **9**, 676-682.
- Shimizu, M., and Yamada, J.** (1980). Ultrastructural aspects of yolk absorption in the vitelline syncytium of the embryonic rockfish, *Sebastes schlegeli*. *Jpn. J. Ichthyol.*, **27**(1), 56-63.
- Sire, M. F., Babin, P. J., and Vernier, J. M.** (1994). Involvement of the lysosomal system in yolk protein deposit and degradation during vitellogenesis and embryonic development in trout. *J. Exp. Zool.*, **269**(1), 69-83.
- Skjærven, K. H., Finn, R. N., Kryvi, H., and Fyhn, H. J.** (2003). Yolk resorption in

- developing plaice (*Pleuronectes platessa*). In The big fish bang. *Proceedings of the 26th annual larval fish conference*. Bergen: Institute of Marine Research (pp. 193-209).
- Smith, B. G.** (1942). The Heterodontid sharks, their natural history, and the external development of *Heterodontus japonicus* based on notes and drawings by Bashford Dean. In The Bashford Dean Memorial Volume Archiac Fishes (Gudger, E. W., ed.), pp. 649–770. New York: The American Museum of Natural History.
- Smith, H. W.** (1936). The retention and physiological role of urea in the Elasmobranchii. *Biol. Rev.*, **11**, 49-82.
- Speake, B. K., Murray, A. M., and Noble, R. C.** (1998). Transport and transformations of yolk lipids during development of the avian embryo. *Prog. Lipid Res.*, **37**, 1-32.
- Speier, J. S., Yadgary, L., Uni, Z., and Wong, E. A.** (2012). Gene expression of nutrient transporters and digestive enzymes in the yolk sac membrane and small intestine of the developing embryonic chick. *Poult. Sci.*, **91**(8), 1941-1949.
- Stoka, V., Turk, V., and Turk, B.** (2016). Lysosomal cathepsins and their regulation in aging and neurodegeneration. *Ageing Res. Rev.*, **32**, 22-37.
- Sveier, H., Kvamme, B. O., and Rae, A. J.** (2001). Growth and protein utilization in Atlantic salmon (*Salmo salar* L.) given a protease inhibitor in the diet. *Aquacult. Nutr.*, **7**, 255-264.
- Takabe, S., Teranishi, K., Takaki, S., Kusakabe, M., Hirose, S., Kaneko, T., and Hyodo, S.** (2012). Morphological and functional characterization of a novel Na⁺/K⁺-ATPase-immunoreactive, follicle-like structure on the gill septum of Japanese banded houndshark, *Triakis scyllium*. *Cell Tissue Res.*, **348**, 141-153.
- Takagi, W., Kajimura, M., Tanaka, H., Hasegawa, K., Bell, J. D., Toop, T., Donald, J. A., and Hyodo, S.** (2014). Urea-based osmoregulation in the developing embryo of oviparous cartilaginous fish (*Callorhynchus milii*): contribution of the extraembryonic yolk sac during the early developmental period. *J. Exp. Biol.*, **217**,

1353-1362.

- Takagi, W., Kajimura, M., Tanaka, H., Hasegawa, K., Ogawa, S., and Hyodo, S.** (2017). Distributional shift of urea production site from the extraembryonic yolk sac membrane to the embryonic liver during the development of cloudy catshark (*Scyliorhinus torazame*). *Comp. Biochem. Physiol. A Mol. Integr. Physiol.*, **211**, 7-16.
- Tatsumi, K., Nishimura, O., Itomi, K., Tanegashima, C., and Kuraku, S.** (2015). Optimization and cost-saving in tagmentation-based mate-pair library preparation and sequencing. *BioTechniques.*, **58**, 253-257.
- Terova, G., Corà, S., Verri, T., Rimoldi, S., Bernardini, G., and Saroglia, M.** (2009). Impact of feed availability on PepT1 mRNA expression levels in sea bass (*Dicentrarchus labrax*). *Aquaculture*, **294**, 288-299.
- Teshima, K., and Tomonaga, S.** (2016). Freshwater stingray embryos store yolk in their intestinal epithelial cells. *J. Natl. Fish. Univ.*, **64**, 182-187.
- Tewinkel, L. E.** (1943). Observations on later phases of embryonic nutrition in *Squalus acanthias*. *J. Morphol.*, **73**(1), 177-205.
- Theodosiou, N. A., Hall, D. A., and Jowdry, A. L.** (2007). Comparison of acid mucin goblet cell distribution and Hox13 expression patterns in the developing vertebrate digestive tract. *J. Exp. Zool. B Mol. Dev. Evol.*, **308**(4), 442-453.
- Theodosiou, N. A., and Simeone, A.** (2012). Evidence of a rudimentary colon in the elasmobranch, *Leucoraja erinacea*. *Dev. Genes Evol.*, **222**(4), 237-243.
- Theodosiou, N. A., and Oppong, E.** (2019). 3D morphological analysis of spiral intestine morphogenesis in the little skate, *Leucoraja erinacea*. *Dev. Dyn.*, **248**, 688-701.
- Thomason, J. C., Davenport, J., and Rogerson, A.** (1994). Antifouling performance of the embryo and eggcase of the dogfish *Scyliorhinus canicula*. *J. Mar. Biolog. Assoc. U.K.*, **74**(4), 823-836.
- Tingaud-Sequeira, A., and Cerdà, J.** (2007). Phylogenetic relationships and gene

- expression pattern of three different cathepsin L (Ctsl) isoforms in zebrafish: Ctsla is the putative yolk processing enzyme. *Gene*, **386**(1-2), 98-106.
- Tingaud-Sequeira, A., Carnevali, O., and Cerdà, J.** (2011). Cathepsin B differential expression and enzyme processing and activity during *Fundulus heteroclitus* embryogenesis. *Comp. Biochem. Physiol. A, Mol. Integr. Physiol.*, **158**(2), 221-228.
- Tomita, T., Nakamura, M., Sato, K., Takaoka, H., Toda, M., Kawauchi, J., and Nakaya, K.** (2014). Onset of buccal pumping in catshark embryos: how breathing develops in the egg capsule. *PLoS ONE*, **9**, e109504.
- van der Wagt, I., de Jong, I. C., Mitchell, M. A., Molenaar, R., and van den Brand, H.** (2020). A review on yolk sac utilization in poultry. *Poult. Sci.*, **99**(4), 2162-2175.
- Verri, T., Kottra, G., Romano, A., Tiso, N., Peric, M., Maffia, M., Boll, M., Argenton, F., Daniel, H., and Storelli, C.** (2003). Molecular and functional characterisation of the zebrafish (*Danio rerio*) PEPT1-type peptide transporter. *FEBS Lett.*, **549**, 115-122.
- Wallace, K. N., Akhter, S., Smith, E. M., Lorent, K., and Pack, M.** (2005). Intestinal growth and differentiation in zebrafish. *Mech. Dev.*, **122**, 157-173.
- Wallace, R. A.** (1985). Vitellogenesis and oocyte growth in nonmammalian vertebrates. In oogenesis (pp. 127-177). Springer, Boston, MA.
- Walton, K. D., Freddo, A. M., Wang, S., and Gumucio, D. L.** (2016). Generation of intestinal surface: an absorbing tale. *Development*, **143**(13), 2261-2272.
- Walzer, C., and Schönenberger, N.** (1979). Ultrastructure and cytochemistry study of the yolk syncytial layer in the alevin of trout (*Salmo fario trutta L.*) after hatching. *Cell Tissue Res.*, **196**(1), 59-73.
- Wang, T. Y., Liu, M., Portincasa, P., and Wang, D. Q. H.** (2013). New insights into the molecular mechanism of intestinal fatty acid absorption. *Eur. J. Clin. Invest.*, **43**(11), 1203-1223.
- Wetherbee, B. M., Gruber, S. H., and Ramsey, A. L.** (1987). X-radiographic observations of food passage through digestive tracts of lemon sharks. *Trans. Am.*

- Fish. Soc.*, **116**, 763-767.
- Wetherbee, B. M., Gruber, S. H., and Cortés, E.** (1990). Diet feeding habits, digestion and consumption in sharks, with special reference to the lemon shark. *Negrapion brevirostris*. *NOAA tech. rep. NMFS SSRF*, **90**(1), 29-47.
- White, E. G.** (1937). Interrelationships of the elasmobranchs with a key to the order Galea. *Bull. Am. Mus. Nat. Hist.*, **74**, 25-138.
- Wilson, J. M., and Castro, L. F. C.** (2010). Morphological diversity of the gastrointestinal tract in fishes. *Fish Physiol.*, **30**, 1-55.
- Wong, E. A., and Uni, Z.** (2020). The chicken yolk sac is a multifunctional organ. *Poult. Sci.*, in press.
- Wouters, J., Goethals, M., and Stockx, J.** (1985). Acid proteases from the yolk and the yolk-sac of the hen's egg. Purification, properties and identification as cathepsin D. *Int. J. Biochem.*, **17**(3), 405-413.
- Wriesez, F., Lechenault, H., Leray, C., Haye, B., and Mellinger, J.** (1993). Fate of yolk lipid in an oviparous elasmobranch fish *Scyliorhinus canicula* (L.). In *Physiological and Biochemical Aspects of Fish* (B. T. Walther and H. J. Fyhn, eds), pp. 315-322. Bergen: University of Bergen Press.
- Xu, D., He, G., Mai, K., Zhou, H., Xu, W., and Song, F.** (2016). Expression pattern of peptide and amino acid genes in digestive tract of transporter juvenile turbot (*Scophthalmus maximus* L.). *J. Ocean Univ. China*, **15**, 334-340.
- Xu, X., Qin, Y., Luo, G., Huang, X., Zou, W.-Z., Zheng, L., Wang, J., and Su, Y.** (2015). Ontogeny of digestive organs during early developmental stages of the tropical whitespotted bamboo shark, *Chiloscyllium plagiosum* – a histological study. *Mar. Freshw. Behav. Physiol.*, **48**, 253-266.
- Yadgary, L., Yair, R., and Uni, Z.** (2011). The chick embryo yolk sac membrane expresses nutrient transporter and digestive enzyme genes. *Poult. Sci.*, **90**(2), 410-416.
- Yadgary, L., Wong, E. A., and Uni, Z.** (2014). Temporal transcriptome analysis of the

- chicken embryo yolk sac. *BMC genomics*, **15**(1), 690.
- Yamamura, J. I., Adachi, T., Aoki, N., Nakajima, H., Nakamura, R., and Matsuda, T.** (1995). Precursor-product relationship between chicken vitellogenin and the yolk proteins: the 40 kDa yolk plasma glycoprotein is derived from the C-terminal cysteine-rich domain of vitellogenin II. *Biochim Biophys Acta Gen Subj*, **1244**(2-3), 384-394.
- Yano, K.** (1992). Comments on the reproductive mode of the false cat shark *Pseudotriakis microdon*. *Copeia*, **1992**, 460-468.
- Yoshizaki, N., Soga, M., Ito, Y., Mao, K. M., Sultana, F., and Yonezawa, S.** (2004). Two-step consumption of yolk granules during the development of quail embryos. *Dev. Growth Differ.*, **46**(3), 229-238.
- Zhang, H., and Wong, E. A.** (2017). Spatial transcriptional profile of PepT1 mRNA in the yolk sac and small intestine in broiler chickens. *Poult. Sci.*, **96**(8), 2871-2876.